AD-766 309

SPRING OVERRIDING AIRCRAFT CLUTCH

P. Lynwander, et al

Avco Lycoming Division

Prepared for:

Army Air Mobility Research and Development Laboratory

May 1973

VH

AD

USAAMRDL TECHNICAL REPORT 73-17

SPRING OVERRIDING AIRCRAFT CLUTCH

By

P. Lynwander
A. G. Meyer
S. Chachakis

May 1973

EUSTIS DIRECTORATE
U. S. ARMY AIR MOBILITY RESEARCH AND DEVELOPMENT LABORATORY
FORT EUSTIS, VIRGINIA

CONTRACT DAAJ02-71-C-0035
AVCO LYCOMING DIVISION
STRATFORD, CONNECTICUT

Approved for public release;
distribution unlimited.

DISCLAIMERS

The findings in this report are not to be construed as an official Department of the Army position unless so designated by other authorized documents.

When Government drawings, specifications, or other data are used for any purpose other than in connection with a definitely related Government procurement operation, the U. S. Government thereby incurs no responsibility nor any obligation whatsoever; and the fact that the Government may have formulated, furnished, or in any way supplied the said drawings, specifications, or other data is not to be regarded by implication or otherwise as in any manner licensing the holder or any other person or corporation, or conveying and rights or permission, to manufacture, use, or sell any patented invention that may in any way be related thereto.

Trade names cited in this report do not constitute an official endorsement or approval of the use of such commercial hardware or software.

DISPOSITION INSTRUCTIONS

Destroy this report when no longer needed. Do not return it to the originator.

Unclassified

Security Classification

DOCUMENT CONTROL DATA - R & D

(Security classification of title, body of abstract and indexing annotation must be entered when the overall report is classified)

1. ORIGINATING ACTIVITY *(Corporate author)*
Avco Lycoming Division
Stratford, Connecticut

2a. REPORT SECURITY CLASSIFICATION
Unclassified

2b. GROUP

3. REPORT TITLE
SPRING OVERRIDING AIRCRAFT CLUTCH

4. DESCRIPTIVE NOTES *(Type of report and inclusive dates)*
Final Report

5. AUTHOR(S) *(First name, middle initial, last name)*
P. Lynwander
A. G. Meyer
S. Chachakis

6. REPORT DATE
May 1973

7a. TOTAL NO. OF PAGES
~~147~~ 150

7b. NO. OF REFS
4

8a. CONTRACT OR GRANT NO.
DAAJ02-71-C-0035

b. PROJECT NO.
1G162207AA72

c.

d.

9a. ORIGINATOR'S REPORT NUMBER(S)
USAAMRDL Technical Report 73-17

9b. OTHER REPORT NO(S) *(Any other numbers that may be assigned this report)*
Avco Lycoming Report No. 105.7.12

10. DISTRIBUTION STATEMENT
Approved for public release; distribution unlimited.

11. SUPPLEMENTARY NOTES

12. SPONSORING MILITARY ACTIVITY
Eustis Directorate
U.S. Army Air Mobility R&D Laboratory
Fort Eustis, Virginia

13. ABSTRACT

The purpose of this program was to investigate the performance of high-speed overriding spring clutch assemblies for use in a multiengine helicopter application. The design operating conditions were 3,570 inch-pounds torque transmitted at 26,500 rpm. Two clutch configurations were evaluated. On design A, the input member of the clutch is a drum into which a variable-cross-section spring is expanded. The large end of the spring butts up against a lug on an output shaft through which the torque is transmitted. The spring is mechanically energized on its small end, and during overriding the small end ratchets past the energizing device. Design B has both an input and an output drum connected by an expanding variable-cross-section spring. The small end coils of the spring are raised slightly and are always in contact with the drums. The clutch is energized by friction between the drum and spring end, and during overriding rubs at this interface. An extensive test program was conducted as follows: 1. Full-Speed Dynamic Clutch Override Test - Operation at zero input speed and 26,500 rpm output speed for 5-hour runs at each of five levels of oil flow; 2. Differential Speed Dynamic Clutch Override Test - Operation at output speed of 26,500 rpm and input speeds of 13,250 (50 percent normal rated), 17,755 (67 percent normal rated) and 19,875 (75 percent normal rated) rpm; 3. Dynamic Engagement Test - Simulated high-speed engagements; 4. Static Cyclic Torque Fatigue Test - Operation at 7,140 ± 900 inch-pounds for 10^7 cycles; 5. Static Overload Test - Torque application to 18,000 inch-pounds. Measurements of drag torque and metal and oil temperatures were made during the dynamic testing. Results of the test program indicated that design A clutch had several failings and would require redesign and extensive development to operate successfully. The design B clutch completed all tests with no significant difficulties.

DD FORM 1 NOV 68 1473 REPLACES DD FORM 1473, 1 JAN 64, WHICH IS OBSOLETE FOR ARMY USE.

Unclassified

Security Classification

14. KEY WORDS	LINK A		LINK B		LINK C	
	ROLE	WT	ROLE	WT	ROLE	WT
Clutch						

4876-73

DEPARTMENT OF THE ARMY
U. S. ARMY AIR MOBILITY RESEARCH & DEVELOPMENT LABORATORY
EUSTIS DIRECTORATE
FORT EUSTIS, VIRGINIA 23604

The research described herein was conducted by Avco Lycoming Division under the terms of Contract DAAJ02-71-C-0035. The work was performed under the technical management of Mr. E. R. Givens and Mr. D. P. Lubrano, Technology Applications Division, Eustis Directorate.

V/STOL drive systems must incorporate an overrunning (freewheel) clutch unit so that in the event of engine malfunction, the aircraft can safely autorotate or, in the case of multiengines, proceed on single-engine operation. Current overrunning speeds are limited to approximately 12,000 rpm or less, depending on the torque transmitted. The objective of this program was to evaluate spring-type clutches operating at engine input conditions of 26,500 rpm and 1500 hp.

Appropriate technical personnel of this Directorate have reviewed this report and concur with the conclusions contained herein.

Project 1G162207AA72
Contract DAAJ02-71-C-0035
USAAMRDL Technical Report 73-17
May 1973

SPRING OVERRIDING AIRCRAFT CLUTCH

Final Report

Avco Lycoming Report No. 105.7.12

By

P. Lynwander
A. G. Meyer
S. Chachakis

Prepared by

Avco Lycoming Division
Stratford, Connecticut

for

EUSTIS DIRECTORATE
U. S. ARMY AIR MOBILITY RESEARCH
AND DEVELOPMENT LABORATORY
FORT EUSTIS, VIRGINIA

SUMMARY

The purpose of this program was to investigate the performance of high-speed overriding spring clutch assemblies for use in a multiengine helicopter application. The design operating conditions were 3,570 inch-pounds torque transmitted at 26,500 rpm. Two clutch configurations were evaluated. On design A, the input member of the clutch is a drum into which a variable-cross-section spring is expanded. The large end of the spring butts up against a lug on an output shaft through which the torque is transmitted. The spring is mechanically energized on its small end, and during overriding the small end ratchets past the energizing device. Design B has both an input and an output drum connected by an expanding variable-cross-section spring. The small end coils of the spring are raised slightly and are always in contact with the drums. The clutch is energized by friction between the drum and spring end, and during overriding rubs at this interface.

An extensive test program was conducted as follows:

1. Full-Speed Dynamic Clutch Override Test - Operation at zero input speed and 26,500 rpm output speed for 5-hour runs at each of five levels of oil flow

2. Differential Speed Dynamic Clutch Override Test - Operation at output speed of 26,500 rpm and input speeds of 13,250 (50 percent normal rated), 17,755 (67 percent normal rated) and 19,875 (75 percent normal rated) rpm

3. Dynamic Engagement Test - Simulated high-speed engagements

4. Static Cyclic Torque Fatigue Test - Operation at 7,140 ± 900 inch-pounds for 10^7 cycles

5. Static Overload Test - Torque application to 18,000 inch-pounds

Measurements of drag torque and metal and oil temperatures were made during the dynamic testing.

Results of the test program indicated that design A clutch had several failings and would require redesign and extensive development to operate successfully. The design B clutch completed all tests with no significant difficulties.

FOREWORD

This program was conducted for the Eustis Directorate, U.S. Army Air Mobility Research and Development Laboratory under Contract DAAJ02-71-C-0035, DA Project 1G162207AA72. The period of performance was 15 April 1971 through 6 December 1972.

U.S. Army technical direction was provided by Mr. R. Givens and Mr. D. Lubrano.

Acknowledgement is made to the engineering staff of Curtiss-Wright Corporation for their assistance in this program.

TABLE OF CONTENTS

LIST OF ILLUSTRATIONS

LIST OF TABLES

LIST OF SYMBOLS

A	cross-sectional area of a coil - $in.^2$
A_C	contact area of spring on shaft - $in.^2$
a	moment arm - in.
b	width of energizing end coil - in.
b_i	width of a spring coil - in.
b_M	mean coil width - in.
b_N	width of lug end coil - in.
b_3	width of third coil - in.
D	ductility
D_{ME}	mean diameter of the spring as assembled onto the output shaft - in.
D_{MF}	mean diameter of the free spring in the free state - in.
D_{MO}	mean diameter of the spring when unwrapped into the drum - in.
d_{d_i}	drum inside diameter - in.
d_{d_o}	drum outside diameter - in.
d_{s_i}	shaft inside diameter - in.
d_{s_o}	shaft outside diameter - in.
E	modulus of elasticity - psi
e	2.72 base natural logarithm

F	force through spring element - lb
F_C	spring centrifugal force - lb
F_{CG}	centrifugal force due to the last coil - lb
F_{N_T}	normal force due to the transmitted load - lb
f	distance from point of load application to point of maximum tensile fillet stress - in.
G	modulus of rigidity = 10.2×10^6 - psi
G_i	gain of a given coil
G_{i-1}	gain of the previous coil
G_N	gain or amplification factor of the spring $e^{2\pi\mu N}$
G_{N-1}	gain of next to last coil
g	acceleration due to gravity - 386.4 in./sec^2
h	spring radial height - in.
i	dimension defining weakest semisection - in.
K	stress concentration factor
L	proximity stress - psi
l	spring length - in.
M	nominal bending stress - psi
M_{CL}	energizing moment to reduce drum clearance to zero - in.-lb
M_D	energizing moment to reduce press fit to zero - in.-lb
M_t	bending moment required to unwrap spring off shaft and into drum - in.-lb

m	mass of the last coil - lb mass
m_S	spring mass - lb mass
N	number of coils in torque spring
N_f	cyclic life - cycles of load
P	applied force - lb
P_N	maximum normal force between ratcheting end faces of springs - lb
P_o	internal pressure at drum inside diameter due to transmitted load plus centrifugal force of the spring - psi
P_T	tangential force between ratcheting ends of springs - lb
p_c	pressure between spring and shaft due to centrifugal force - psi
p_d	pressure between spring and shaft due to expansion of spring onto shaft - psi
R	fillet radius - in.
R^1	projection radius - in.
RA	reduction in area
r_1	output shaft radius - in.
r_2	lug outer radius - in.
r_m	lug mean radius - in.
S_{AV}	average stress component - psi
S_b	bending stress - psi
S_c	compressive stress - psi

S_s	shear stress in the output shaft - psi
S_{t_i}	total stress at the inner surface of the spring - psi
$S_{t\,max}$	maximum total stress - psi
$S_{t\,min}$	minimum total stress - psi
S_{t_o}	total stress at the outer surface of the spring - psi
S_{t_R}	maximum drum hoop stress - psi
S_r	fluctuating stress component - psi
T	total energizing moment - in.-lb
Ta	applied torque - in.-lb
T_D	drag torque during overriding - in.-lb
T_S	moment required to unwrap the free spring to the diameter of the shaft - in.-lb
T_{S_N}	torque transmitted through the outer surface of the last coil - in.-lb
T_T	design point torque - in.-lb
T_3	torque transmitted through third coil - in.-lb
t	width of section - in.
Z	section modulus - $in.^3$
β	semiangle of projection - deg
γ	spring factor
ΔCL	initial drum clearance - in.

ΔD	growth of the free spring due to centrifugal force - in.
ΔX	axial displacement - in.
$\Delta \epsilon_t$	total strain range - in./in.
δ	weight density constant = 0.282 lb/in.^{3}
η	design point speed - rpm
θ_{CL}	actuation angle to reduce drum clearance to zero - deg
θ_D	actuation angle to redue press fit to zero - deg
θ_E	free spring angle of wrap - rad
θ_F	deflected spring angle of wrap - rad
μ	coefficient of static friction at contact surface between drum and spring
μ_{SL}	coefficient of sliding friction between end faces of springs
ν	Poisson's ratio - 0.25
π	constant - 3.14159263
σ	bending stress - psi
σ_{max}	maximum tensile fillet stress - psi
σ_u	ultimate tensile strength - psi
τ	torsional shear stress - psi
ϕ	spring angular deflection, one end relative to the other - turns
ψ	angle of inclination of load from surface normal - deg
ω	angular velocity at design point speed - rad/sec

INTRODUCTION

The purpose of this program was to advance the technology of overriding spring clutch units to allow for reliable and efficient operation at speeds and loads commensurate with advanced aircraft turboshaft engines. The design operating conditions for this program were 26, 500 rpm and 3, 570 inch-pounds torque.

The overriding clutch is a critical helicopter component that transmits engine torque in normal operation and allows the rotors to autorotate in case of engine malfunction. With the advent of multiple engine configurations, the overriding clutch assumes an even greater role since the aircraft must be capable of operation with an engine shut down or with engines operating at different speeds.

Current transmission designs locate the clutch after the first or second gear reduction stage from the engine in order to eliminate problems associated with high-speed operation; however, this practice is costly in terms of component size, weight, and oil flow. To achieve the lightest configuration, the overriding clutch must be located on the high-speed shaft before or in combination with the first gear reduction.

Difficulties associated with high-speed overriding clutches fall into two categories:

1. Fatigue and overload capability

2. Problems associated with high-speed overriding operation

Also, clutch engagement and disengagement at high rates of speed and acceleration with attendant shock loads are a potential source of difficulties.

The approach taken to investigate these problems and to advance the technology of overriding spring clutches in the subject program follows:

1. An analytical study was conducted to arrive at the spring clutch configurations best suited for high-speed aircraft operation. The configuration chosen, designated design A,

features a variable lead spring that expands into an input shaft drum and drives the output shaft at the heavy end of the spring through a lug. This spring clutch configuration minimizes the space required and is lightweight. A drawback of design A is that all output torque must pass through the lug end.

A second clutch configuration, designated design B, was made available for evaluation by the U. S. Army Air Mobility Research and Development Laboratory. Design B features a variable lead spring that expands into drums on both the input and output shafts to transmit torque from one to the other. This configuration overcomes the problem of transmitting all the torque from the spring to a connection on the output shaft.

2. A computer program was developed to provide an analytical tool for the analysis of high-speed spring clutches of the design A configuration.

3. An extensive test program was conducted on both design A and B configurations as follows:

   a. Full-Speed Dynamic Clutch Override Test - Operation at zero input speed and 26, 500 rpm output speed for 5-hour runs at various oil flows

   b. Differential Speed Dynamic Clutch Override Test - Operation at output speed of 26, 500 rpm and input speeds of 13, 250 (50 percent normal rated), 17, 755 (67 percent normal rated), and 19, 875 (75 percent normal rated) rpm

   c. Dynamic Engagement Test - Simulated high-speed engagement

   d. Static Cyclic Torque Fatigue Test - Operation at 7, 140 $\pm$ 900 inch-pounds for ten million cycles

   e. Static Overload Test - Torque application in increments to 18, 000 inch-pounds (Design B only)

DESIGN AND ANALYSIS

DESCRIPTION OF CLUTCH OPERATION

The principle of spring clutch operation is presented in simplified form in Figure 1. Figure 1(A) shows a contracting configuration where a spring is wrapped around two shafts with an interference fit; Figure 1(B) shows an expanding configuration with a spring pressed into the bores of two drums.

Rotation of the input shaft or drum in one direction grips the spring and transmits torque into the output shaft or drum. In the case of the shaft-mounted configuration, Figure 1(A), the spring is in tension, whereas in the drum-mounted configuration, Figure 1(B), the spring is in compression while transmitting torque.

Rotation in the opposite direction will produce slippage between the spring and the shaft or drum.

The coils carry an increasingly greater load along the spring. In the case of the clutches pictured in Figure 1, the coil with the highest load is at the crossover. Because the load in the spring coils varies exponentially, it is efficient to vary the coil cross section in order to achieve constant stress along the spring. This action will reduce the size and weight of the clutch.

The clutches pictured in Figure 1 are actuated through friction between the spring and shaft or drum. It is possible to actuate the clutch mechanically by means of an obstruction placed in the path of the end coil. The end coil transmits only a small portion of the total torque; therefore, the energizing force required is low.

DESCRIPTION OF TEST CLUTCHES

Two clutch designs suitable for use in aircraft applications were evaluated. They are designated "clutch design A" and "clutch design B."

Clutch Design A

Clutch design A is shown in cross section in Figure 2. An input drum (1) contains an energizing spring coil (2) through which the clutch is activated. (See Figure 3.) The eight-coil torque transmittal spring (3) drives the output shaft (4) through the torque transmittal lug (5). The output shaft is supported by a roller bearing (6) on the lug end and a

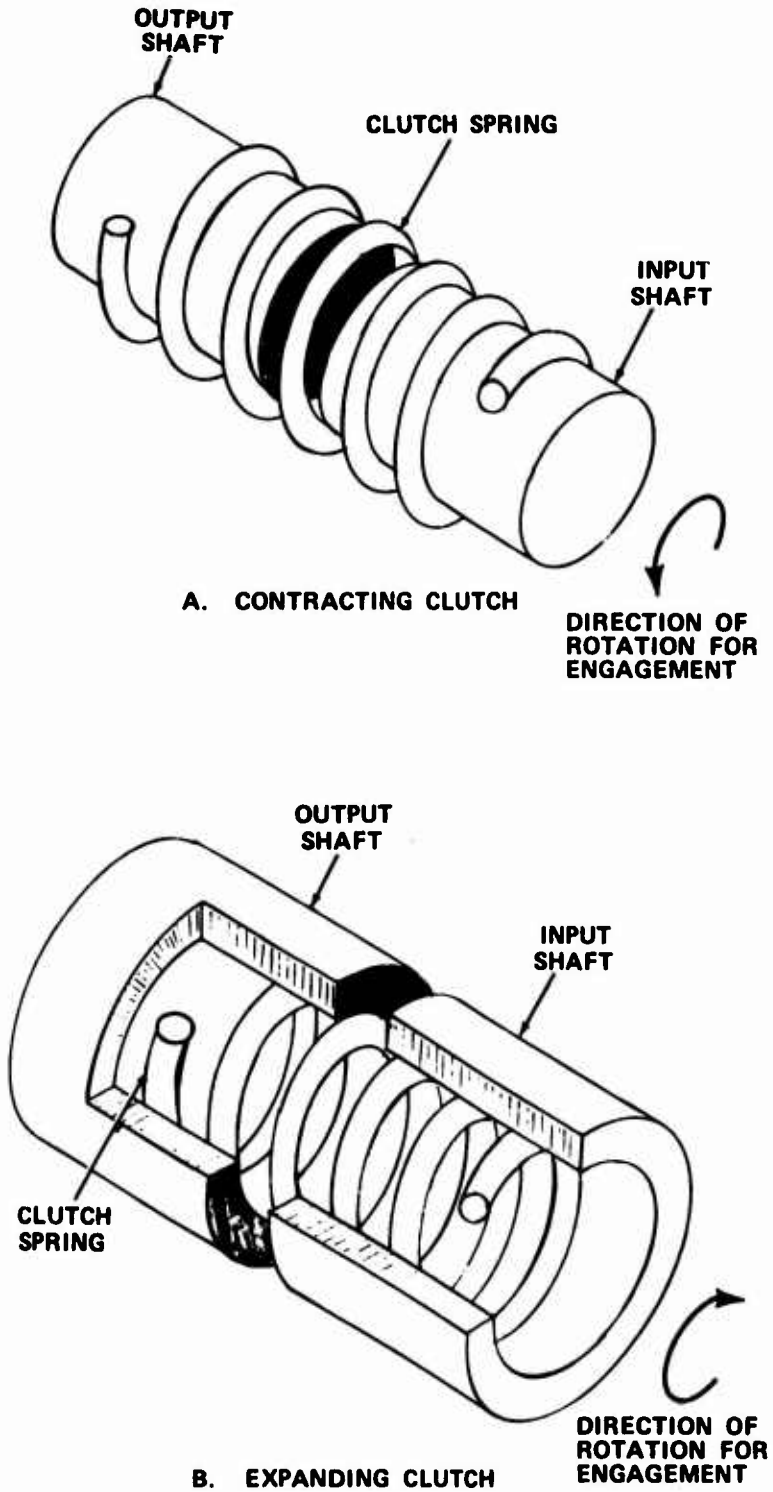

Figure 1. Principle of Spring Clutch Operation.

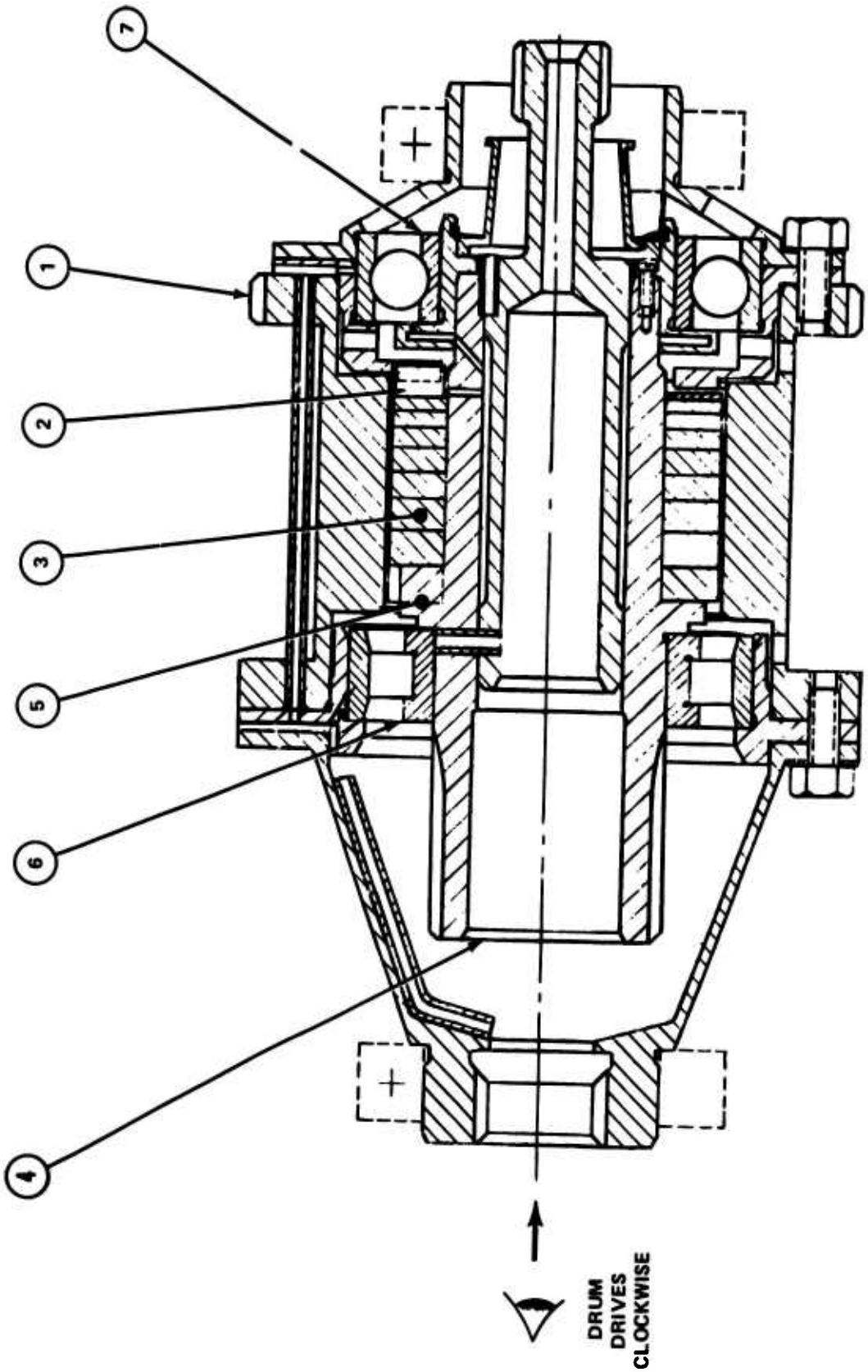

Figure 2. Clutch Design A Description.

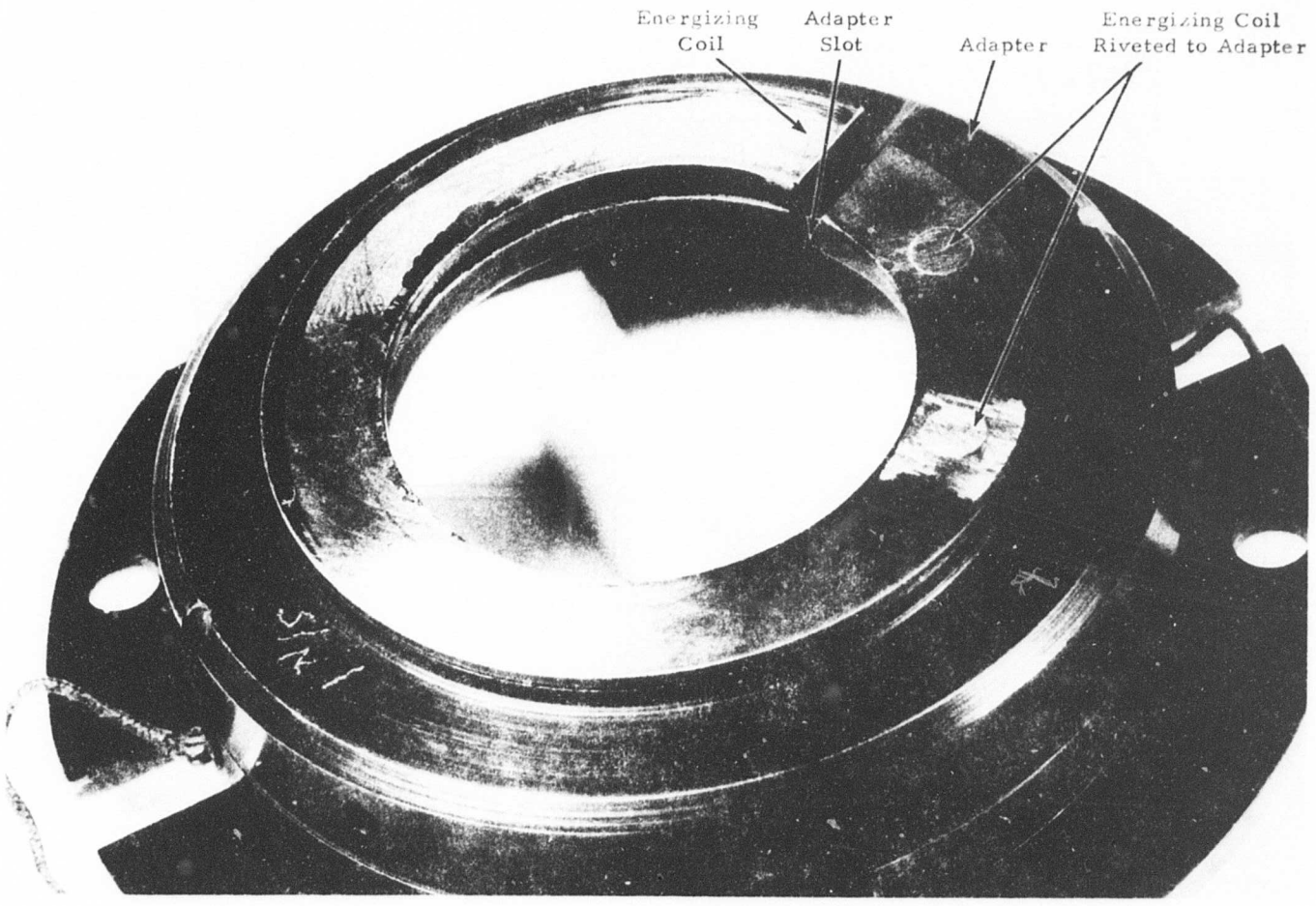

Figure 3. Energizing Coil Assembly.

ball bearing (7), which locates the assembly axially. The spring is mounted onto the output shaft with a press fit, and in the assembled condition there is clearance between the spring outside diameter and drum inside diameter.

For the driving mode of operation, the input drum (engine) drives clockwise as shown in Figure 2. The energizing coil rotates with the drum. When the input lug on the energizing coil butts up against the torque spring end, load is transmitted through the spring, thus driving the output shaft, Figure 4(A). As the torque is increased, the first active coil of the torque spring unwinds into the drum. Torque is now being transmitted through the energizing end face of the spring and through the outside diameter of the spring via friction, Figure 4(B). As more torque is transmitted, more coils unwind into the drum until at some point before the design point torque is reached, all of the coils are unwound from the shaft and wrapped into the drum, Figure 4(C). The energizing end coil carries a small amount of the torque, and each succeeding coil carries a proportionately larger share. At the torque transmittal end of the spring, all of the torque must now pass through the lug cross section. A constant-height variable lead spring was chosen for this program. The energizing end has the smallest cross section to reduce the amount of torque needed for energization. The axial thickness of the spring increases towards the torque delivery end because more torque is being transmitted through each succeeding coil. Pertinent clutch geometry is listed in Table I.

Overriding occurs when the input shaft speed goes to zero (engine is shut down) while the output shaft continues to rotate at constant speed. The spring will now wind down off of the drum since torque is no longer being transmitted by friction through the drum. At the design point overriding speed of 26,500 rpm, the spring was designed to rest lightly on the output shaft, centrifugal force on the spring overcoming the assembled press fit of the spring on the shaft, and the spring maintains clearance with the drum. The energizing end lugs of the springs will ratchet past each other, and the energizing spring coil that is attached to the drum can recede axially into a slot provided for in the adapter (Figure 3). Since the clutch is designed to operate with clearance at the spring outside diameter during overriding, the only components in direct contact will be the energizing ends that ratchet past each other. Lubrication has been provided for in this area to reduce heat generation and wear.

Lubrication for design A clutch components is provided centrifugally by holes drilled through the clutch output shaft (Figure 5). The lubrication

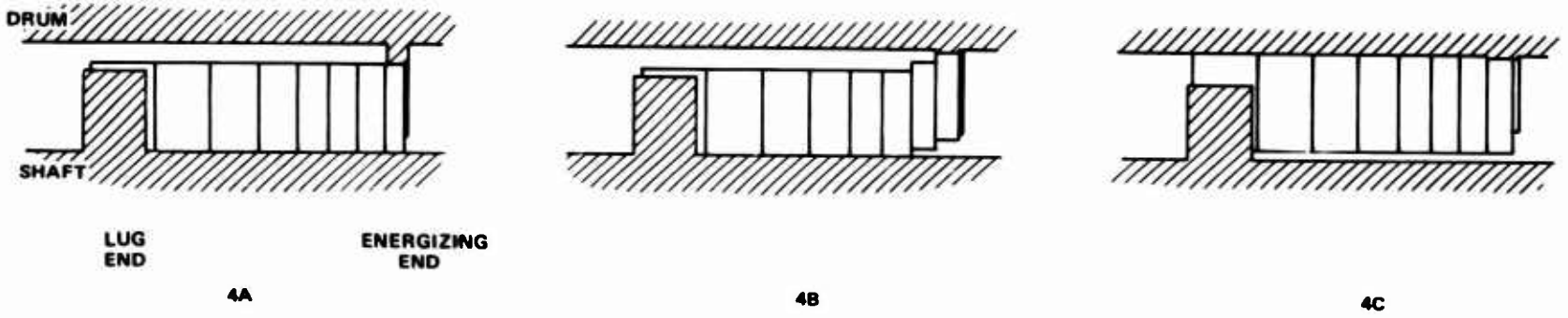

Figure 4. Design A Operation.

TABLE I. CLUTCH GEOMETRY

	Design A	Design B
Drum Dimensions		
Outside diameter (in.)	3.120	3.16*
Inside diameter (in.)	2.200	
Concentricity	0.0005	
Surface finish (AA)	20	
Shaft Dimensions		
Outside diameter (in.)	1.465	
Inside diameter (in.)	1.000	
Concentricity	0.001	
Surface finish (AA)	32	
Torque Spring Dimensions		
Outside diameter, free (in.)	2.163	
Mean diameter, free (in.)	1.803	
Inside diameter, free (in.)	1.443	
Outside diameter, assembled (in.)	2.183	1.380
Mean diameter, assembled (in.)	1.823	
Inside diameter, assembled (in.)	1.463	0.875
Radial height (in.)	0.360	
Axial length, energizing end (in.)	0.050	
Axial length, torque end (in.)	0.250	
Axial length overall, nominal (in.)	1.350	3.120
Number of coils	8	36
Hand of spring	left	
Concentricity	0.001	
Surface finish (AA)	32	
Energizing Coil Dimensions		
Outside diameter (in.)	2.189	
Inside diameter (in.)	1.473	
Axial length (in.)	0.050	
Number of coils	1	
Hand of spring	left	
Overall Clutch Length (in.)		
End of input spline to end of output spline	4.30	9.75
Clutch Weight (lb)	7.8	8.0

* Maximum outside diameter at output end. See Figure 6.

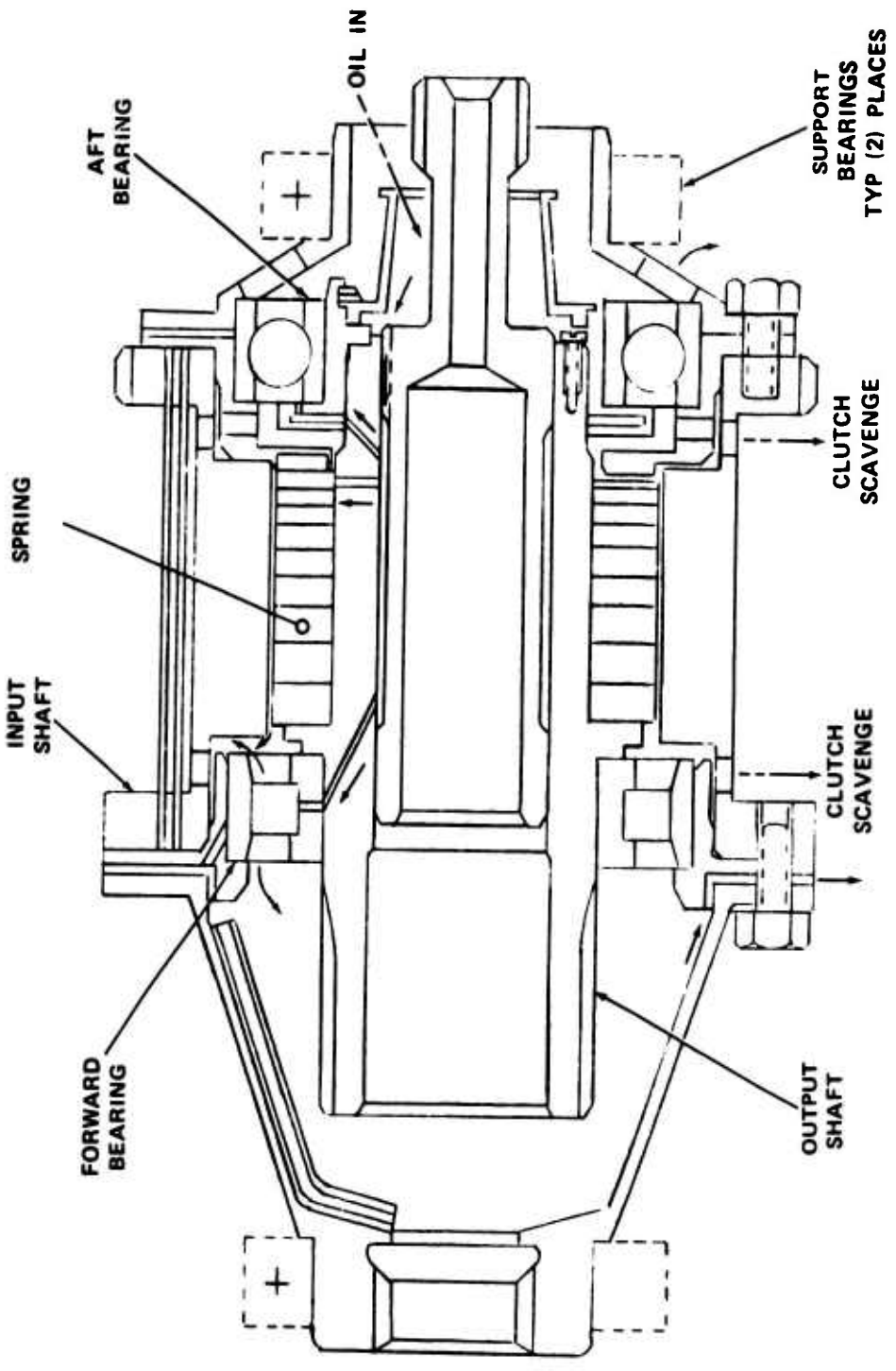

Figure 5. Lubrication and Scavenge Paths, Design A.

and scavenge paths for the clutch components are depicted with arrows. Clutch lubrication is accomplished with two 0.032- to 0.035-inch-diameter jets drilled radially through the clutch output shaft as shown in Section C-C of Figure 6. The forward bearing, not shown, is lubricated centrifugally by the oil reservoir developed in the circular groove area of Section D-D. Three 0.023- to 0.025-inch-diameter holes drilled through the roller bearing inner race provide the lubrication path through the bearing. It is noted that the bearing race is positioned over the grooved section of the clutch output shaft so that only two holes carry the oil to the roller bearing. The third hole was added to the bearing race to ensure two-hole lubrication in the event relative motion occurred between the bearing race and output shaft. The aft bearing was lubricated with two 0.032- to 0.035-inch-diameter jets drilled through the clutch output shaft at an angle of 45 degrees as shown in Section C-C.

Ample scavenge ports for the clutch assembly were provided by drilling eight 0.190-inch-diameter holes in two places through the clutch input shaft. The clutch scavenge ports were positioned between the spring clutch and the bearings. This arrangement prevents clutch particles from contaminating the bearings and eliminates oil churning in the bearings. Axial grooves, machined in the output shaft, extend to the forward bearing and away from the feed oil so as not to starve this area in case of low oil flow.

The test program was designed to evaluate oil flows from 33 to 300 percent of design flow. A design flow of 0.8 gpm (376 pph) was selected as being reasonable for this type of transmission component. Fifty-nine percent of the flow lubricates the clutch bearings, and the remainder lubricates the spring clutch assembly.

The forward roller bearing is 40-68-15 MM of ABEC 5 quality. It incorporates a one-piece bronze retainer, straight-through outer race, and flanged inner race. The aft ball bearing is a 40-68-15 MM of the Conrad configuration. The retainer is a riveted phenolic. The bearing was not preloaded.

Clutches were dynamically balanced to 0.25 inch-grams prior to operation. This procedure is standard for high-speed rotating components.

To afford the minimum size and weight configuration, hardening was required for all torque transmitting surfaces to take advantage of the higher allowable stresses. The torque capacity of a spring clutch is a function of the cross section of the wire, the ultimate strength of the wire, and the mean radius of the coil. Clutch materials are chosen on

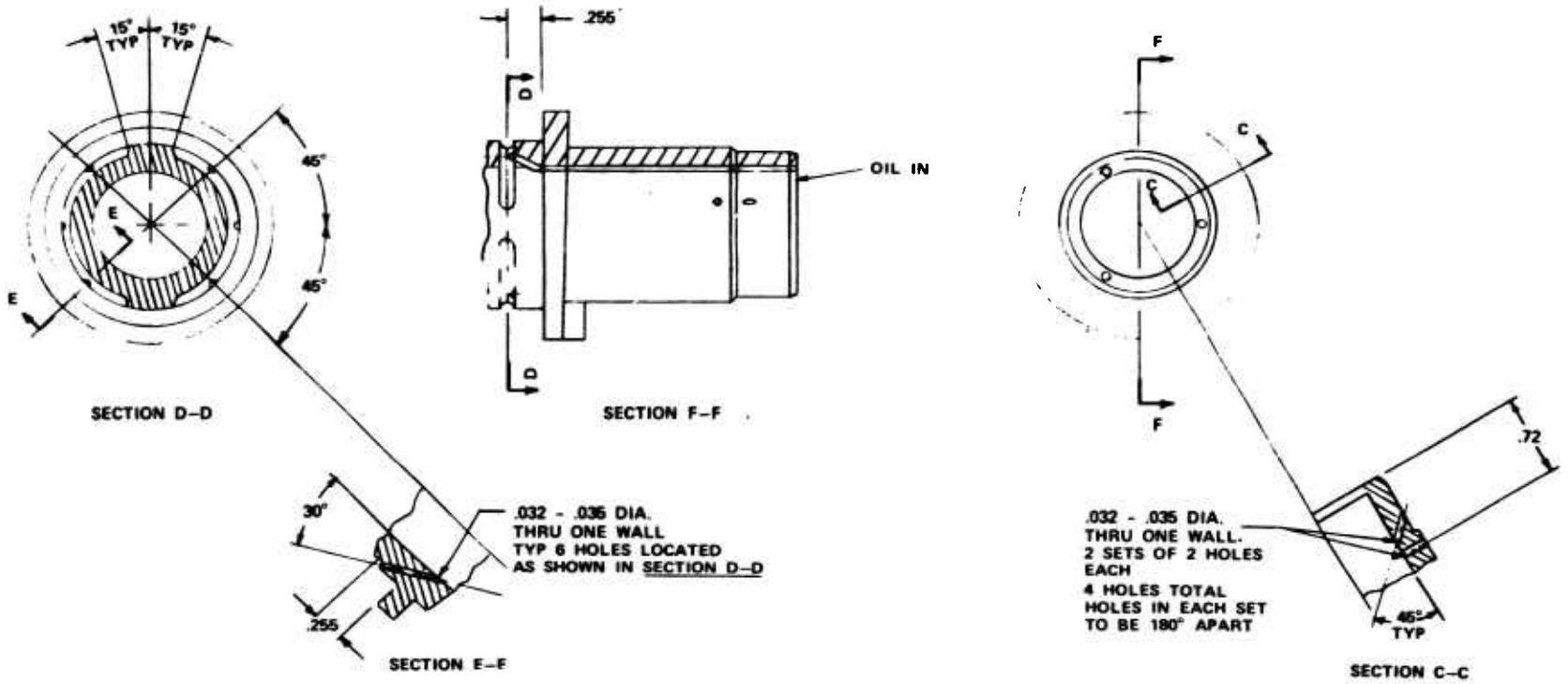

Figure 6. Output Shaft Lubrication, Design A.

the basis of hoop stress and shear stress, respectively. The materials data are listed in Table II.

Clutch design A components are shown in Figure 7.

TABLE II. TEST CLUTCH MATERIALS, DESIGN A

Shaft and Drum	
Material specification	AMS 6265
Heat treatment	Carburize
Case depth - (in.)	.050 - .065
Max. stock removal (after heat treatment) - (in.)	.010
Case hardness	R_C 60-63
Core hardness	R_C 32-40
Torque Spring and Energizing Coil	
Material specification	Vasco 350
Heat treatment	Thru hardened
Surface hardness	R_C 56-60
Oil	MIL-L-23699

Clutch Design B

Clutch design B is shown in cross section in Figure 8. The clutch is composed of an input housing (1) and an output housing (2), which are held in relative position by a preloaded duplex bearing (3). The torque element is a one-piece double-ended spring (4) with wide coils at the center and progressively narrower coils approaching each end of the spring. One end of the spring fits into a counterbore in the input housing while the other end fits into a similar counterbore in the output housing. Three coils at each end of the spring are larger in outside diameter than the remainder of the spring, and they fit their respective counterbores with a small amount of interference. The three end coils are silver plated at the outside diameter to reduce wear. The central portion of the spring does not contact the inside of the counterbores unless the clutch is transmitting torque.

A central mandrel (5) is piloted and pinned (6) in the input housing. The mandrel fits the inside diameter of the spring and holds it in the center of the housing bores to reduce overriding drag torque. Friction during overriding is thus limited to the sliding between the outside diameter of the three end coils of the spring and the inside diameter of the output housing.

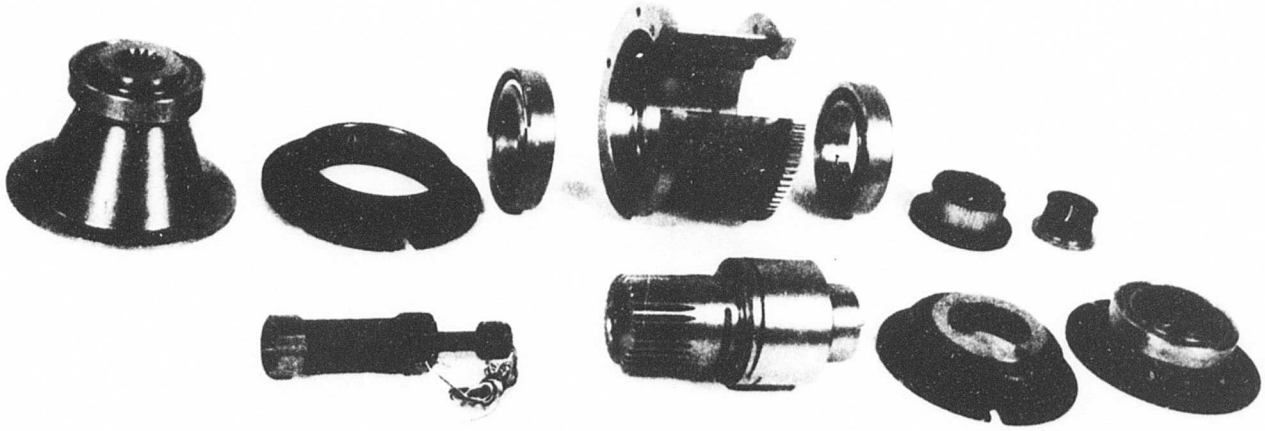

Figure 7. Clutch A Components.

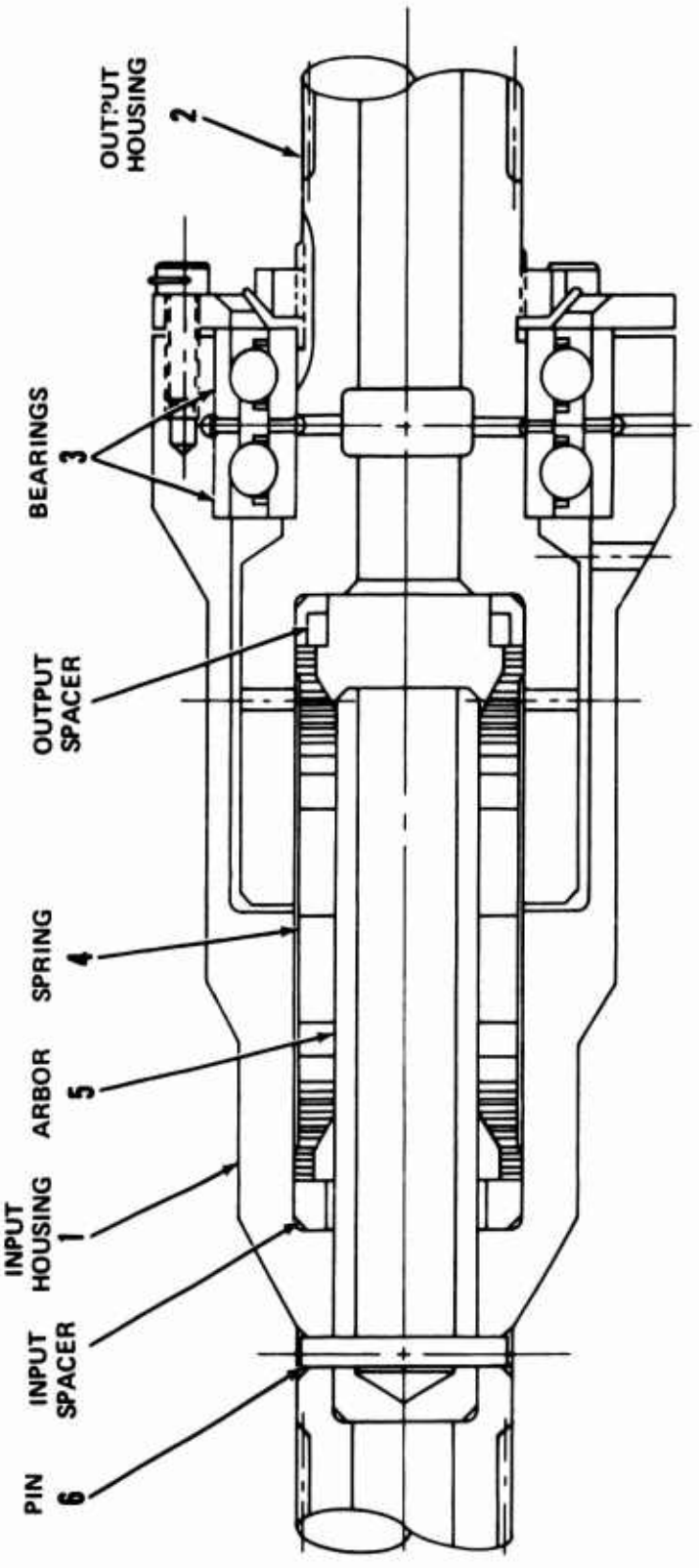

Figure 8. Clutch Design B Description.

During engagement, the torque applied to the spring through the friction on the end coils causes the spring to enlarge progressively until the entire spring fits tightly in the bores of the housings. The spring then acts as a common pilot in the counterbores of the input and output housings, thus providing the reaction to the shear load between the housings. This relieves the duplex bearing of the moment related to the shear forces caused by any driving torque above 600 inch-pounds.

Lubrication and cooling of the duplex bearing are provided by oil paths between and through the bearings. Lubrication and cooling paths at the end of the spring are provided by reliefs in the face and outside of the output washer, grooves in the end coils of the spring, and holes in the housings.

The lubrication and scavenge paths for the clutch components are shown in Figure 9.

Two 0.026- to 0.027-inch-diameter holes lubricate the back-to-back bearings, and the remainder of the flow passes through scallops and lubricates the spring clutch assembly.

Twenty-four percent of the flow lubricates the clutch bearings, and the remainder lubricates the spring clutch assembly.

Design B geometry is listed in Table I, and test clutch materials are listed in Table III. Design B clutch components are shown in Figure 10.

TABLE III. TEST CLUTCH MATERIALS, DESIGN B

Spring, Output Housing, Input Housing	
Material specification	H-11
Heat treatment	Thru hardened
Hardness	R_C 54-56
Spring end coils surface treatment	Silver plate
Arbor	
Material specification	SAE 4340
Heat treatment	Thru hardened
Hardness	R_C 32-40
Input and Output Spacers	
Material	Phosphor bronze

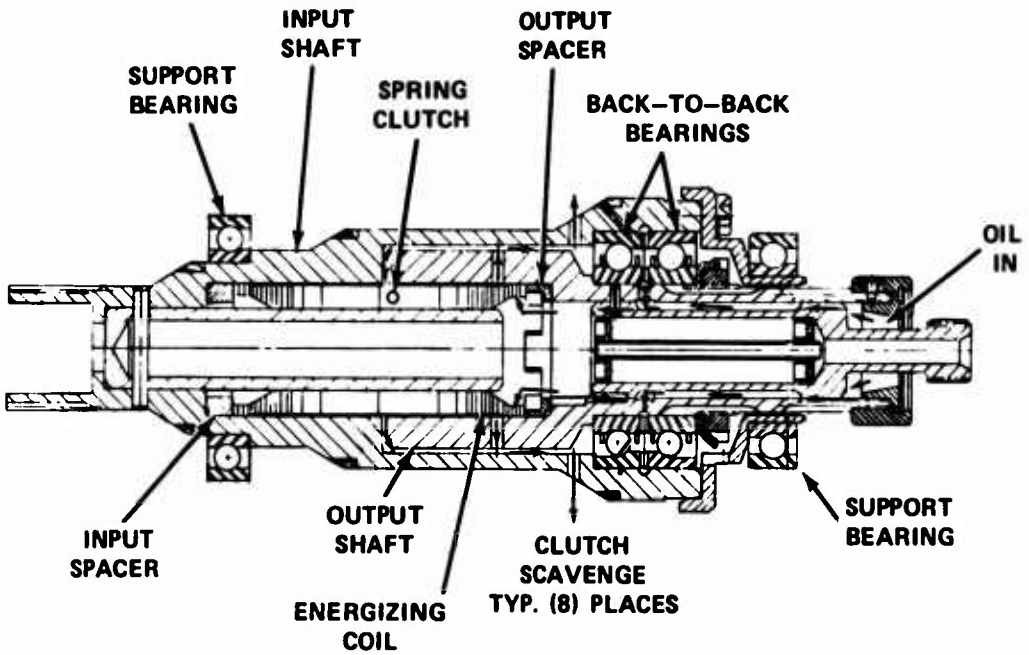

Figure 9. Lubrication and Scavenge Paths, Design B.

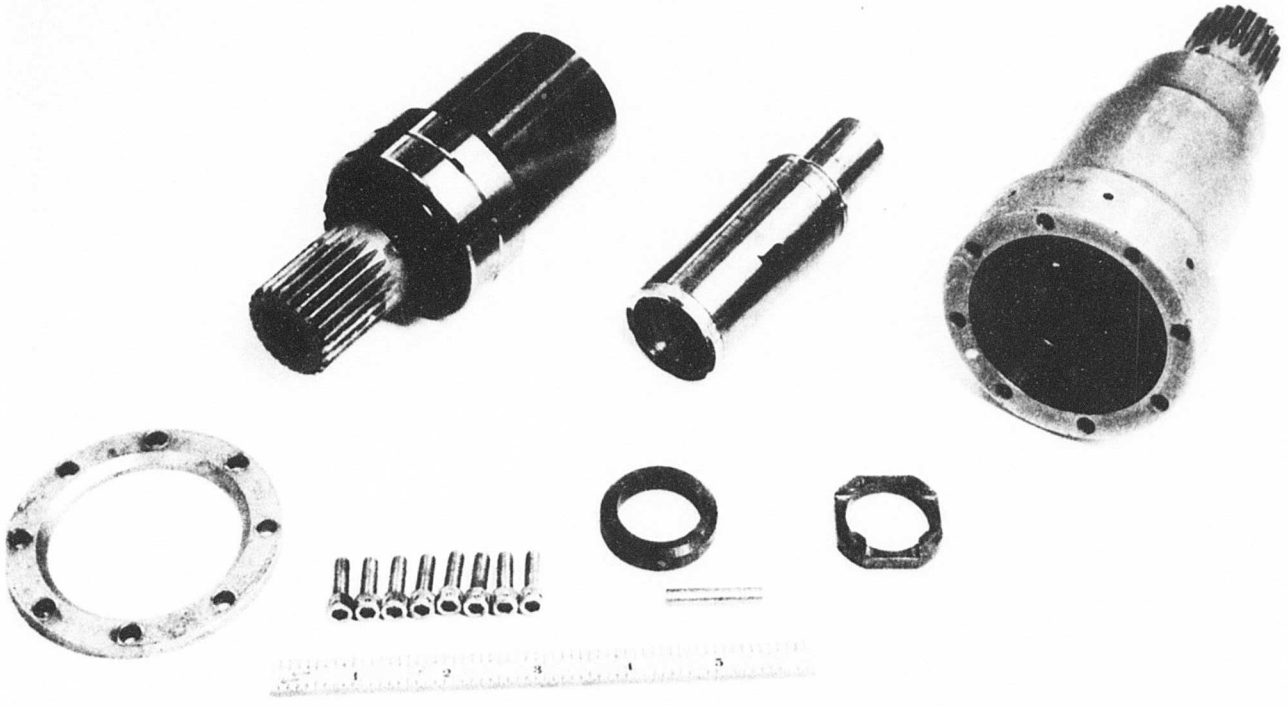

Figure 10. Clutch B Components.

CLUTCH ANALYSIS, DESIGN A

The successful design of a high-speed overriding spring clutch requires consideration not only of the load-carrying capability but also the energy losses during overriding and differential speed operation.

The critical parameters for load-carrying capability are hoop stress in the drum, shear stress in the shaft, and compressive and tensile stresses in the spring. For the override and differential speed modes of operation, the critical parameter is the drag torque developed as the energizing end faces of the springs ratchet past each other. These modes of operation assume, of course, that the outside diameter of the torque spring does not make contact with the drum. A computer program was developed, Appendix I, and trade-off studies were conducted to optimize the system design.

Following is the analytical approach of the spring system design, the results of which are listed in Table IV for the design point of 3570 inch-pounds at 26,500 rpm.

1. Calculate the growth of the free torque spring due to centrifugal force at the design point speed.

$$\Delta D = \frac{2 \times 10^{-13} (D_{MF}{}^5) (\eta^2)}{h^2} \quad *$$

where D_{MF} = mean diameter of the free spring in the free state, in.

η = design point speed, rpm

h = spring radial height, in.

$$\Delta D = \frac{2 \times 10^{-13} (1.803)^5 (26,500)^2}{(.36)^2} = .02065 \text{ in.}$$

The torque spring is designed to have a 0.020-inch interference fit with the output shaft at assembly. At overriding speed, therefore, the torque spring will unwind from the shaft to reduce the press fit to zero. For any speed above this value, the torque spring will unwind further and also grow radially outward.

* For derivation, refer to Appendix II.

TABLE IV. CLUTCH DESIGN PARAMETERS, DESIGN A

Design Point: 3, 570 in. -lb at 26, 500 rpm	
Speed Parameters	
Diametral spring growth, in.	.021
Spring actuation angle, deg	32.61
Spring energizing moment, in. -lb	193.1
Drum Clearance Parameters	
Diametral clearance, drum to spring, in.	.017
Spring actuation angle, deg	26.60
Spring energizing moment, in. -lb	155.7
Stresses	
Total energizing moment, in. -lb	348.8
Total stress at energizing end lug due to energizing moment, psi	
Inner surface	86, 611
Outer surface	-128, 727
Total stress at output end lug at design point torque, psi	
Inner surface	64, 569
Outer surface	-150, 769
Torque through outer surface of output end coil, in. -lb	1, 665
Drum hoop stress, psi	38, 450
Shaft shear stress, psi	7, 386
Overriding Parameter	
Drag torque at energizing end, in. -lb	0.22

For assembly, assume a diametral clearance (ΔCL) of 0.017 inch between the torque spring outside diameter and drum inside diameter.

2. Calculate spring actuation angle and energizing moment required to reduce the initial press fit to zero.

$$\theta_D = N\left[\frac{2\pi\Delta D}{D_{MF}+\Delta D}\right] \quad \text{(See App II)}$$

where θ_D = actuation angle to reduce press fit to zero, deg

N = number of coils in torque spring

$$\theta_D = 8\left[\frac{2\pi\,(.02065)}{1.803+.02065}\right] = .56938 \text{ rad}$$

$$\theta_D = 32.61 \text{ deg}$$

$$M_D = \frac{Eb_M h^3}{6.6\, D_{MF} N} \cdot \frac{\theta_D}{360} \quad \text{(See App II)}$$

where M_D = energizing moment to reduce press fit to zero, in.-lb

b_M = mean coil width, in.

h = spring radial height, in.

E = modulus of elasticity of spring, psi

$$M_D = \frac{29\times10^6\ (.150)\ (.36)^3}{6.6(1.803)\ (8)} \cdot \frac{32.61}{360}$$

$$M_D = 193.1 \text{ in.-lb}$$

3. Calculate spring actuation angle and energizing moment required to reduce the drum clearance to zero.

$$\theta_{CL} = N\left[\frac{2\pi\Delta CL}{D_{ME}+\Delta CL}\right]$$

where θ_{CL} = actuation angle to reduce drum clearance to zero, deg

Δ_{CL} = initial drum clearance, in.

D_{ME} = mean diameter of the spring as assembled onto the output shaft, in.

$$\theta_{CL} = 8\left[\frac{2\pi(.017)}{1.823+.017}\right] = .46424 \text{ rad}$$

$$\theta_{CL} = 26.60 \text{ deg}$$

$$M_{CL} = \frac{Eb_M h^3}{6.6 D_{ME} N} \cdot \frac{\theta_{CL}}{360}$$

$$M_{CL} = \frac{29x10^6 (.150) (.36)^3}{6.6 (1.823) (8)} \cdot \frac{26.60}{360}$$

$$M_{CL} = 155.7 \text{ in.-lb}$$

If the system is started from rest, it will require $M_D + M_{CL} = 348.8$ inch-pounds of torque to unwrap the spring off of the shaft and into the drum. In a twin-engine installation with one engine already operating, only $M_{CL} = 155.7$ inch-pounds of torque will be required for energizing because the output shaft is already overriding at speed when the second engine is being started up; the speed of the output shaft provides the centrifugal force necessary to reduce the press fit to zero; hence, M_D need no longer be supplied by the second engine.

These calculations have assumed a mean coil axial thickness (b_m) for the energizing moment equations, and as such they are somewhat conservative.

If the energizing end coil width is used, the energizing moments would be one-third of the values just calculated.

4. Calculate the maximum stresses in the spring. See Figure 11 for derivations.

   a. Energizing lug end

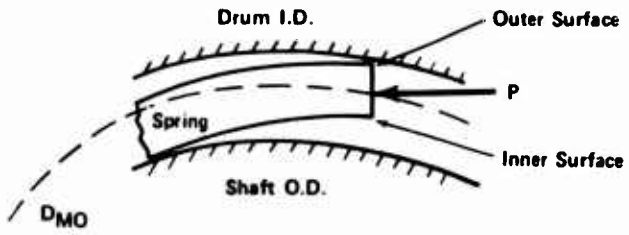

Spring stess due to load P consists of bending plus compressive stresses.

$$S_b = \frac{M_t}{Z}, \quad Z = \frac{bh^2}{6}$$

where S_b = bending stress

M_t = bending moment required to unwrap spring off of shaft and into drum, in.-lb

$$S_b = \frac{6M_t}{bh^2}$$

$$S_c = \frac{P}{A} = \frac{2T}{D_{MO}} = \frac{1}{bh}$$

where S_C = compressive stress

P = applied force, lb

Outer Surface

S_{t_o} = bending stress - compressive stress

$$S_{t_o} = -\frac{6M_t}{bh^2} - \frac{2T}{D_{MO}bh}$$

S_{t_o} = total stress, outer surface, psi

Inner Surface

$$S_{t_i} = +\frac{6M_t}{bh^2} - \frac{2T}{D_{MO}bh}$$

where S_{t_i} = total stress, inner surface, psi

Note: + = Tension
– = Compression

Figure 11. Bending and Compressive Stress Derivations.

$$S_b = \frac{6M_t}{b\,h^2}$$

where S_b = bending stress, psi

M_t = $M_D + M_{CL}$, in.-lb

b = b_1 = width of energizing end coil, in.

$$S_b = \frac{6(348.8)}{(.050)(.36)^2} = 107,669 \text{ psi}$$

$$S_c = \frac{2T}{D_{MO}\,bh}$$

where S_c = compressive stress, psi

T = $M_D + M_{CL}$, in.-lb

D_{MO} = mean diameter of the spring when unwrapped into the drum = $d_{d_i} - h$, in.

d_{d_i} = drum inside diameter, in.

$$S_c = \frac{2(348.8)}{(2.201 - .36)\,(.05)\,(.36)} = 21,058 \text{ psi}$$

$$S_{t_i} = 107,669 - 21,058 = 86,611 \text{ psi}$$

$$S_{t_o} = -107,669 - 21,058 - -128,727 \text{ psi}$$

where S_{t_i} = total stress at the inner surface of the spring, psi

S_{t_o} = total stress at the outer surface of the spring, psi

b. Torque transmittal lug end

$$S_b = 107,669 \text{ psi}$$

Once the spring has been unwrapped into the drum, any further increase in load being transmitted will not affect the bending stress.

$$S_c = \frac{2T_T}{D_{MO}\, b\, h}$$

where T_T = design point torque, in.-lb

$b = b_N$ = width of the lug end coil, in.

$$S_c = \frac{2(3,570)}{(2.201 - .36)\ (.250)\,(.36)} = 43,100 \text{ psi}$$

$$S_{t_i} = 107,669 - 43,100 = 64,569 \text{ psi}$$

$$S_{t_o} = -107,669 - 43,100 = -150,769 \text{ psi}$$

The maximum tensile stress in the spring occurs at the inner surface of the energizing end, while the maximum compressive stress occurs at the outer surface of the torque transmittal end.

5. Check spring life for cyclic fatigue test.

In the cyclic fatigue test, the spring will operate at 7,140 $\pm$ 900 inch-pounds of torque for ten million cycles. From the computer program output, Appendix I, the maximum stress variation will occur at either the energizing or output lug end. The total stress at the inner and outer surfaces is tabulated below for both ends.

	Total Stress			
	Energizing Lug End		Output Lug End	
Torque (in.-lb)	Inner Surface (psi)	Outer Surface (psi)	Inner Surface (psi)	Outer Surface (psi)
6,240	105,200	-110,100	32,300	-183,000
7,140	104,800	-110,500	21,500	-193,900
8,040	104,500	-110,900	10,600	-204,700

Calculation of average and fluctuating components is now necessary for plotting a Goodman diagram.

$$S_{AV} = \frac{S_{t_{max}} + S_{t_{min}}}{2}$$

where S_{AV} = average stress component, psi

$S_{t_{max}}$ = maximum total stress component, psi

$S_{t_{min}}$ = minimum total stress component, psi

$$S_r = \frac{S_{t_{max}} - S_{t_{min}}}{2}$$

where S_r = fluctuating stress component, psi

Tabulation of these calculated stress values is shown below:

	Energizing End		Output End	
	Inner Surface	Outer Surface	Inner Surface	Outer Surface
S_{AV} (psi)	104, 850	-110, 500	21, 450	-193, 850
S_r (psi)	300	400	10, 850	10, 850
Point Designation for Plot (Fig. 12)	A	B	C	D

The fatigue endurance limit (S_e = 120, 000 psi)* for one-hundred million cycles and the ultimate strengths (S_u - 365, 000 psi)* are shown in Figure 12 as ordinate and abscissa, respectively. The plotted points A through D fall within the triangle, showing that the spring design is adequate for the cyclic fatigue test.

* Vascomax 350 material manufactured by Vasco, Latrobe, Pennsylvania.

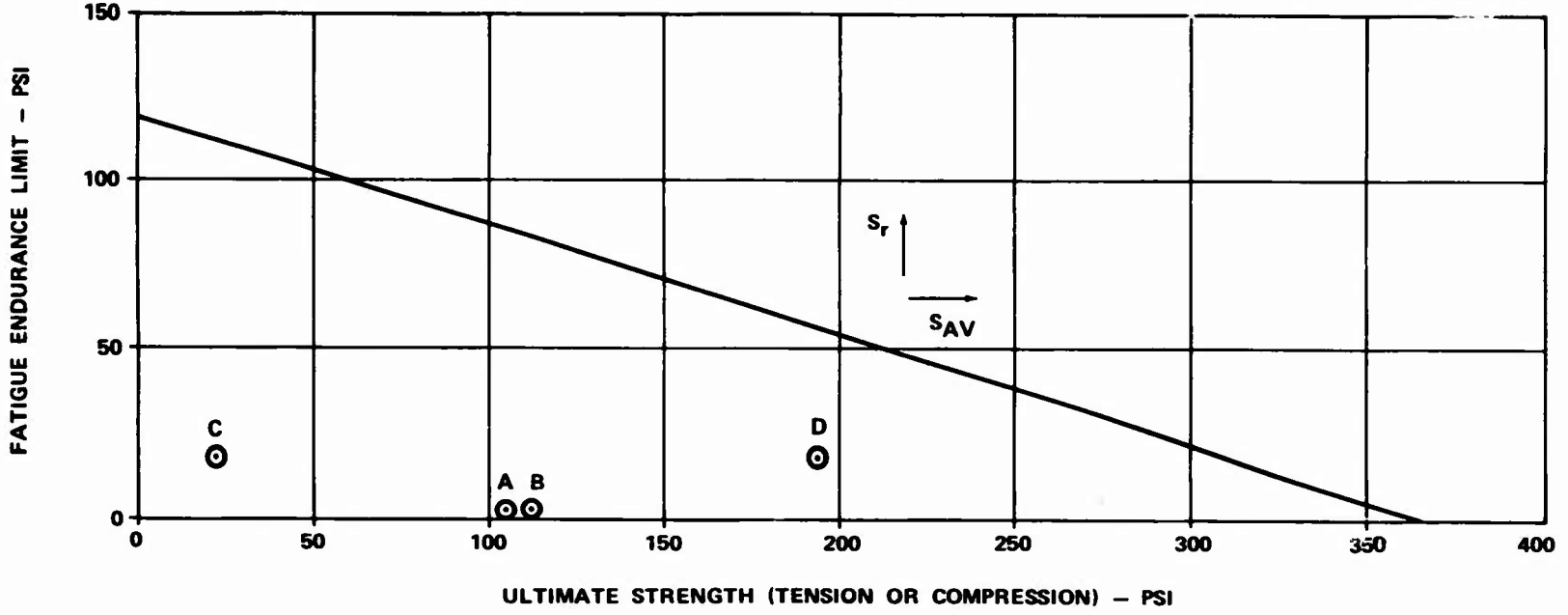

Figure 12. Goodman Diagram for Cyclic Fatigue Test, Design A.

6. Calculate the maximum hoop stress that occurs at the inner surface of the drum. The following equation includes the centrifugal effect of the spring and the rotational stress of the drum.

$$S_{t_R} = P_o \left[\frac{d_{d_o}^2 + d_{d_i}^2}{d_{d_o}^2 - d_{d_i}^2} \right] + \left(\frac{3+\nu}{32} \right) \left(\frac{\delta}{g} \right) \left(\frac{\pi \eta}{30} \right)^2 \left[2d_{d_o}^2 + d_{d_i}^2 - \left(\frac{1+3\nu}{3+\nu} \right) d_{d_i}^2 \right] *$$

where S_{t_R} = maximum hoop stress at drum inside diameter, psi

d_{d_o} = drum outside diameter, in.

d_{d_i} = drum inside diameter, in.

ν = Poisson's ratio = 0.25

δ = weight density constant - .282 lb/in.^{3}

g = acceleration due to gravity - 386.4 in./sec^2

η = design point speed, rpm

P_o = internal pressure at drum inside diameter due to transmitted load plus centrifugal force of the spring, psi

$$P_o = \frac{F_{N_T} + F_{CG}}{A}$$

* Shigley, J. E., MACHINE DESIGN, New York, McGraw-Hill, 1956, p. 446 Equation (14-7), p. 475 Equation (14-21).

$$F_{N_T} = \frac{\frac{2T_{SN}}{d_{d_i}}}{\mu}$$

$$F_{CG} = m \cdot \frac{D_{MO}}{2} \cdot \omega^2 = \left(\frac{2\pi n\, b_N\, \delta}{g}\right)\left(\frac{d_{d_i} - n}{2}\right)\left(\frac{2\pi\eta}{60}\right)^2$$

$$A = \pi\, d_{d_i} \cdot b_N$$

where F_{N_T} = normal force due to the transmitted load, lb

μ = coefficient of static friction at contact surface between drum and spring

F_{CG} = centrifugal force due to the last coil, lb

m = mass of the last coil, lb-mass

ω = angular velocity at the design point speed, rad/sec

A = contact area of the last coil, $in.^2$

T_{SN} = torque transmitted through the outer surface of the last coil, in.-lb

$$T_{SN} = \left[\frac{G_N - G_{N-1}}{G_N}\right](T_T)$$

where $G_N = e^{2\pi\mu N}$ = gain or amplication factor of the spring

T_T = design point torque, in.-lb

e = 2.72 base natural logarithm

$$T_{SN} = \left[\frac{e^{2\pi(.1)(8)} - e^{2\pi(.1)(7)}}{e^{2\pi(.1)(8)}}\right](3570)$$

$$= \left[\frac{152.4 - 81.3}{152.4}\right](3570)$$

$$T_{SN} = 1,665 \text{ in.-lb}$$

$$F_{N_T} = \frac{\frac{2(1665)}{2.200}}{.1} = 15,136 \text{ lb}$$

$$F_{CG} = \left[\frac{2\pi(.36)(.250)(.282)}{386.4}\right] \left[\frac{(2.200)(.36)}{2}\right] \left[\frac{2\pi(26,500)}{60}\right]^2$$

$$F_{CG} = 2,924 \text{ lb}$$

$$A = \pi(2.200)(.250) = 1.7279 \text{ in.}^2$$

$$P_o = \frac{18,060}{1.7279} = 10,450 \text{ psi}$$

$$S_{tR} = 10,450\left(\frac{3.120^2 + 2.200^2}{3.120^2 - 2.200^2}\right) + \left(\frac{3 + 2.5}{32}\right)\left(\frac{.282}{386.4}\right)\left(\frac{\pi\, 26,500}{30}\right)^2$$

$$+ \left[2(3.120)^2 + (2.200)^2 - \left(\frac{1 + .75}{3.25}\right)(2.200)^2\right]$$

$$= 10,450\,(2.980) + 571(21.703) = 31,141 + 12,392$$

$$S_{tR} = 43,533 \text{ psi}$$

7. Calculate the maximum shear stress in the output shaft.

$$S_s = \frac{16T_T d_{s_o}}{\left(d_{s_o}^4 - d_{s_i}^4\right)}$$

where S_s = shear stress in the output shaft, psi

d_{s_o} = shaft outside diameter, in.

d_{s_i} = shaft inside diameter, in.

$$S_s = \frac{16(3570)(1.464)}{\pi(1.464^4 - 1.000^4)} = 7410 \text{ psi}$$

8. Calculate the drag torque at the energizing end coils.

$$T_D = P_T\left(\frac{D_{MO}}{2}\right)$$

where T_D = drag torque during overrunning, in.-lb

P_T = tangential force between ratcheting end faces of springs, lb

$P_T = \mu_{SL} P_N$

μ_{SL} = coefficient of sliding friction between end faces of springs

P_N = maximum normal force between ratcheting end faces of springs, lb

$$\frac{P_N}{\Delta X} = \frac{h^2 b^2 G}{D_{MO}^3 N\delta} *$$

where $\frac{P_N}{\Delta X}$ = spring rate constant, lb/in.

ΔX = axial displacement, in.

---

* Wahl, A.M., MECHANICAL SPRINGS, Second Edition, New York, McGraw-Hill, 1963, p. 129, Figure 10-6.

G = modulus of rigidity = 10.2×10^6 psi

N = number of coils

δ = spring factor *

$$\frac{P_N}{\Delta X} = \frac{(.36)^2 (.050)^2 (10.2 \times 10^6)}{(2.201-.36)^3 (1) (17.8)} = 29.76 \text{ lb/in.}$$

ΔX = axial travel of energizing coil = .10 in.

P_N = 2.98 lb

μ_{SL} = .08

P_T = .238

$$T_D = (.238) \left(\frac{2.201-.36}{2}\right) = .22 \text{ in.-lb}$$

This value of drag torque is to be considered only as a rough approximation. The calculation was made to show that the drag torque for this type of clutch is rather small. The actual measured spring rate of the design A clutch energizing coil was found to be 18.5 pounds per inch.

CLUTCH ANALYSIS, DESIGN B

A complete analysis of clutch B design parameters was not conducted. Table V lists critical stress values as supplied by the vendor.

DYNAMIC VALIDATION OF ANALYTICAL PROCEDURE TO DETERMINE SPRING GROWTH DUE TO CENTRIFUGAL FORCE

The equation used to determine the growth of the free torque spring due to centrifugal growth for clutch design A, namely,

$$\Delta D = \frac{2 \times 10^{-13} (D_{MF}^5) (\eta^2)}{h^2}$$

* Wahl, A.M., MECHANICAL SPRINGS, Second Edition, New York, McGraw-Hill, 1963, p. 129, Figure 10-6.

TABLE V. CLUTCH DESIGN PARAMETERS, DESIGN B	
Design Point: 3570 in.-lb at 26, 500 rpm	
Spring Stress	
Maximum tensile stress to open spring	67, 500 psi
Maximum compressive stress at:	
Maximum operating torque of 3, 570 in.-lb	131, 000 psi
Limit torque of 8, 000 in.-lb	210, 000 psi
Output Housing	
Maximum hoop stress at:	
Maximum operating torque of 3, 570 in.-lb	75, 200 psi
Limit torque of 8, 000 in.-lb	169, 000 psi

is only an approximation for a spring of variable cross section. It was necessary to determine the actual growth versus speed prior to any override or differential speed tests. Initial testing was conducted with a diametral clearance of 0.014 inch, and the spring contacted the drum at an override speed of 22, 500 rpm. The analytical procedure had predicted a growth of 0.020 inch at the design speed of 26, 500, which would just have dissipated the press fit of 0.020 inch between the spring and shaft. Additional tests were run with increased diametral clearance, and the results are plotted in Figure 13. The final test was run with a diametral clearance of 0.087 inch, and the spring did not make contact at an override speed of 26, 000 rpm. The theoretical curve is also shown in Figure 13 for comparison. The actual curve tends to flatten out so rapidly in the 20, 000- to 25, 000-rpm speed range that the initial drum clearance required becomes excessive; i.e., energizing moment and tensile stresses at the energizing end coil exceed the yield point of the material. This condition occurred during the test program, the details of which are discussed under "Test Results and Discussion."

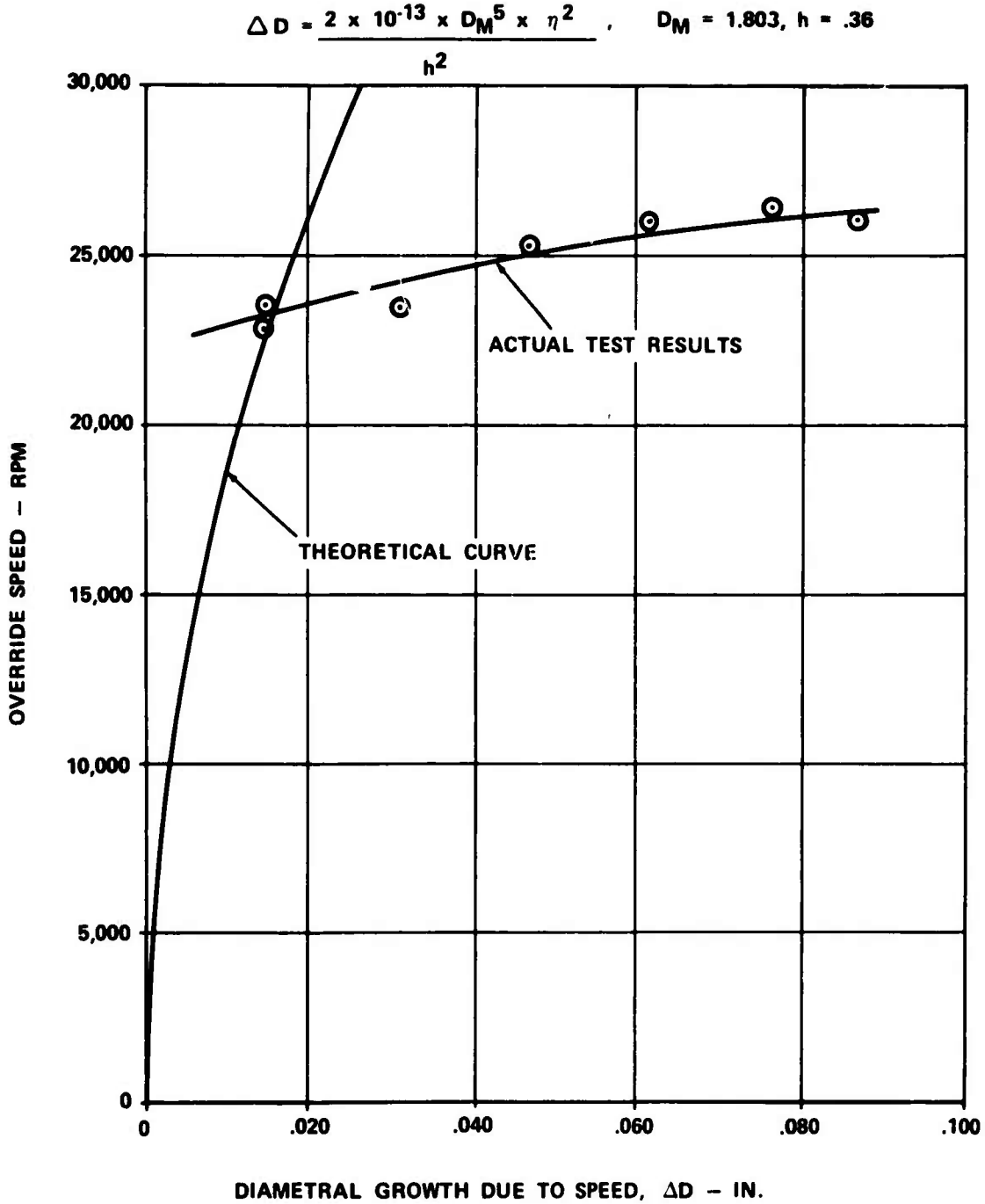

Figure 13. Override Speed Versus Diametral Growth, Design A.

TEST FACILITY

DYNAMIC TESTS

Test Rig

The dynamic tests were conducted on an existing rig especially fabricated for high-speed overriding clutch development. The test vehicle, Figure 14, consists of two independently controlled 8-inch Barbour Stockwell 100-horsepower, 30,000-rpm steam turbine prime movers driving through 3:1 speed increasers. One turbine drives the clutch input shaft, and the second turbine drives the clutch output shaft. A pad is provided on each speed increaser to accommodate slip ring assemblies that transmit data from the rotating shafts. A photograph of the test setup is presented in Figure 15.

The test cartridges for designs A and B are presented in Figures 16 and 17, respectively. The cartridges containing the test clutches have been designed to be installed between the supporting frames without moving either frame. This procedure ensures good alignment for each test increment and rapid turnaround between tests.

MIL-L-23699 lubricant (Hatco 3211) as specified was employed in all tests.

A schematic representation of the lubrication system is presented in Figures 18 and 19 for designs A and B, respectively. Two independent pressure pumps were employed in the tests, one to feed the test clutch and the other for the rig support bearings. A constant flow of 0.17 gpm was supplied to the rig support bearings. High-quality ABEC 7 ball bearings with bronze retainers were utilized.

Instrumentation

A typical console and instrument panel for external control of rig operating environments are shown in Figure 20. Clutch rig instrumentation monitored from the panel included:

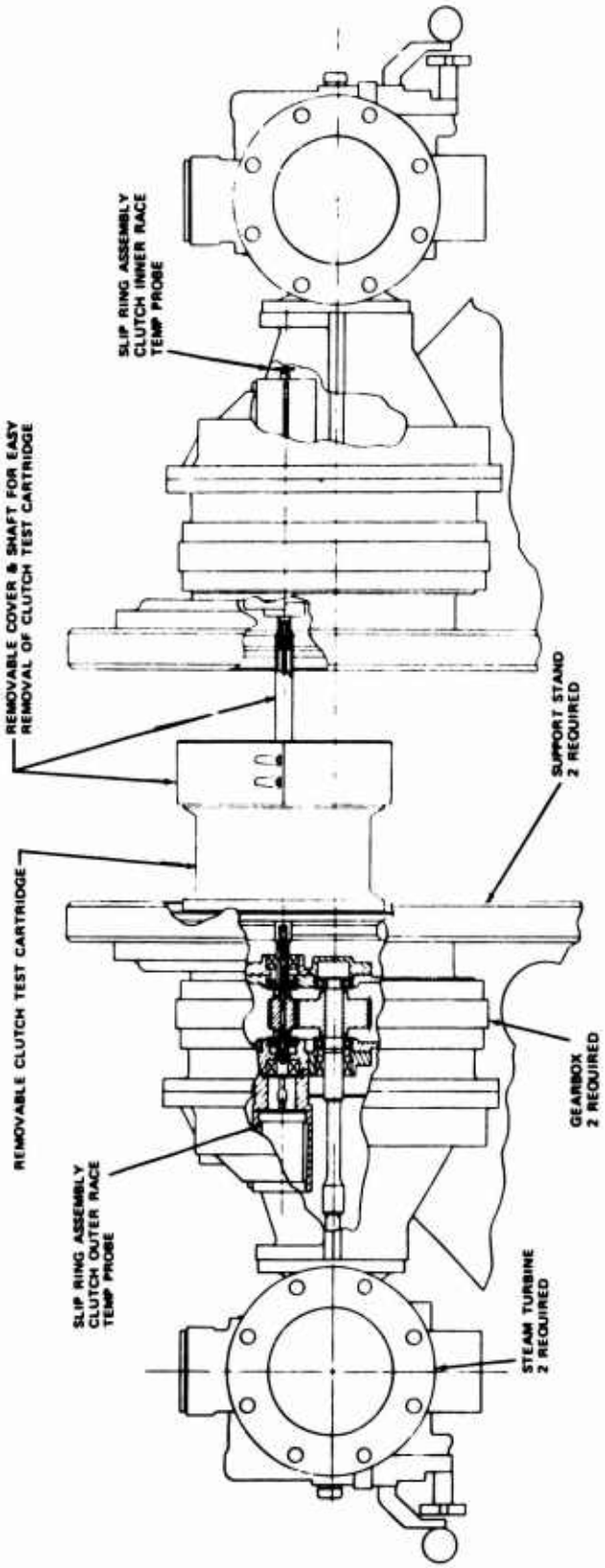

Figure 14. Overall Rig Arrangement.

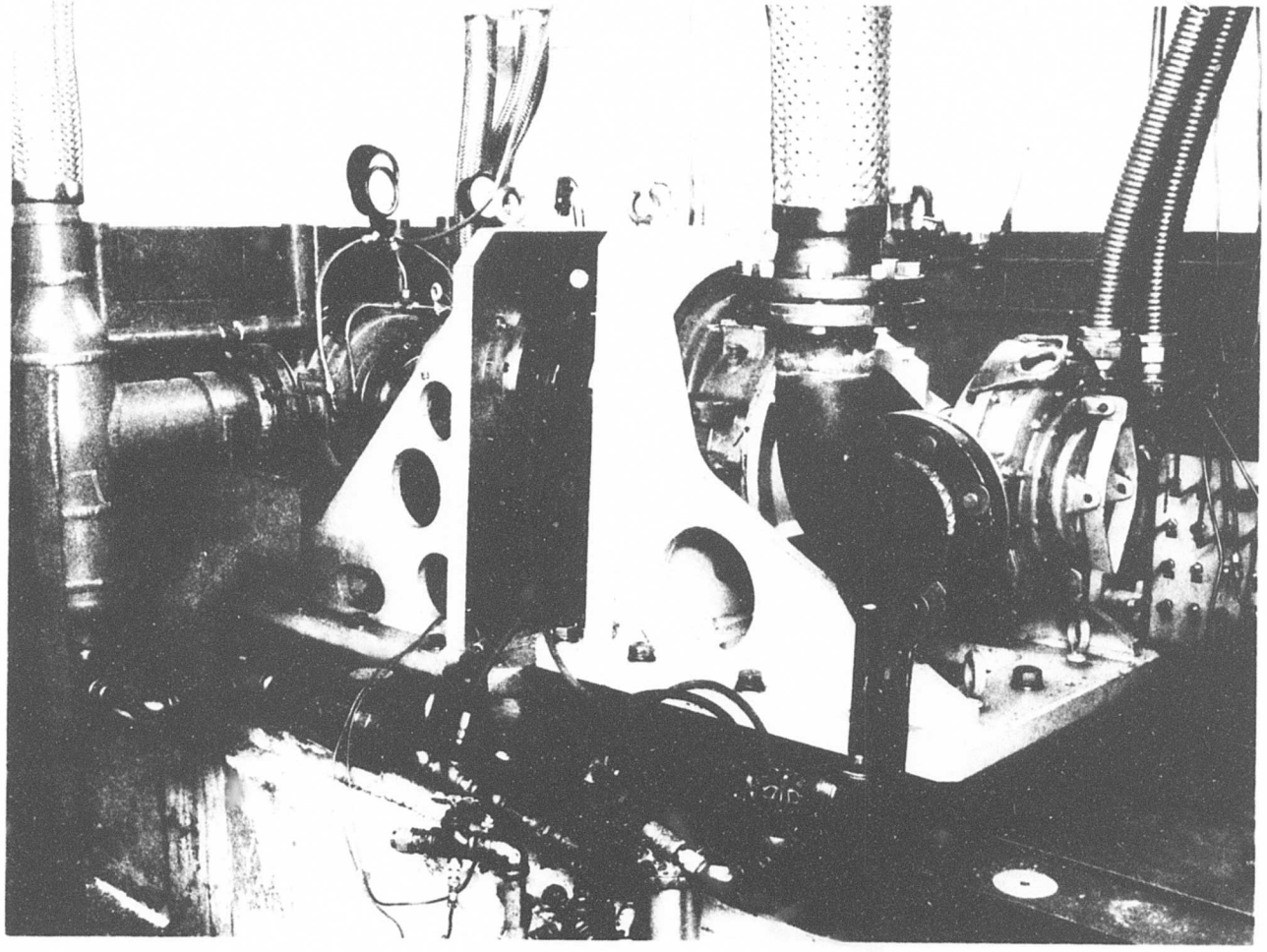

Figure 15. Test Rig Installation.

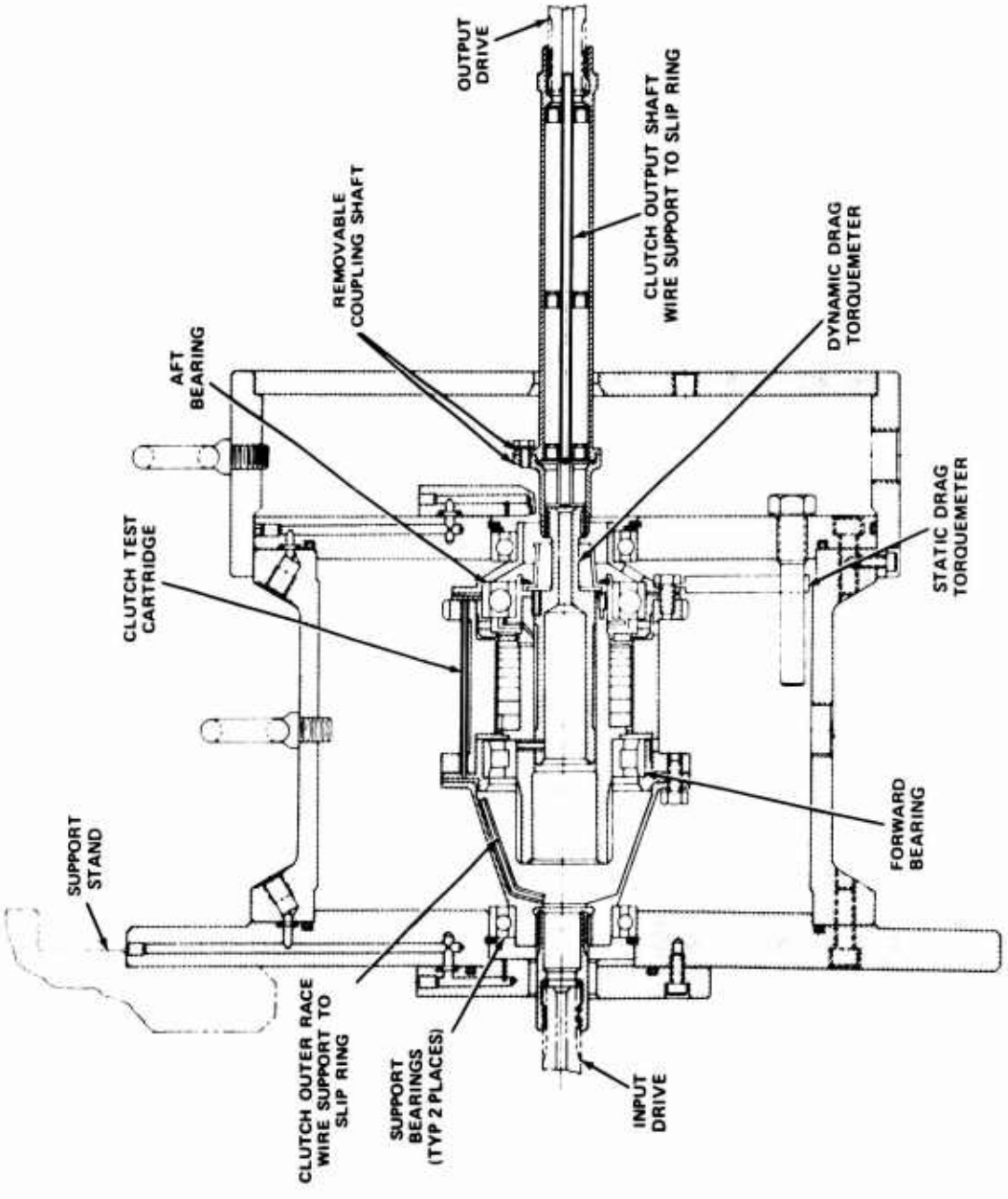

Figure 16. Design A, Test Cartridge Details.

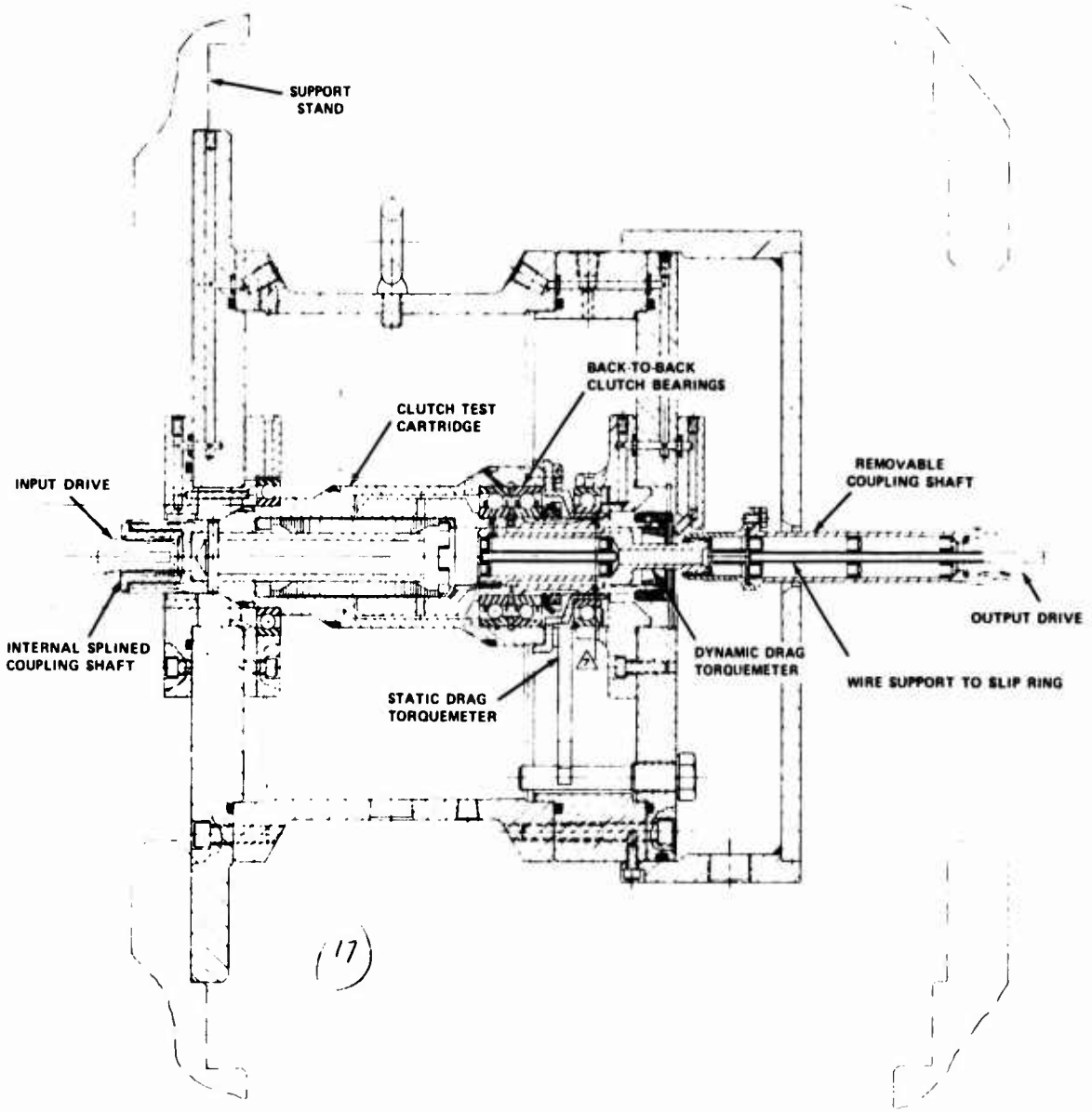

Figure 17. Design B, Test Cartridge Details.

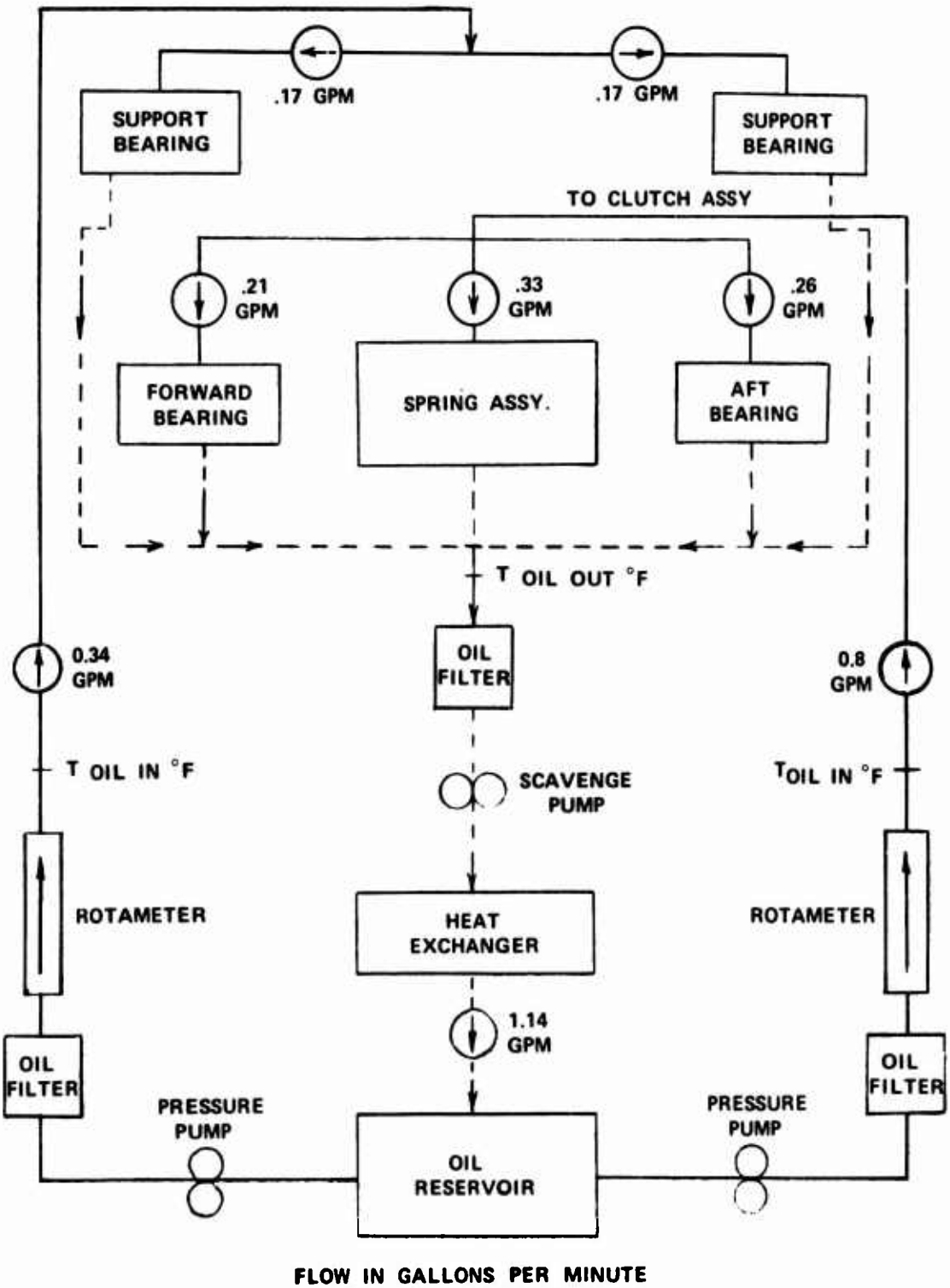

Figure 18. Design A, Lubrication Schematic.

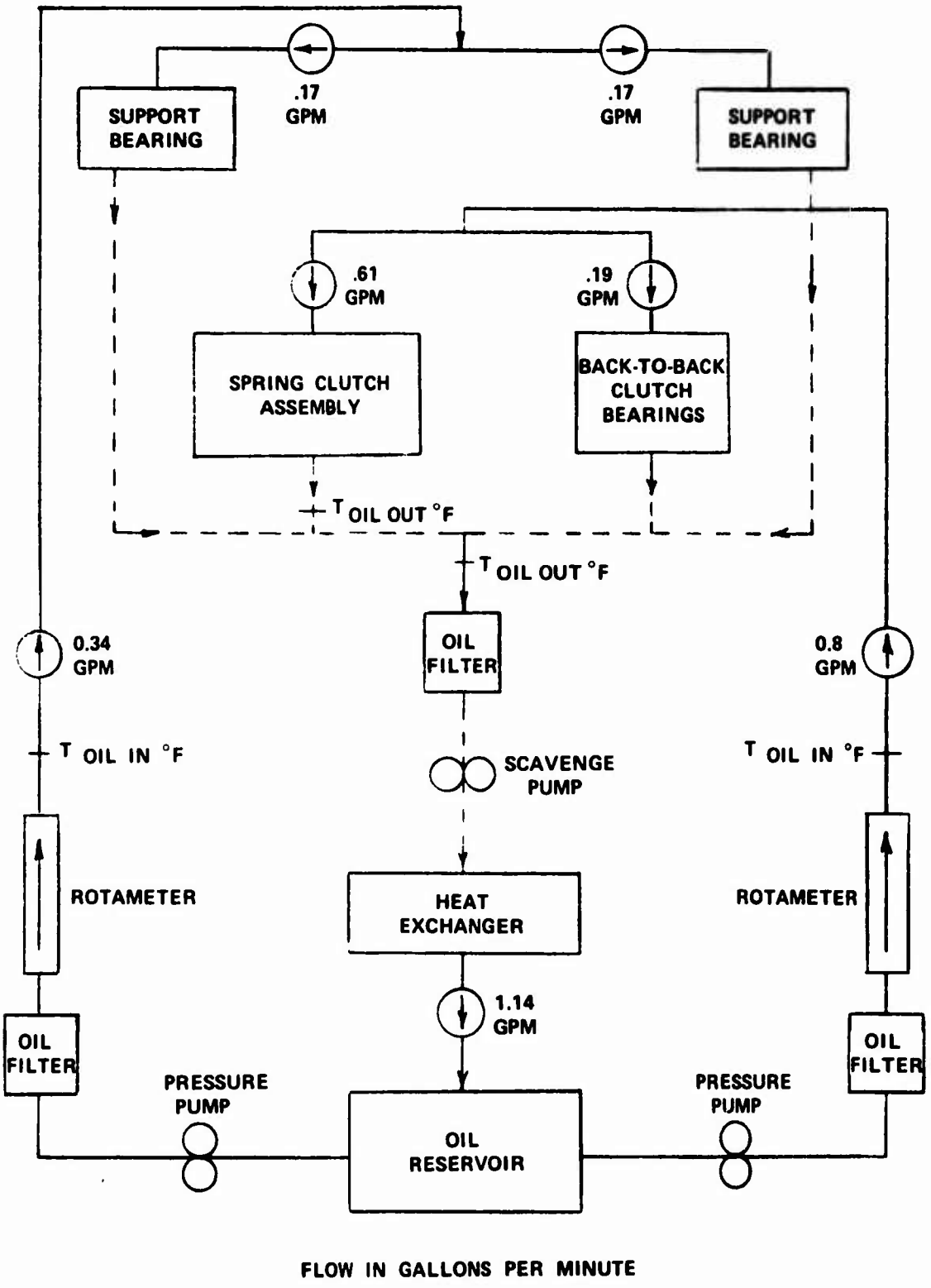

Figure 19. Design B, Lubrication Schematic.

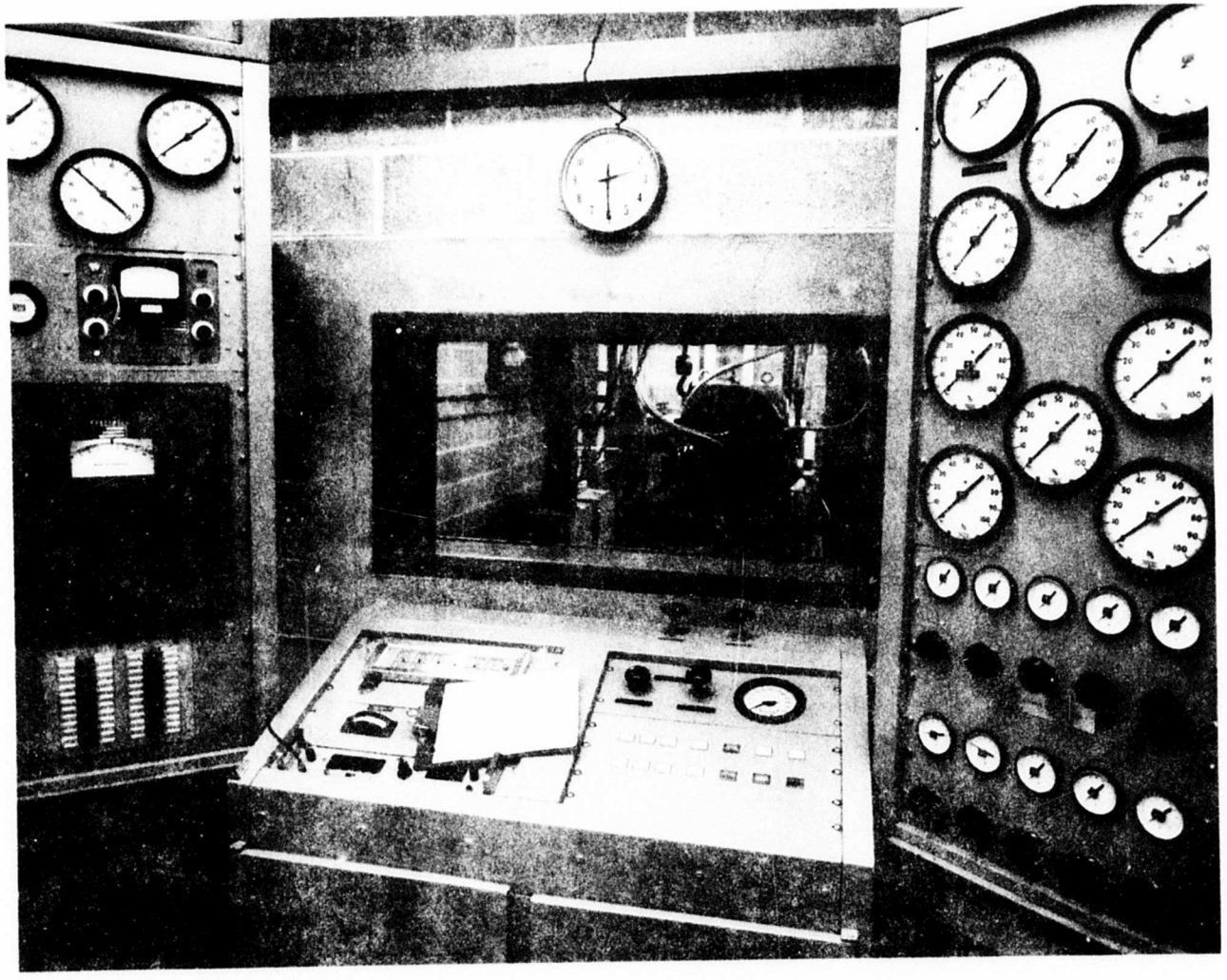

Figure 20. Console and Instrument Panel.

1. Oil flow and pressure

2. Oil temperature in and out

3. Rig vibration

4. Rig speeds

5. Clutch outer shaft temperature (design A)

6. Clutch inner shaft and energizing coil temperature (design B)

7. Bearing inner and outer race temperature

8. Energizing coil temperature (design A)

9. Clutch drag torque

10. Chip detectors

The locations where measurements were obtained are shown schematically in Figures 21 and 22 for designs A and B, respectively. Iron-Constantan thermocouples were employed throughout. Clutch scavenge oil temperature was measured at the test clutch oil ports rather than at the rig scavenge port so that no heat would be lost to the rig housing.

Clutch torque was measured by two methods in the overriding tests. One method measured driving shaft torque (Figure 21). Foil resistance strain gages were mounted on a reduced section of the inner-race drive shaft. The gages were located to form a torque bridge at 45 degrees to the axis of the shaft. The shaft and gage installation was calibrated for torque versus bridge output over the expected torque range (0 to 250 inch-ounces). The calibration was accomplished through the application of weights on a specially constructed fixture. Corrections were made for extraneous loads and temperature effects.

The other method of measuring shaft torque was to restrain the outer race from rotating with an instrumented beam (Figure 16). Foil resistance strain gages were mounted on the beam to form a

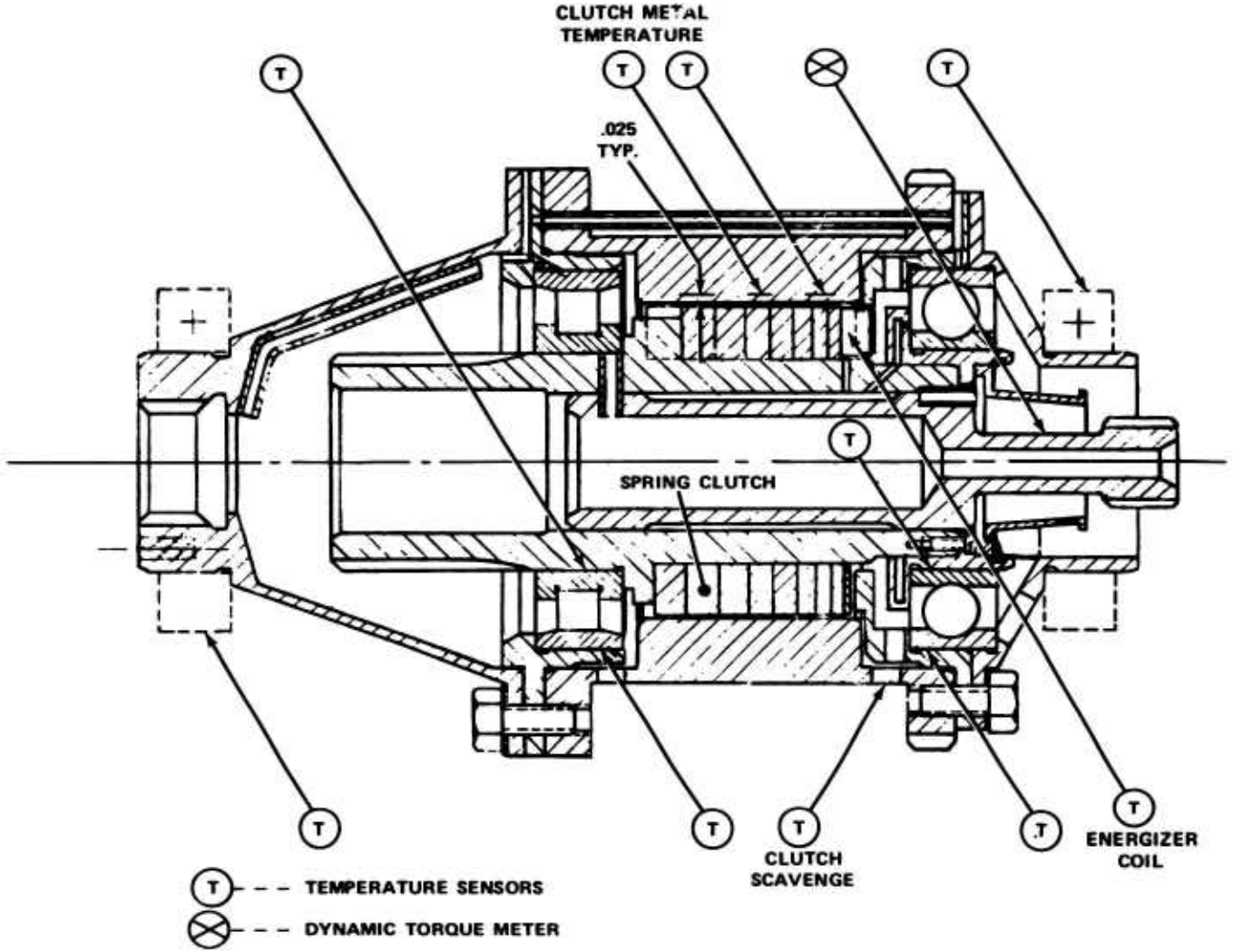

Figure 21. Design A, Instrumentation Schematic.

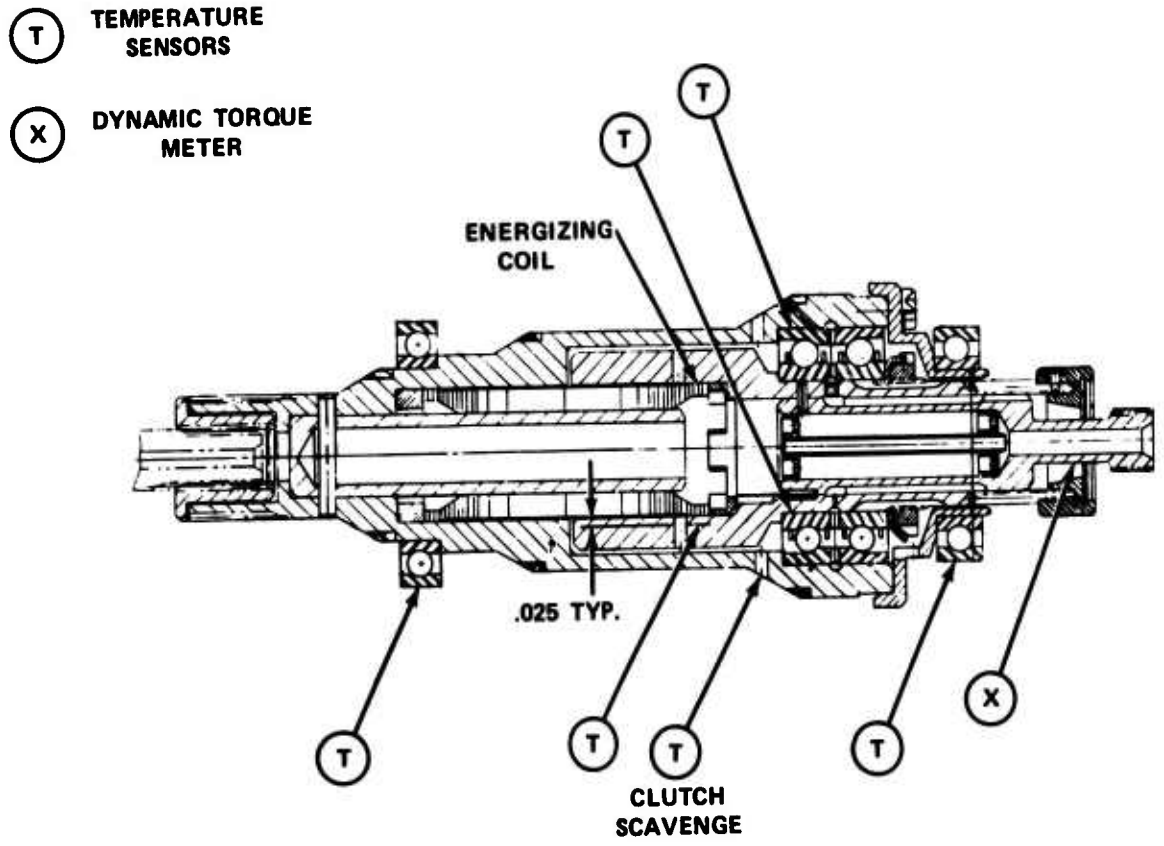

Figure 22. Design B, Instrumentation Schematic.

shear bridge. The beam was calibrated for point load versus bridge output over the expected load range. Corrections were made for extraneous loads and temperature effects. The shear bridge was chosen to eliminate any need to correct the calibration for variations in the point of load application relative to the strain gage locations. During the second override test for design B, the instrumented beam used to measure static drag torque was damaged. As a substitute, a force gage and lever were employed to measure static drag torque. The lever was fixed to the internal spline coupling shaft shown in Figure 17. A calibrated mechanical force gage fixed to ground was used to measure the force exerted by the lever. The gage is fully jeweled and measures pound force from 0 to 5 pounds in increments of 0.05 pound. The effective lever length was 6 inches. The static drag torque is simply the product of the gage force and the effective length of the lever. When the differential speed tests were conducted with both shafts rotating, only the drive shaft torque could be measured.

STATIC TESTS

Test Rig

The cyclic fatigue tests were conducted in the experimental mechanical laboratory using electrohydraulic closed-loop, servo-controlled, rotary actuator systems. A cross section of a typical installation is shown in Figure 23. The system utilizes a rotary actuator and provides the required torque load of 7,140 $\pm$ 900 inch-pounds at a frequency of 10 Hertz. The torque load was applied, using the hydraulic rotary actuator, through a bolted adaptor splined to the clutch outer race. The load was then reacted through a torque sensor bolted to an adaptor and splined to the clutch inner race. Continuous oil flow of 0.5 gpm was maintained within the clutch assembly at a pressure of 20 psig for design A and 4 psig for design B using MIL-L-23699 oil. The system uses a full-flow chip detector and is instrumented for an automatic shutdown in the event of chip detection or component failure. The equipment compares input and output torque and shuts down automatically if the difference is greater than 1/2 percent of full torque. Torque load, angular displacement between input and output races, and outer race radial deflections were monitored every one million cycles. The torque readouts were observed with an oscilloscope, digital voltmeter,

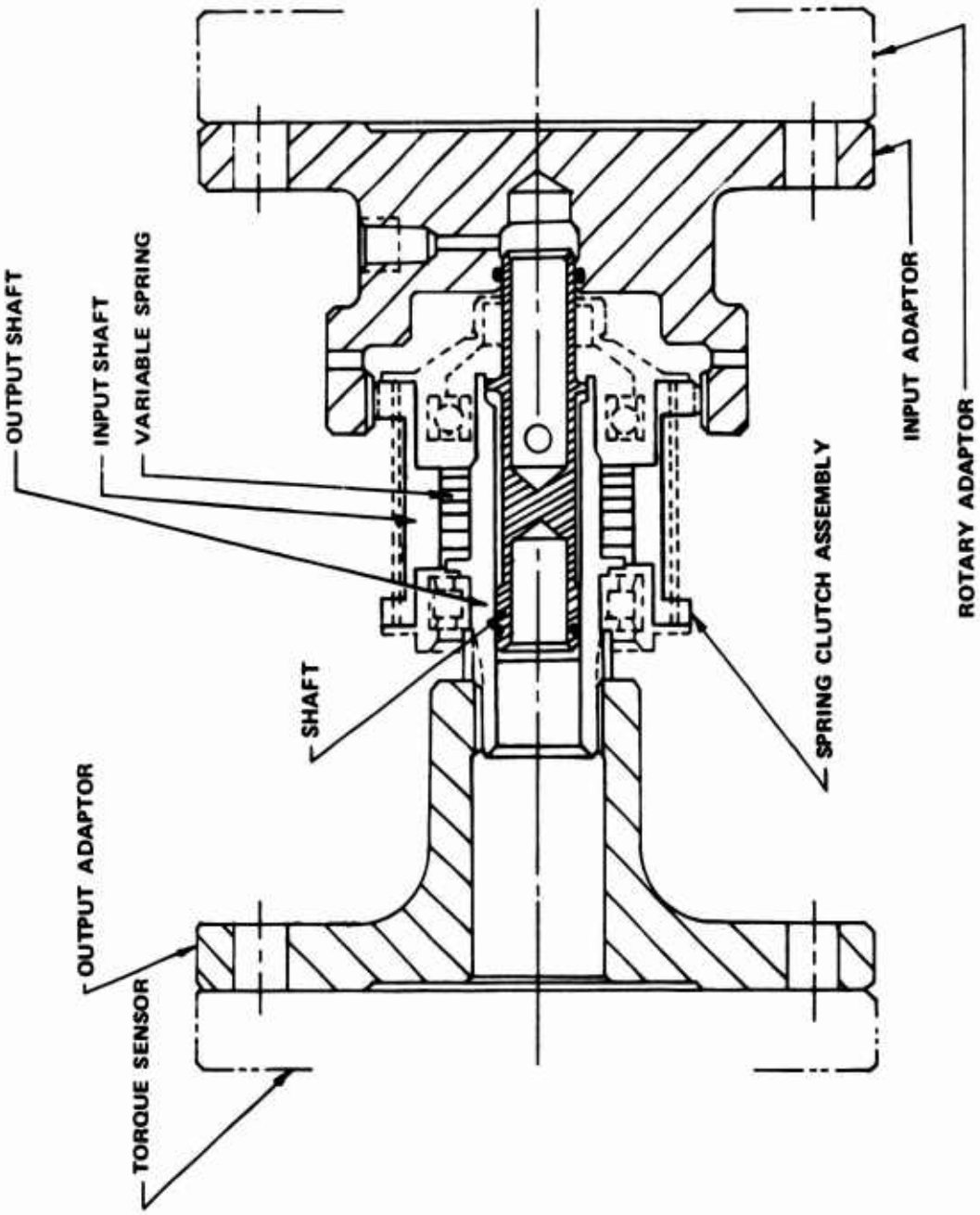

Figure 23. Cyclic Fatigue Test Schematic.

and load amplitude measurement system. Angular displacement between outer and inner races was measured with graduated scales, located on the input and output adaptor flanges, and with pointers attached to ground. The outer race radial deflection of design A and the inner race radial deflection of design B were determined by averaging the output of eight strain gages tangentially oriented and equally spaced around the shaft circumference. The rig utilizes a rotary actuator that is rated at 8,020 inch-pounds dynamic and 12,000 inch-pounds static. Maximum travel is 90 degrees ($\pm$ 45 degrees). A 10-gpm hydraulic power supply at 3,000 psi source pressure is employed. A photograph of the cyclic fatigue test installation is shown in Figure 24.

The overload tests were performed on a second rotary actuator that is rated at 72,000 inch-pounds static torque. Instrumentation utilized was the same as that in the cyclic fatigue test. A photograph of the overload test installation is shown in Figure 25.

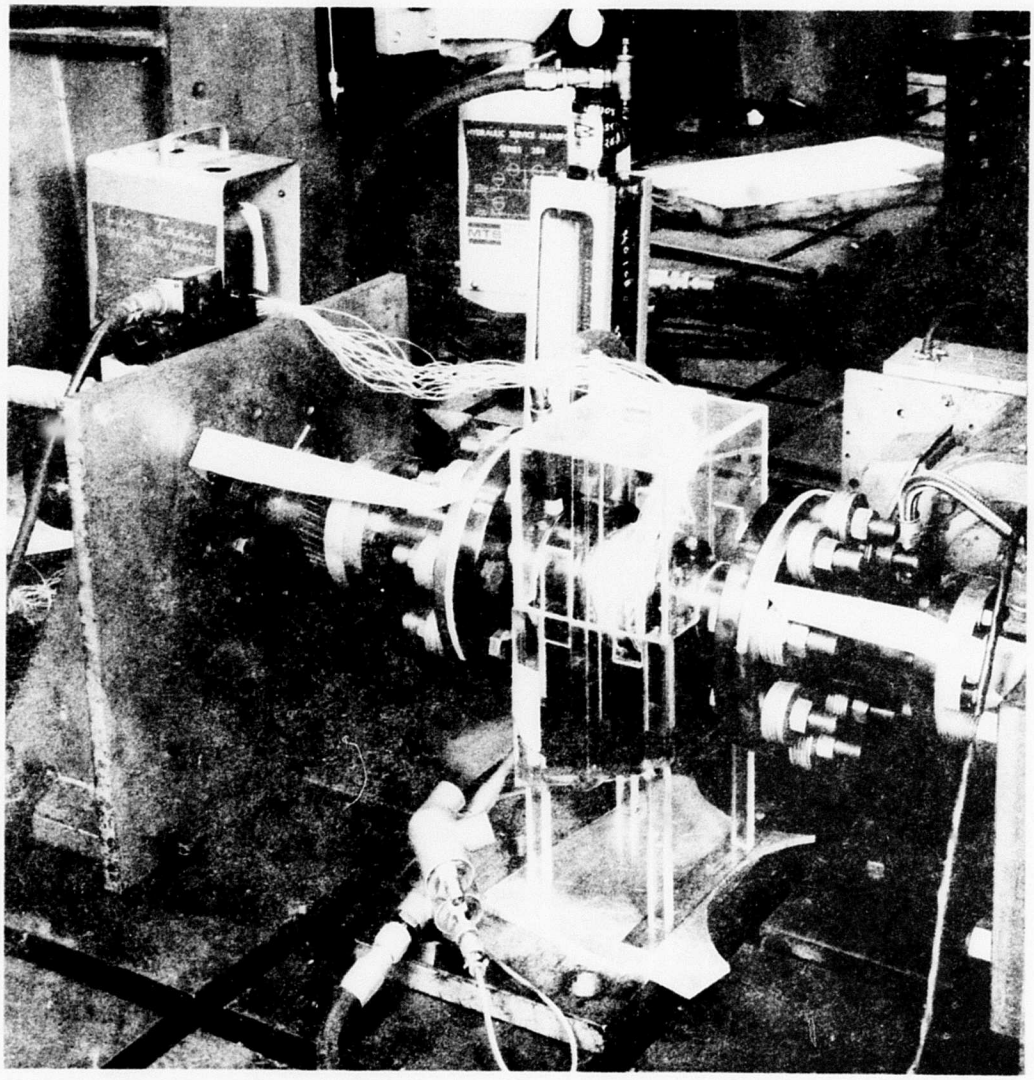

Figure 24. Cyclic Fatigue Test Installation.

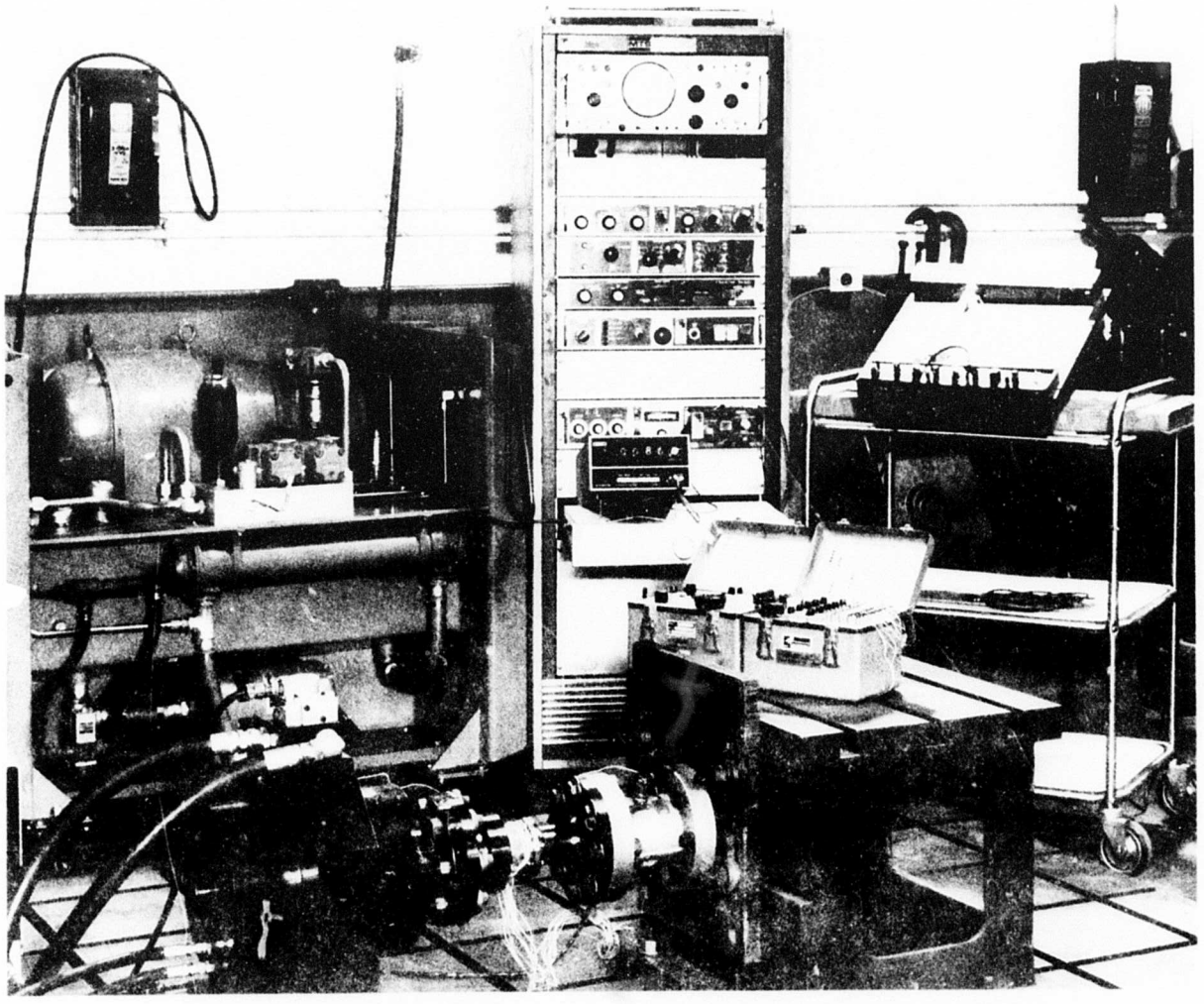

Figure 25. Static Overload Test Installation.

TEST PROCEDURE

GENERAL

Five series of tests were conducted as follows:

1. Full-speed dynamic clutch override test
2. Differential-speed dynamic clutch override test
3. Dynamic engagement tests
4. Static cyclic torque fatigue test
5. Static overload test

One design A clutch and one design B clutch were subjected to tests 1 through 3.

Two design A clutches and two design B clutches were to be subjected to tests 4 and 5.

For the dynamic tests, data were recorded every 15 minutes. A typical log sheet is shown in Figure 26. Data points taken were averaged for presentation under "Test Results and Discussion".

FULL-SPEED DYNAMIC CLUTCH OVERRIDE TEST

The objective of this test was to determine the optimum clutch oil flow in terms of heat generation, drag torque, and component wear.

Prior to testing, the clutch rig was fully instrumented to monitor the following parameters, which were recorded every 15 minutes:

Parameters	Number of Positions	
	Design A	Design B
Outer race temperature of bearing - ^{o}F	5	4
Inner race temperature of bearing - ^{o}F	4	2
Clutch outer shaft temperature - ^{o}F	4	-
Clutch inner shaft temperature - ^{o}F	-	2

LYCOMING GAS TURBINE TEST DATA

ENGINE DESIGN A CONFIGURATION _____ CONTRACT _____ DATE 5-1-72 TEST CELL 9

TEST TITLE AVCO SPRING CLUTCH OPERATOR H. TRUCHON OBSERVER S. CHAKHAKIS

RUN NO. TIME OF DAY	TIME TEST TIME	SPEED OUTER	SPEED INNER	OIL-IN SCAV.	CLU MID OUTER	TE TCH AFT OUTER	MP OIL OUT	ER #2 OUTER	AT BEA #1 INNER	UR BEARING #3 OUTER SPRING END	ES #3 INNER	OUTER 144	OIL IN BAGS. 144		PRESS. CLUTCH BAGS 144	FLOW CLUTCH BAGS. 144	TOR SHAFT IN-OZ	QUE BEAM IN-OZ	V #1 VEL. DISP.	VB. #2 VEL. DISP.
10:30	2:30			25	27	29	41	31	33	35	37	39	44							
				26	28	30	42	32	34	36	38	40								
10:45			26000	200	258	250	204	277	220	244	243	174	200		41	130	101.8	49.9	.35	.35
				211	254	250	218	277	215	226	246	202			68	160			.4	.35
11:00	3 HRS.		26000	200	258	250	204	276	218	244	243	175	201		41	130	100.8	48.9	.4	.4
				210	258	250	214	276	216	228	246	202			68	160			.4	.35
11:15			26000	200	254	250	205	277	219	244	242	175	200		41	130	101.4	49.8	.4	.4
				211	254	250	218	277	217	230	246	202			68	160			.4	.4
11:30			26000	200	254	250	204	277	220	244	242	176	201		41	130	101.4	49.6	.4	.35
				211	254	250	218	277	216	224	245	203			68	160			.35	.35
11:45	3:45	STOP	24,000	200	256	250	205	277	222	244	246	176	201		41	130	101.4	49.6	.4	.4
12:45		START		210	256	250	214	278	220	224	248	203			68	160			.4	.4
1300	4 HRS.		26000	198	253	245	200	273	218	240	238	173	200		41	130	105.6	49.5	.4	.35
				208	253	245	206	273	215	226	244	198			67	155			.4	.4
13:15			26000	200	257	247	204	277	223	244	243	175	201		41	130	99.6	48.1	.4	.35
				211	257	247	218	277	218	224	246	202			67	155			.35	.35
13:30			26000	200	257	250	205	277	224	244	244	176	201		41	130	103.8	49.5	.4	.35
				211	257	250	217	277	220	230	247	203			67	155			.35	.35
13:45			26000	201	257	250	206	277	222	244	243	176	201		41	130	103.0	49.5	.4	.4
				211	257	250	213	277	218	230	246	203			67	155			.4	.4
14:00	5 HRS.		26000	201	256	251	206	278	220	245	244	176	201		41	130	102.4	49.8	.4	.4
				212	258	251	215	278	216	230	244	204			67	155			.4	.35
	TEST	NO.	12					HOURS/SHEET			2½				SHEET NO.		2	OF	3	

GTE-9

Figure 26. Typical Log Sheet.

Parameters	Number of Positions	
	Design A	Design B
Spring pickup temperature - °F	1	-
Clutch oil-in temperature - °F	1	1
Clutch oil-out temperature - °F	2	2
Clutch drag torque, dynamic - in.-oz	1	1
Clutch drag torque, static - in.-oz	1	1
Clutch oil flow - pph	1	1
Rig housing vibration (displacement and velocity)	2	2
Chip detectors	2	2
Clutch oil pressure at rig housing - psig	1	1
Output shaft speed - rpm	1	1

The clutch was operated at zero input speed and 26,500 rpm output speed. Tests were conducted with oil flows of 300, 200, 100, 67, and 33 percent of design flow (design flow = 0.8 gpm). Each test was of 6 hours duration, of which 1 hour was used for a speed rundown. The oil inlet temperature was held to a minimum of 195°F and did not exceed 215°F. The oil inlet pressure did not exceed 100 psig nor did it go below 40 psig throughout the dynamic test program. It must be remembered that this is the oil fed to the inside of the clutch inner race. Test oil flows and pressures are listed in Table VI.

At the end of each oil flow level test, i.e., 300 percent oil flow, 200 percent oil flow, etc., a speed rundown was conducted. For this portion of the test, the variable was clutch output speed, and the operating oil flow was maintained at a steady state. The output speed levels selected are listed below:

Output Speed Level (rpm)
25,000
20,000
15,000
10,000
5,000

Each output speed level was maintained until steady-state temperature condition was achieved. Temperatures were stabilized for

TABLE VI. FULL-SPEED DYNAMIC CLUTCH OVERRIDE OIL FLOWS AND PRESSURES

Test	Design Flow (pct)	GPM	PPH	Feed Pressure (psig) Design A	Design B
1	300	2.4	1125	95	100
2	200	1.6	750	87	76
3	100	.8	375	66	58
4	67	.54	250	46	50
5	33	.26	125	41	43

approximately 15 minutes at each speed level. After testing, the test rig was dismantled and the clutch components were inspected visually and analytically.

The test procedure for the full-speed override test including the speed rundown was repeated for each design without the spring clutch assembly installed. The purpose was to resolve clutch drag torque into individual components produced by bearings and shafts on one hand and the spring clutch on the other hand. One clutch each of designs A and B was subjected to the full-speed override test.

DIFFERENTIAL SPEED DYNAMIC CLUTCH OVERRIDE TEST

The objective of this test was to determine the maximum drag condition. The test objective was accomplished by adjusting the clutch output speed to 26,500 rpm (100 percent normal rated) and then adjusting the clutch input speed to the values noted below:

Output Speed (rpm)	Normal Rated (pct)	Input Speed (rpm)	Normal Rated (pct)
26,500	100	13,250	50
26,500	100	17,667	67
26,500	100	19,875	75

The optimum oil flow rates established during the full-speed override test were used during this test. Oil inlet temperatures and pressures were maintained at 195°F minimum and 100 psig maximum, respectively. After conditions were stabilized, each speed condition was maintained for 1 hour and the following parameters were monitored every 15 minutes:

Parameter	Number of Positions	
	Design A	Design B
Outer race temperature of bearings - °F	5	4
Inner race temperature of bearings - °F	2	2
Clutch shaft temperature - °F	4	2
Temperature of clutch oil-out - °F	2	2
Clutch drag torque dynamic measurement - in.-oz	1	1
Clutch assembly oil-in temperature - °F	1	1
Oil flow to clutch assembly - pph	1	1
Rig housing vibration (displacement and velocity)	2	2
Chip detectors	2	2
Oil pressure at rig housing for clutch assembly - psig	1	1
Output shaft speed - rpm	1	1
Input shaft speed - rpm	1	1

After completing the three 1-hour speed runs, i.e., input clutch speed adjusted to 50, 67, and 75 percent normal rated, the clutch input speed associated with the highest drag torque was selected as the next operating point, and a 5-hour test was conducted at the selected clutch input speed. All other test parameters were the same as before.

At the end of the differential speed dynamic override test, the clutch rig was dismantled and clutch components were visually and analytically inspected. One clutch each of designs A and B was subjected to the differential speed test.

DYNAMIC ENGAGEMENT TEST

The objective of this test was to investigate the engagement and disengagement characteristics of the clutch.

The test procedure employed was to adjust the output speed of the clutch to 13, 250 rpm (50 percent normal rated). The input speed of the clutch was then accelerated to exceed 13, 250 rpm, such that clutch engagement occurred. As the input speed increased, the output prime mover was shut down to impart a shock load to the clutch components, an operation that was accomplished twice.

The procedure was repeated at output speeds of 19, 875 rpm (75 percent normal rated) for two engagements and of 26, 500 rpm (100 percent) for five engagements. The optimum oil flow established in the full-speed override test was utilized.

For this test series, the strain-gaged drive shaft, capable of monitoring clutch drag torque, was not used. The shaft was designed to measure only small values of drag torque and would fail if subjected to the shock loads. Accordingly, another drive shaft capable of withstanding shock loads was used.

One clutch each of designs A and B was subjected to the dynamic engagement test.

Following the test, clutch components were visually and analytically inspected.

STATIC CYCLIC TORQUE FATIGUE TEST

The objective of this test was to determine the fatigue characteristics of the clutch.

A torque load of 7, 140 $\pm$ 900 inch-pounds was applied to both designs A and B clutches for ten million cycles. The cyclic fatigue test program was conducted at twice the design torque, reflecting safety factors commonly used in the aircraft industry to account for torsionals, shock loads, etc. Load application frequency was 10 Hertz using sine wave excitation. The following parameters were monitored:

Torque - in.-lb
Angular Displacement - deg
Outer Shaft Radial Deflection - in.

A continuous oil flow of 0.5 gpm at room temperature was maintained in both design A and B clutches with the use of special fixtures. For design A the pressure was 20 psig, and for design B the pressure was 4 psig.

Three clutches of design A and two clutches of design B were subjected to the cyclic fatigue test.

Following the test, clutch components were visually and analytically inspected.

STATIC OVERLOAD TEST

The objective of this test was to determine the clutch's ultimate capacity and the overload mode of failure.

Static torque load, in increasing increments of 500 inch-pounds, was applied until slippage or component failure occurred. The following parameters were monitored:

Torque - in.-lb
Angular Displacement - deg
Outer Shaft Radial Deflection - in.

Internal clutch components were lubricated with MIL-L-23699 oil prior to testing.

Following the test, clutch components were visually and analytically inspected.

INSPECTION

Prior to testing, all clutch components were completely dimensionally inspected. Clutch shafts were measured on the Indi-Ron (Figure 27) to determine roundness to 1.5×10^{-6} inch and on the Proficorder (Figure 28) to determine surface texture to 3×10^{-6} inch. Proficorder traces were also taken on the spring clutch in the axial direction.

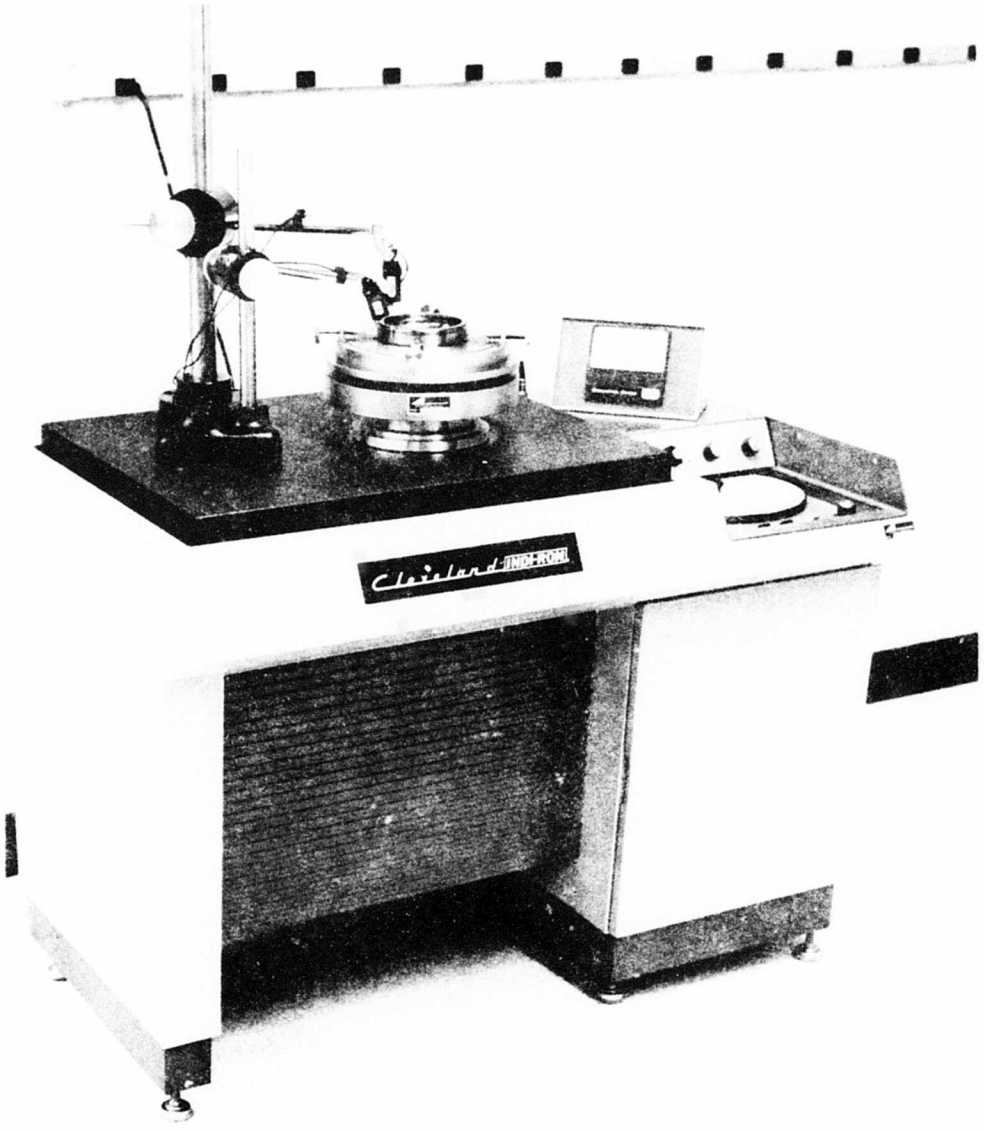

Figure 27. Indi-Ron.

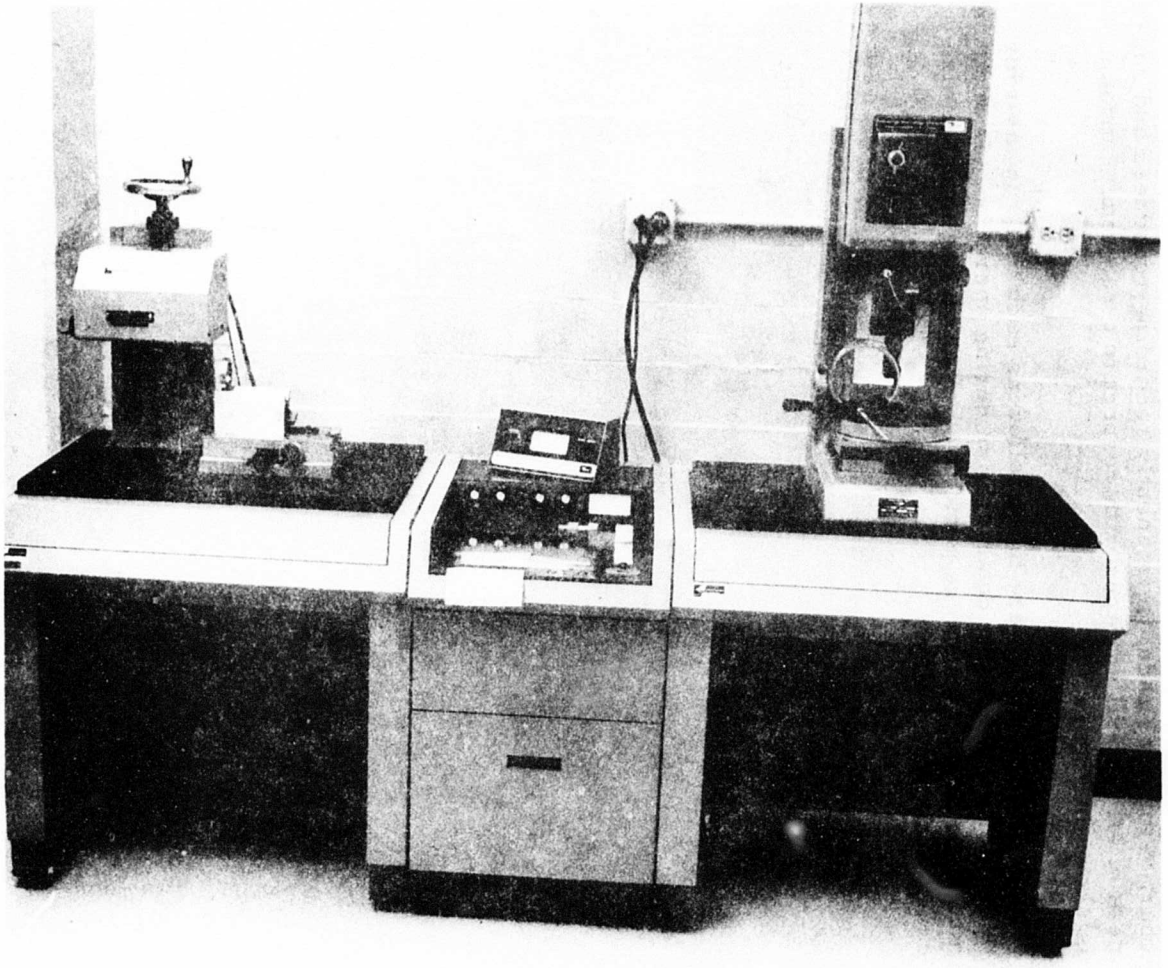

Figure 28. Proficorder.

A typical Proficorder chart, which provides a permanent record of component surface texture, is shown in Figure 29. An Indi-Ron chart of an inner race, permanently recording roundness and squareness of all critical surfaces with respect to a reference surface, is shown in Figure 30.

These measurements were taken following each test run in order to determine component deterioration during operation. In addition, magnaflux inspections were performed after testing to determine crack initiation, if any.

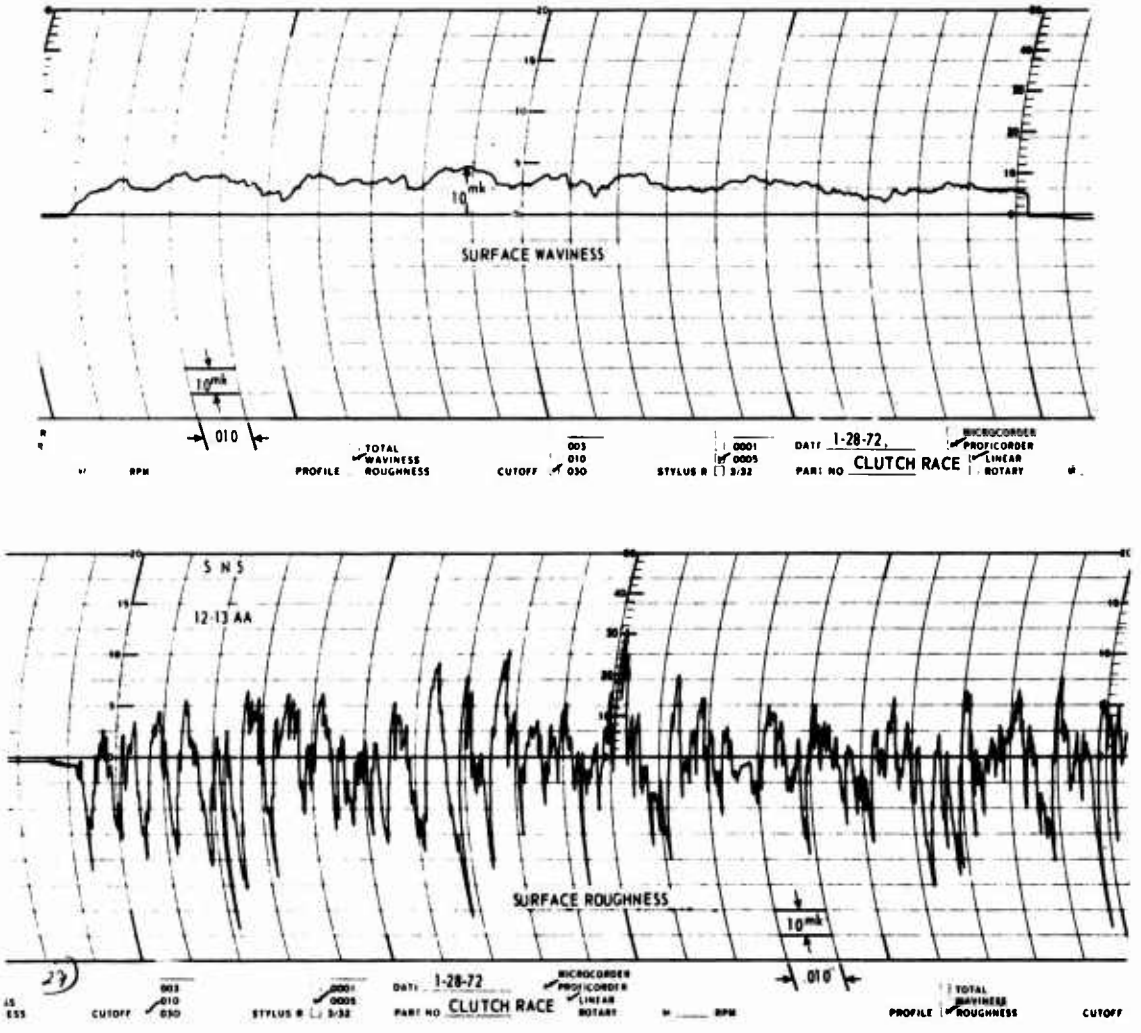

Figure 29. Typical Proficorder Chart.

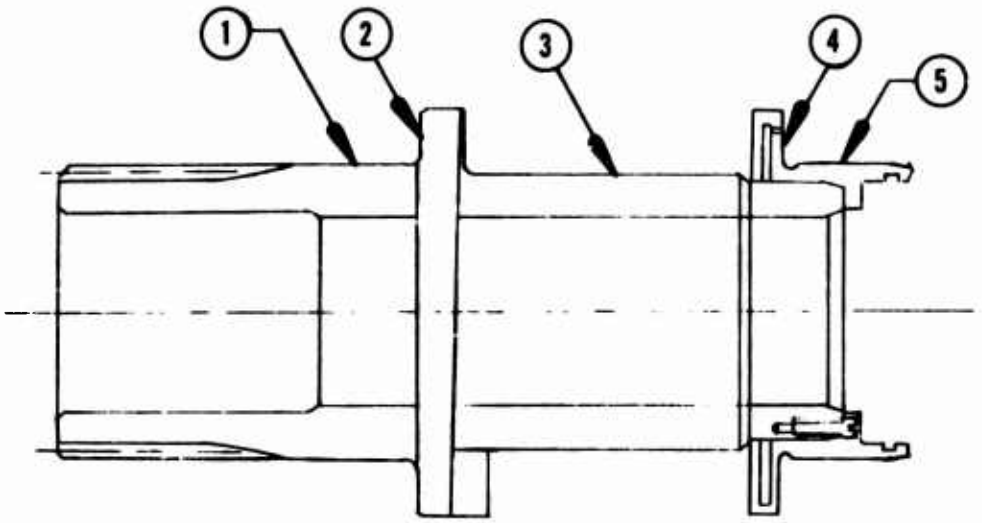

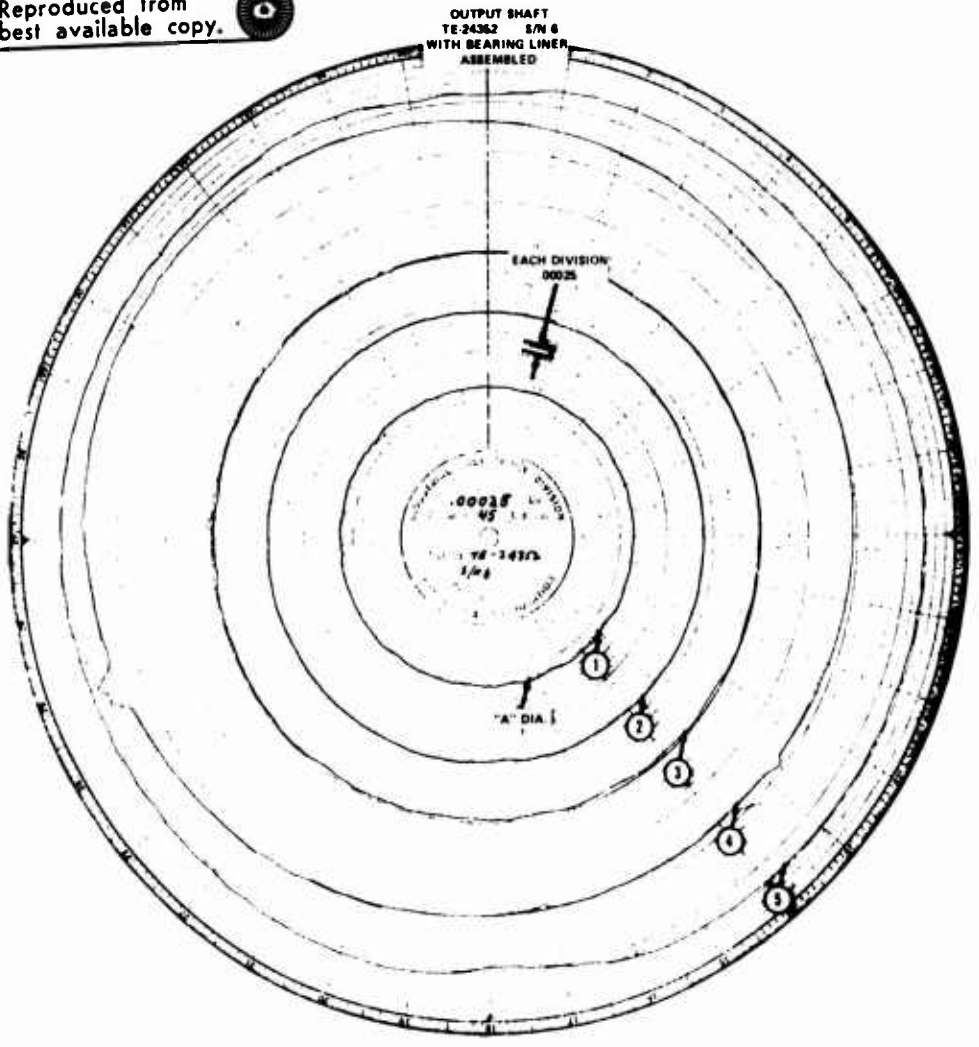

Figure 30. Typical Indi-Ron Chart.

TEST RESULTS AND DISCUSSION

FULL-SPEED DYNAMIC CLUTCH OVERRIDE TEST

The design A clutch survived all oil flow runs down to 33 percent (.27 gpm) in good condition. As determined in the initial testing described on page 33, an .087-inch diametral gap was required between the spring OD and the drum ID to preclude interference at a speed of 26,000 rpm. Therefore, the test was conducted with a maximum speed of 26,000 rpm rather than the design speed of 26,500 rpm.

The clutch was designed so that during overriding, contact would occur only on the ratcheting coils on the energizing end. Some axial wear was evident on these coils as illustrated in Figures 31 and 32. The stationary coil, Figure 31, exhibited more wear than the rotating coil. The depth of wear versus hours of operation, plotted in Figure 33, shows that wear rate is independent of oil flow.

The design B clutch also survived all flow runs down to 33 percent (.27 gpm) in good condition. In the overriding mode, all rubbing takes place between the OD of the silver-plated end coils and the rotating output shaft. The amount of silver-plate wear after testing was measured to be .002 inch. Figure 34 shows a plot of wear versus time. Figures 35, 36, and 37 illustrate the condition of the design B clutch after the override test. Some flaking can be seen on the silver-plated end coils.

The energy loss in the clutch due to overriding was measured in three ways: oil temperature increase, reaction torque on the stationary input shaft, and shaft torque on the rotating output shaft. In some test runs, difficulty was experienced with the slip-ring readout, and erroneous data was obtained. At the higher oil flows, the torque calculated from oil in and out temperatures was higher than shaft or reaction torque, which indicates that a percentage of the oil flow was lost in leakage and was not passing through the spring and bearings. At the lower flows, in some cases, there was no oil temperature rise, which indicates that test rig parts had cooled the oil prior to the temperature measurement. The reaction torque gave the most accurate and consistent readings throughout the test, and this data is presented for designs A and B in Figures 38 and 39 respectively. In order to determine the energy loss due to the spring assembly alone, the rig was operated both with and without the spring assembly installed. The results are reflected in the solid and dotted lines of Figures 38 and 39. The raw data for shaft torque, reaction torque, and oil temperature are shown in Appendix III.

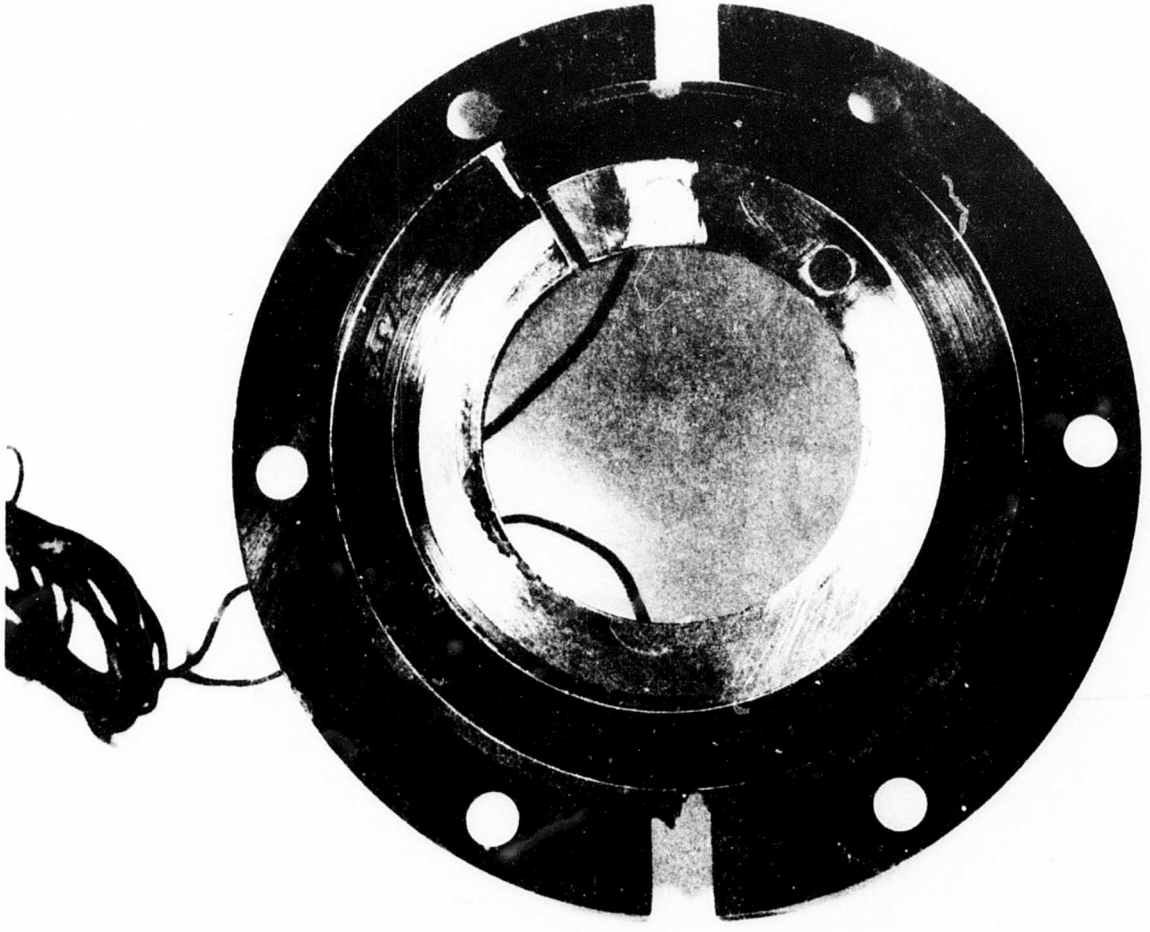

Figure 31. Energizing Coil Wear Due to Override Test, Design A.

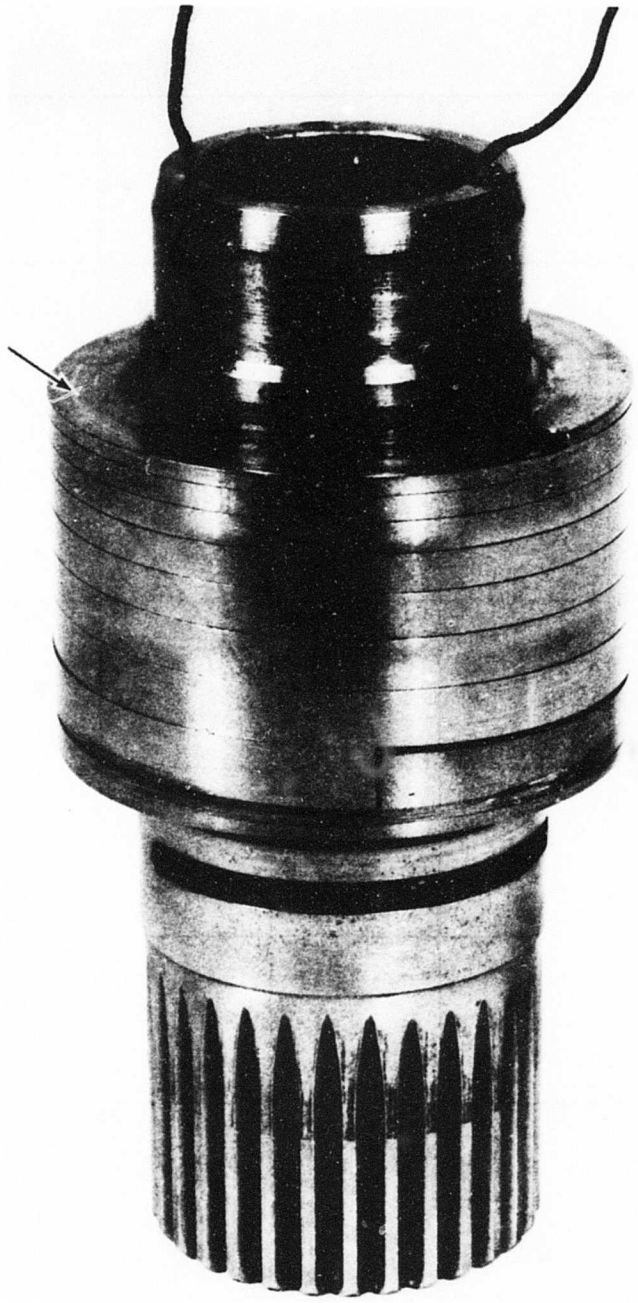

Figure 32. Spring Condition Following Override Test, Design A.

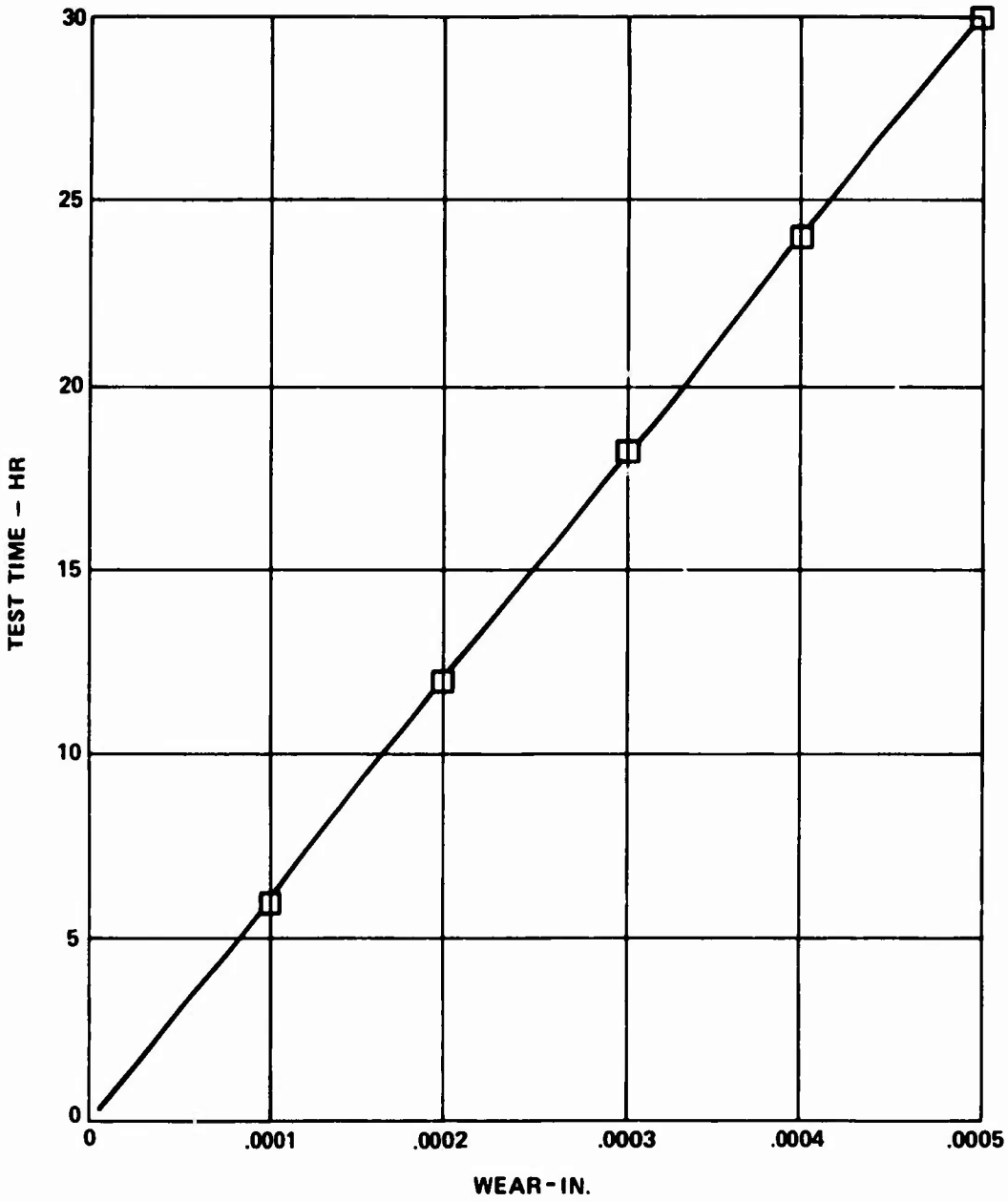

Figure 33. End Coil Wear Versus Test Hours, Design A.

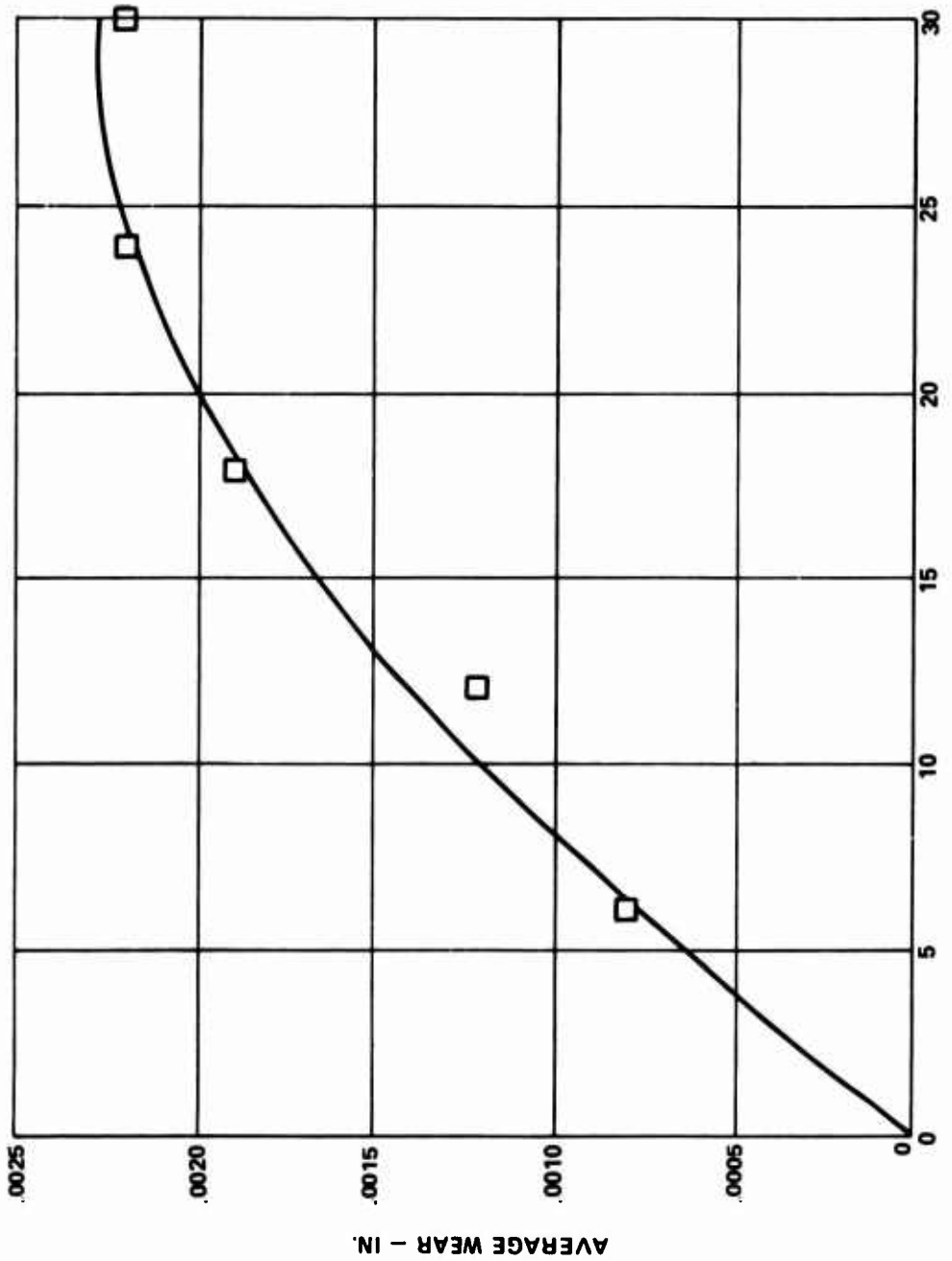

Figure 24. Energizing Coil Wear Versus Test Hours, Design B.

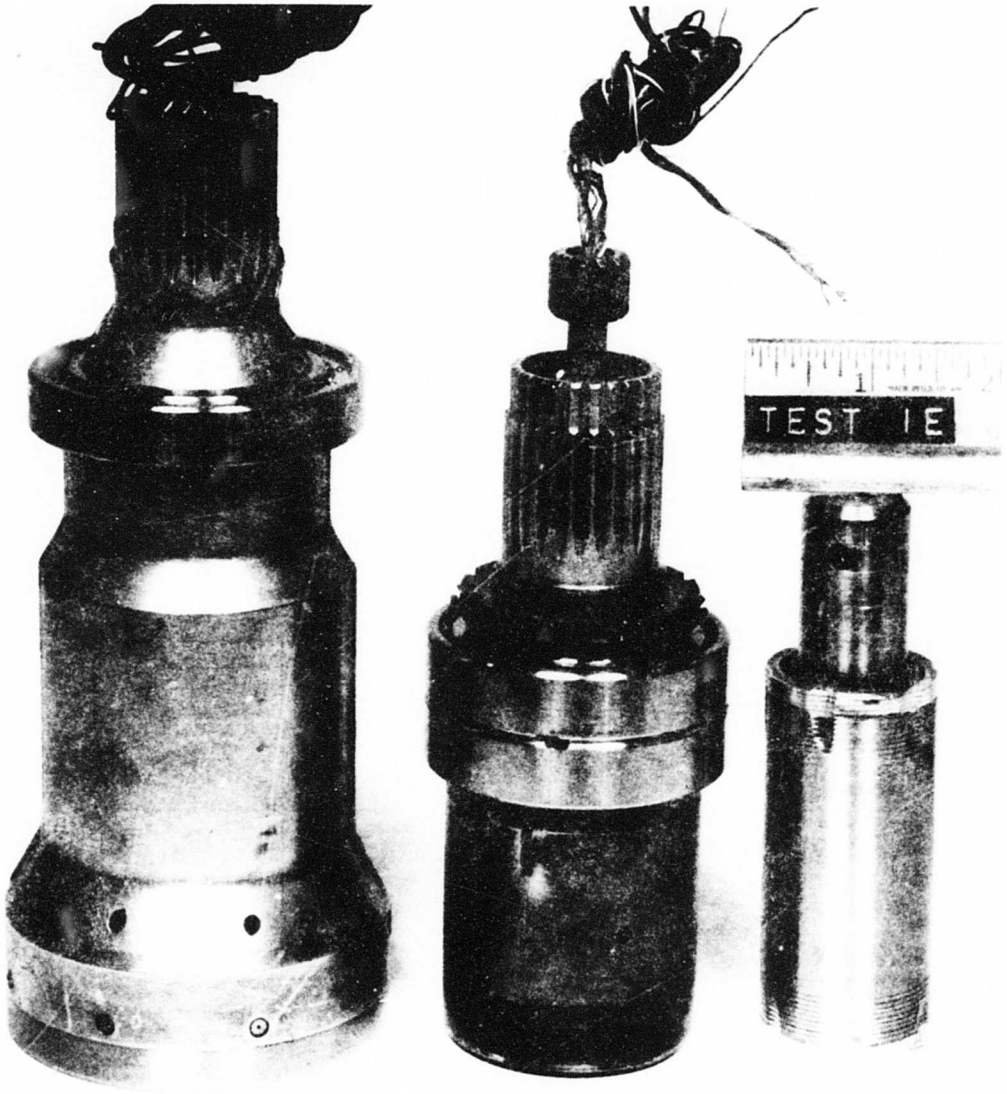

Figure 35. Design B Components Following Override Test.

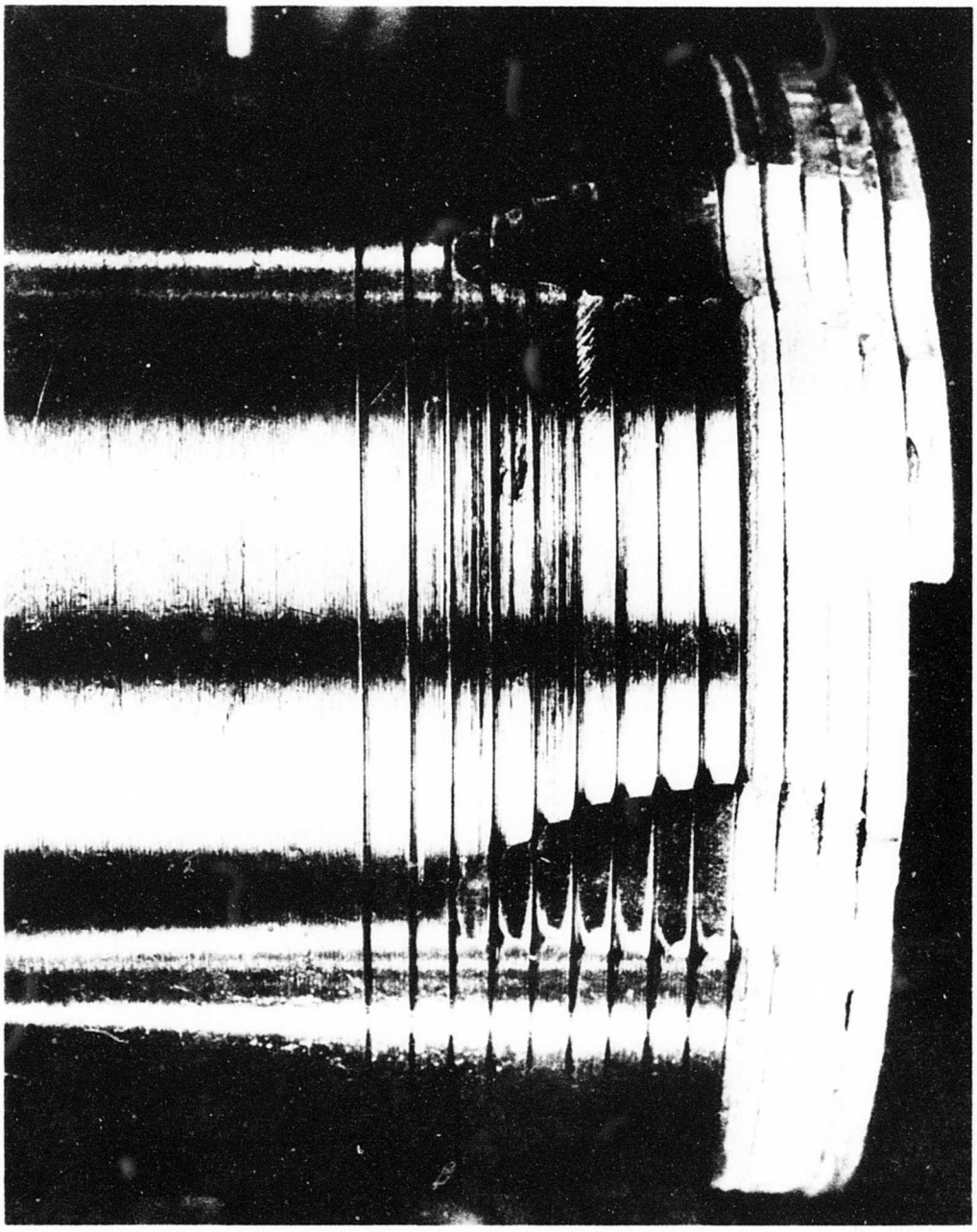

Figure 36. Design B Energizing Spring Following Override Test.

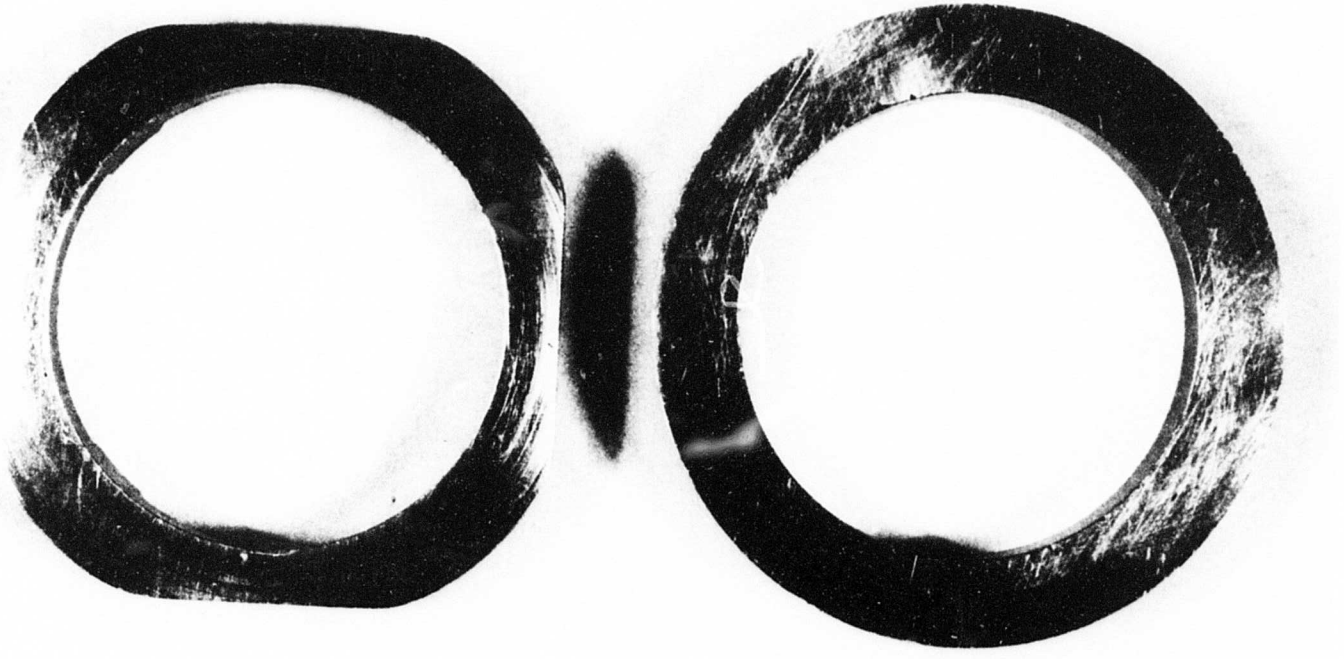

Figure 37. Design B Spacers Following Override Test.

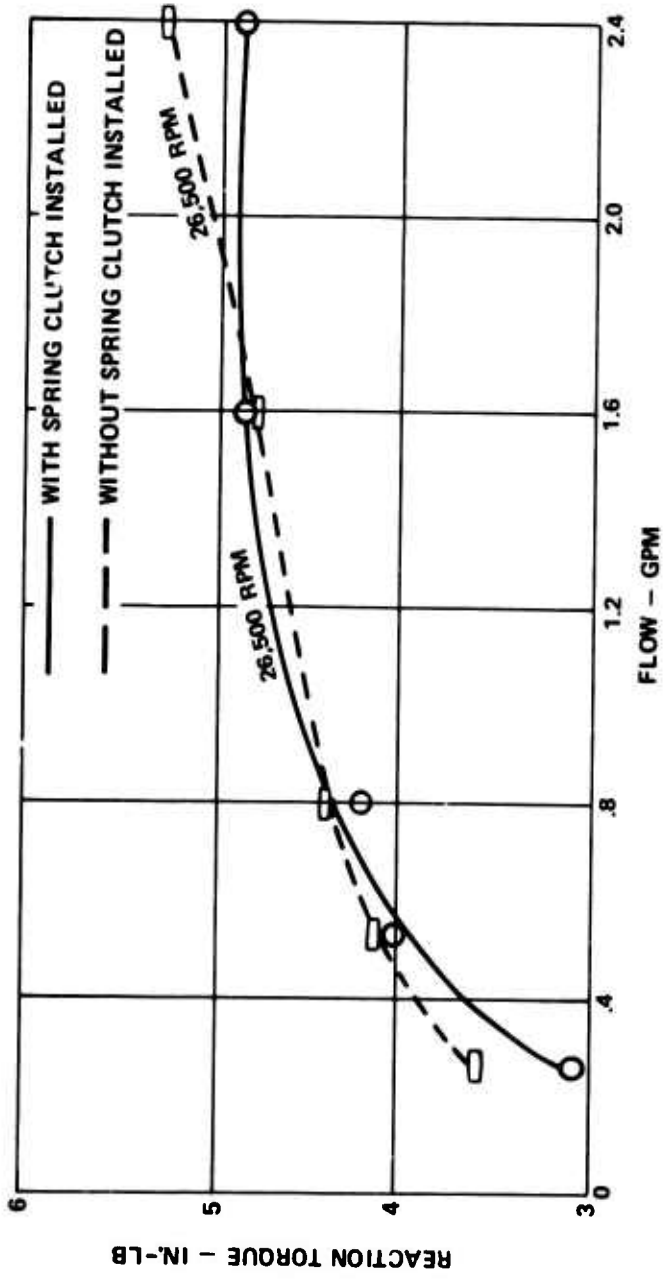

Figure 38. Reaction Torque Versus Oil Flow, Design A.

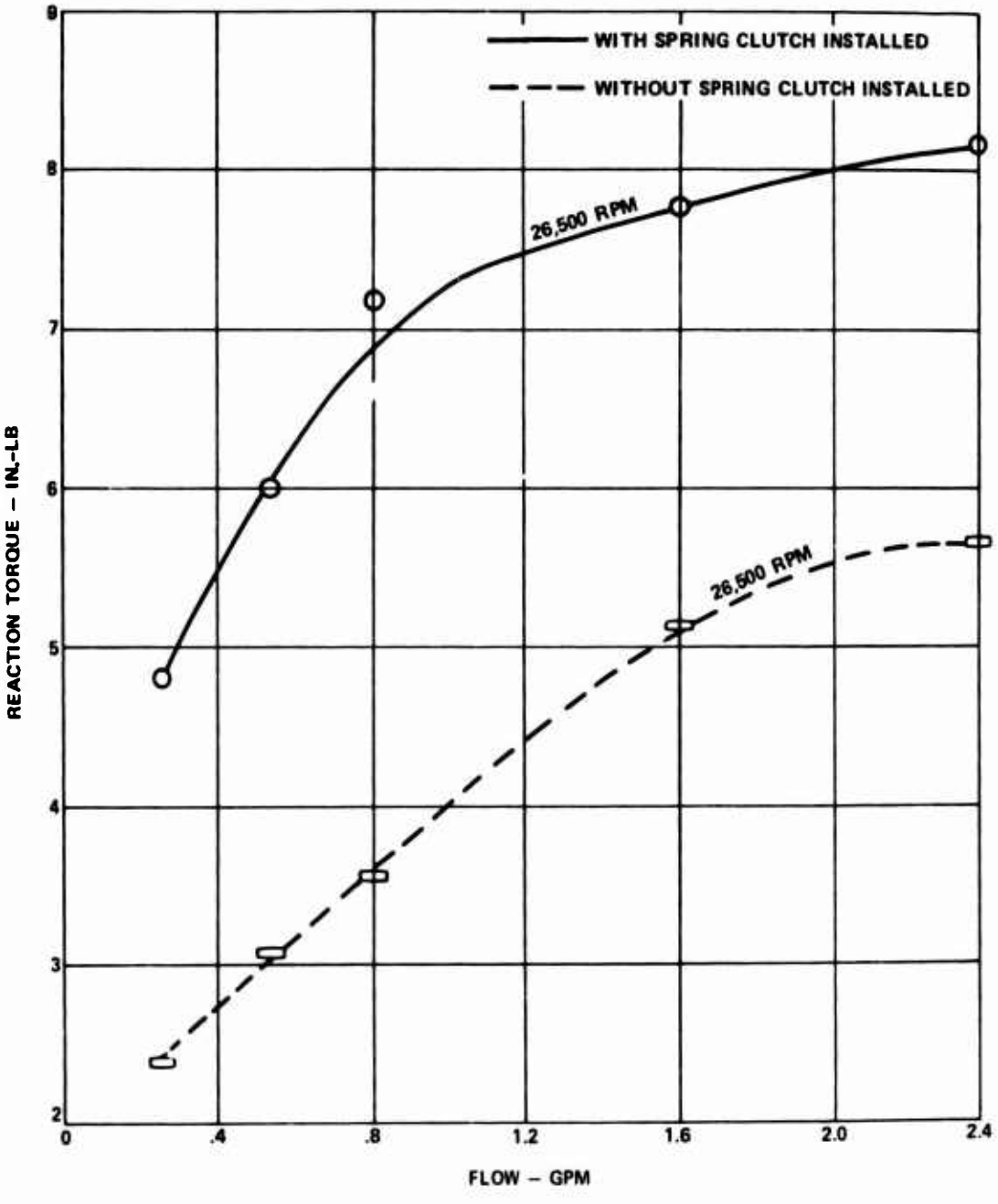

Figure 39. Reaction Torque Versus Oil Flow, Design B.

Oil temperature changes versus oil flow at 26,500 rpm for designs A and B are shown in Figures 40 and 41. Clutch temperatures at the rubbing interfaces of designs A and B are presented in Figures 42 and 43. Bearing race temperatures are presented in Figures 44 and 45.

The 67 percent design flow (.54 gpm) was designated as the optimum oil flow for use in the differential-speed and high-speed engagement tests. Although 33 percent flow (.27 gpm) operation was acceptable, test results indicated a significant temperature increase between 67 percent and 33 percent (Figures 40 to 45); therefore, 67 percent flow was chosen to be conservative.

DIFFERENTIAL-SPEED DYNAMIC CLUTCH OVERRIDE TEST

Both design A and B clutches were tested at 67 percent design oil flow (.54 gpm). Table VII presents drag torque and temperature data for the override test. Values presented are averages for the test; however, actual readings varied only ± 5 percent.

Inspection of the design A clutch after eight hours of differential speed testing revealed an average of .0088 inch of axial wear on the energizing coil. Figure 46 illustrates the location of wear on the coil. Figures 47 and 48 illustrate clutch component condition following test. The axial wear on the energizing coil is difficult to explain since relative sliding of the end coils is less during differential speed than during override, yet wear measured during the override testing was only .0005 inch. The wear also cannot be reconciled with the temperature readings (Table VII), which were lower than those of the overriding test at the 67 percent oil flow (.54 gpm). The drag torque readings, however, were higher during differential speed than override. The spring rate of the energizing coil is 18.5 pounds per inch, and the axial force at assembly was 1.85 pounds.

Inspection of clutch design B after completing eight hours of differential speed testing revealed .0014 inch of diametral wear on the output end of the silver-plated energizing coils. No wear was measured on the input end coils. In the differential speed mode, the design B clutch spring rotates with the input shaft; therefore, centrifugal force presses the spring ends out against the input and output shafts as rubbing takes place at the interface. The measured shaft torque, however, was only slightly higher than that of the overriding test at 67 percent oil flow (.54 gpm), and the measured temperature was slightly lower.

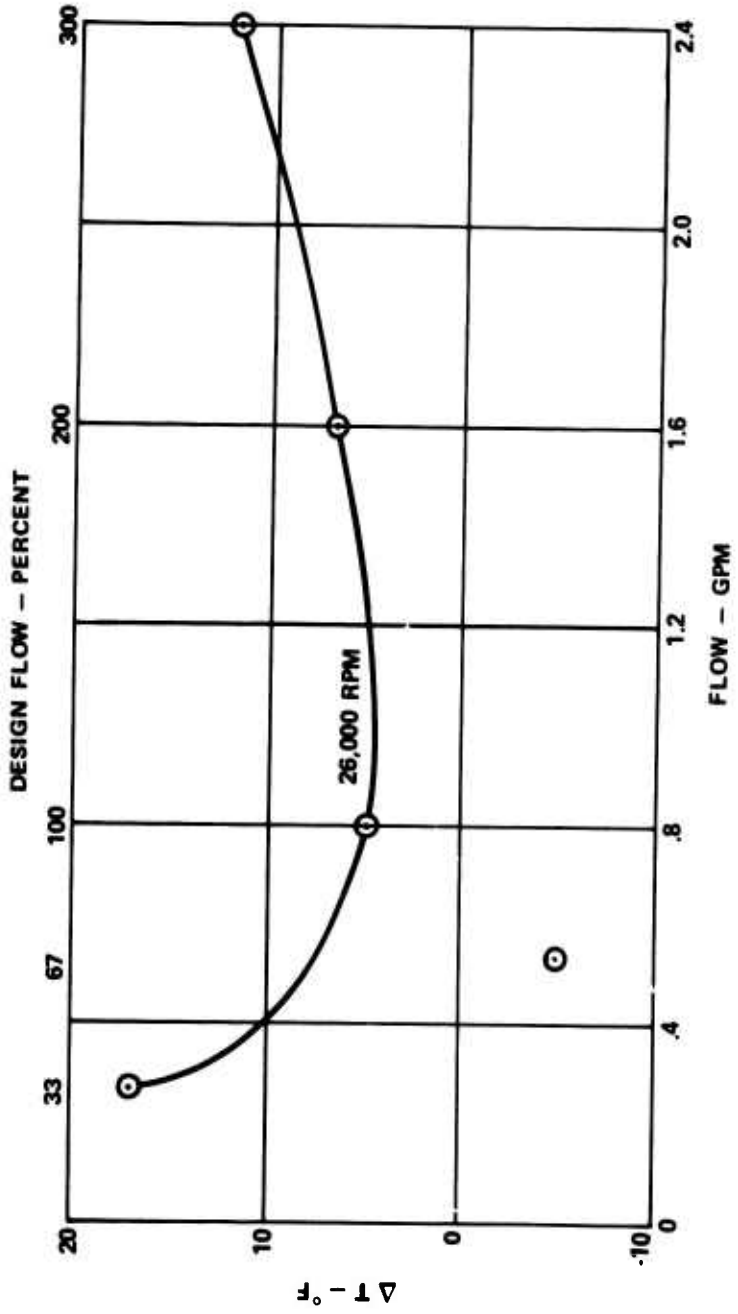

Figure 40. Oil ΔT Versus Flow, Design A.

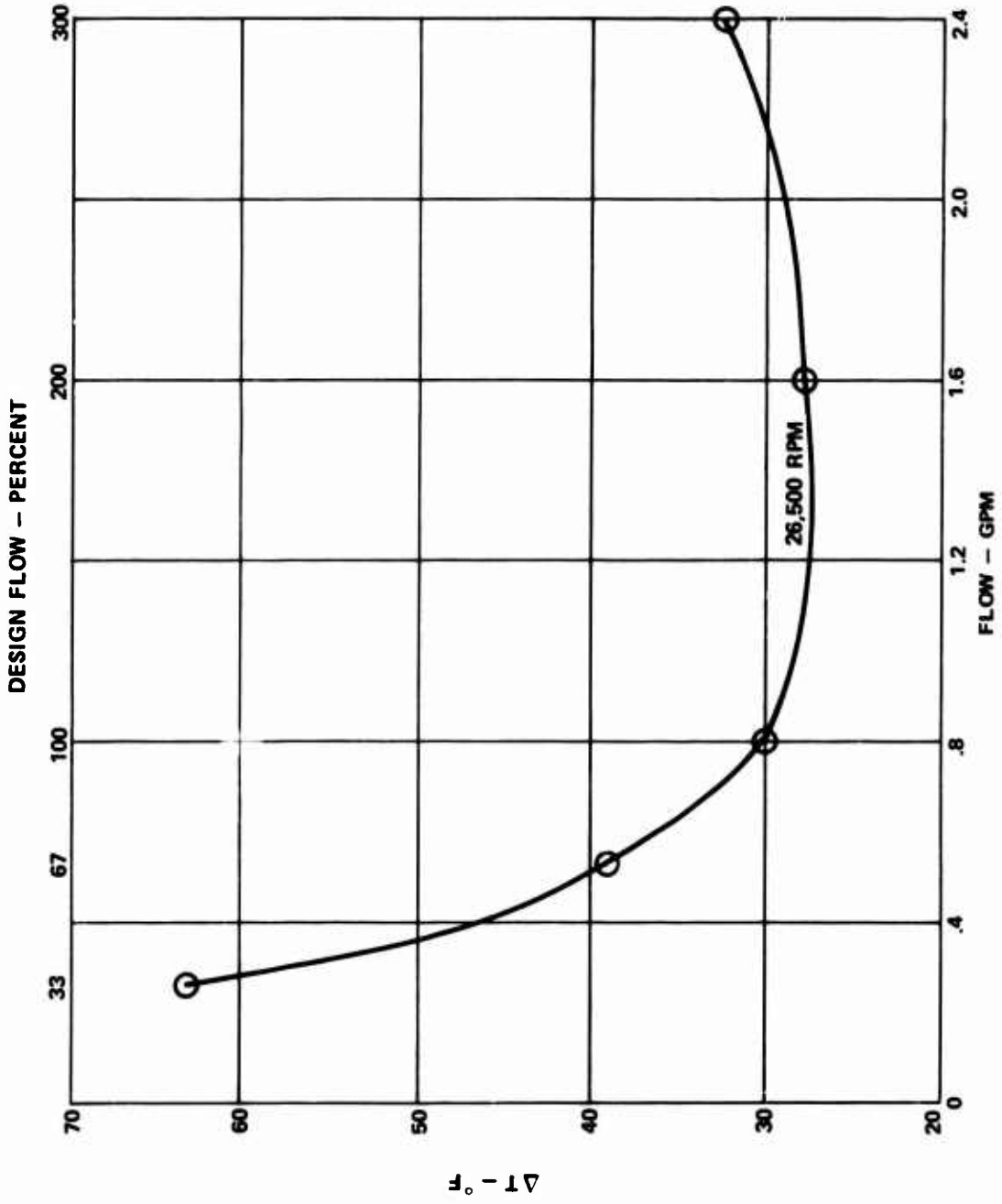

Figure 41. Oil ΔT Versus Flow, D

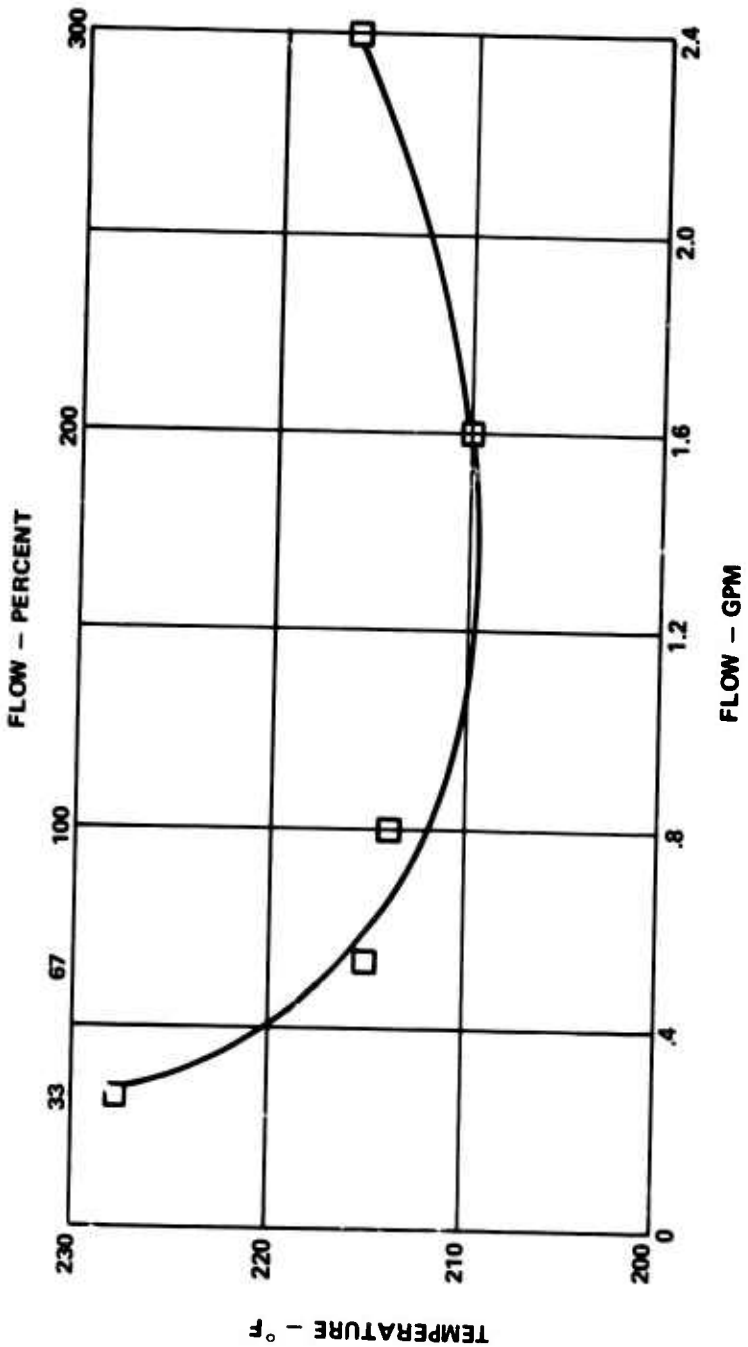

Figure 42. Energizing Coil Temperature Versus Flow, Design A.

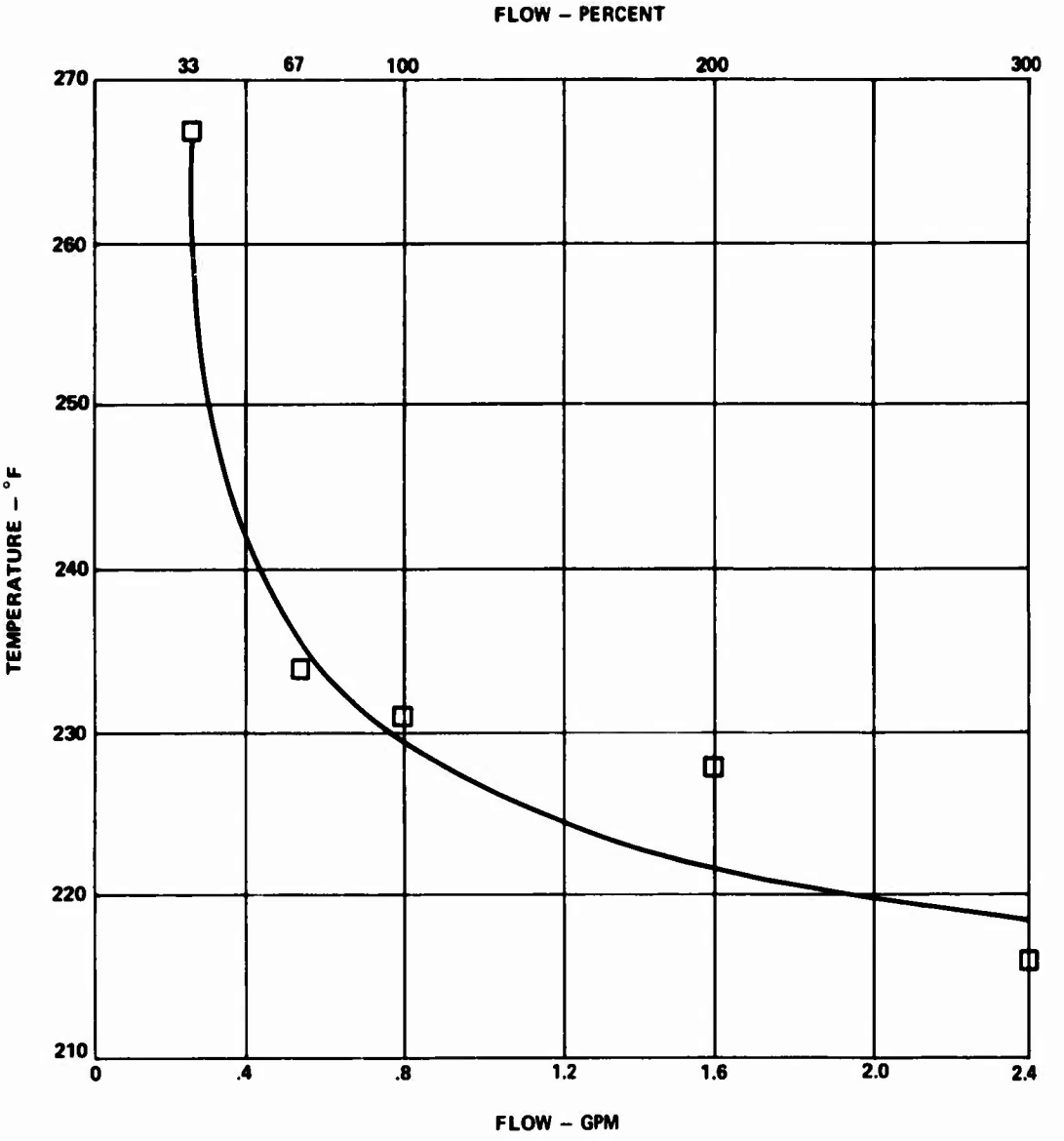

Figure 43. Energizing Coil Temperature Versus Flow, Design B.

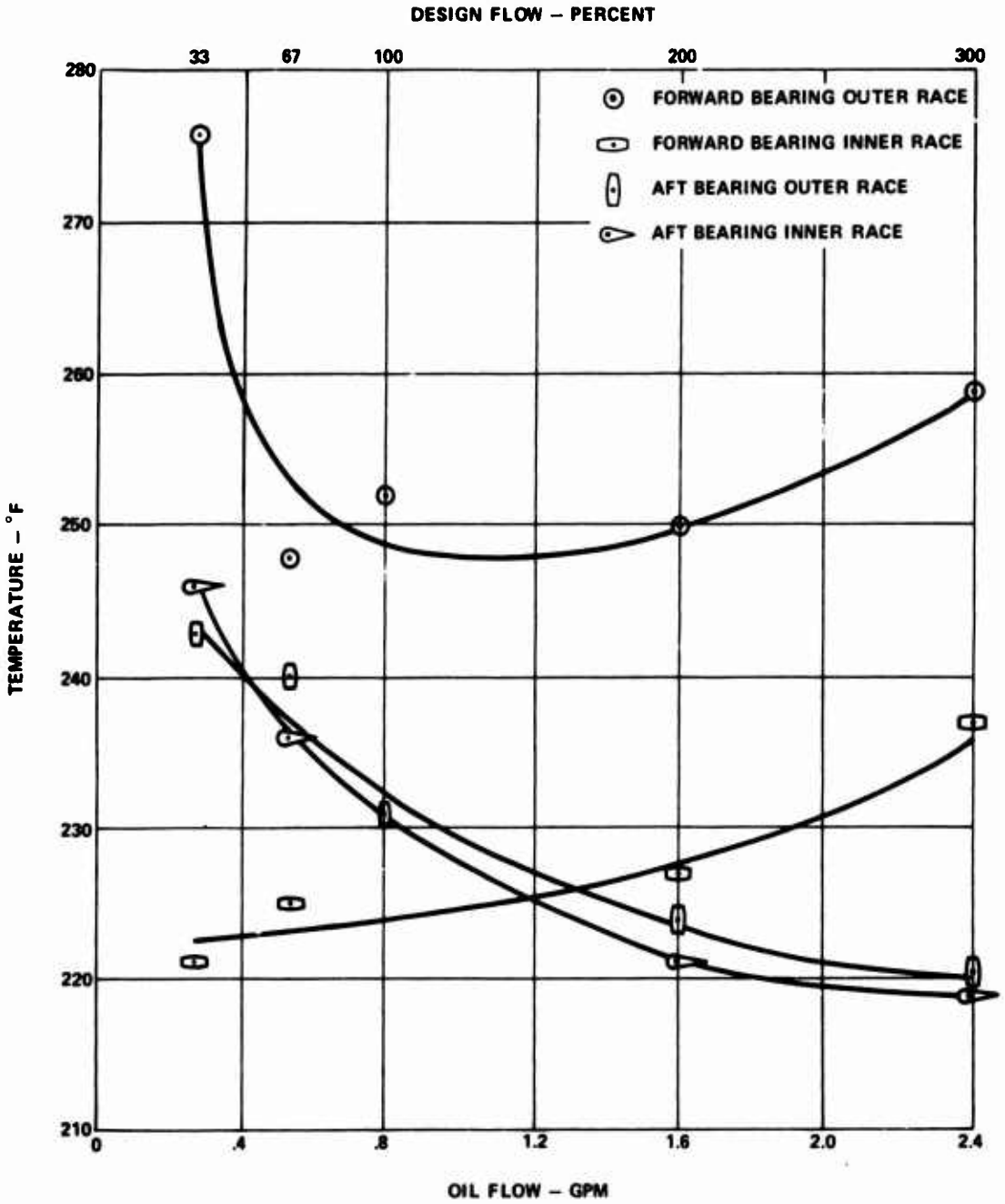

Figure 44. Bearing Race Temperatures Versus Flow, Design A.

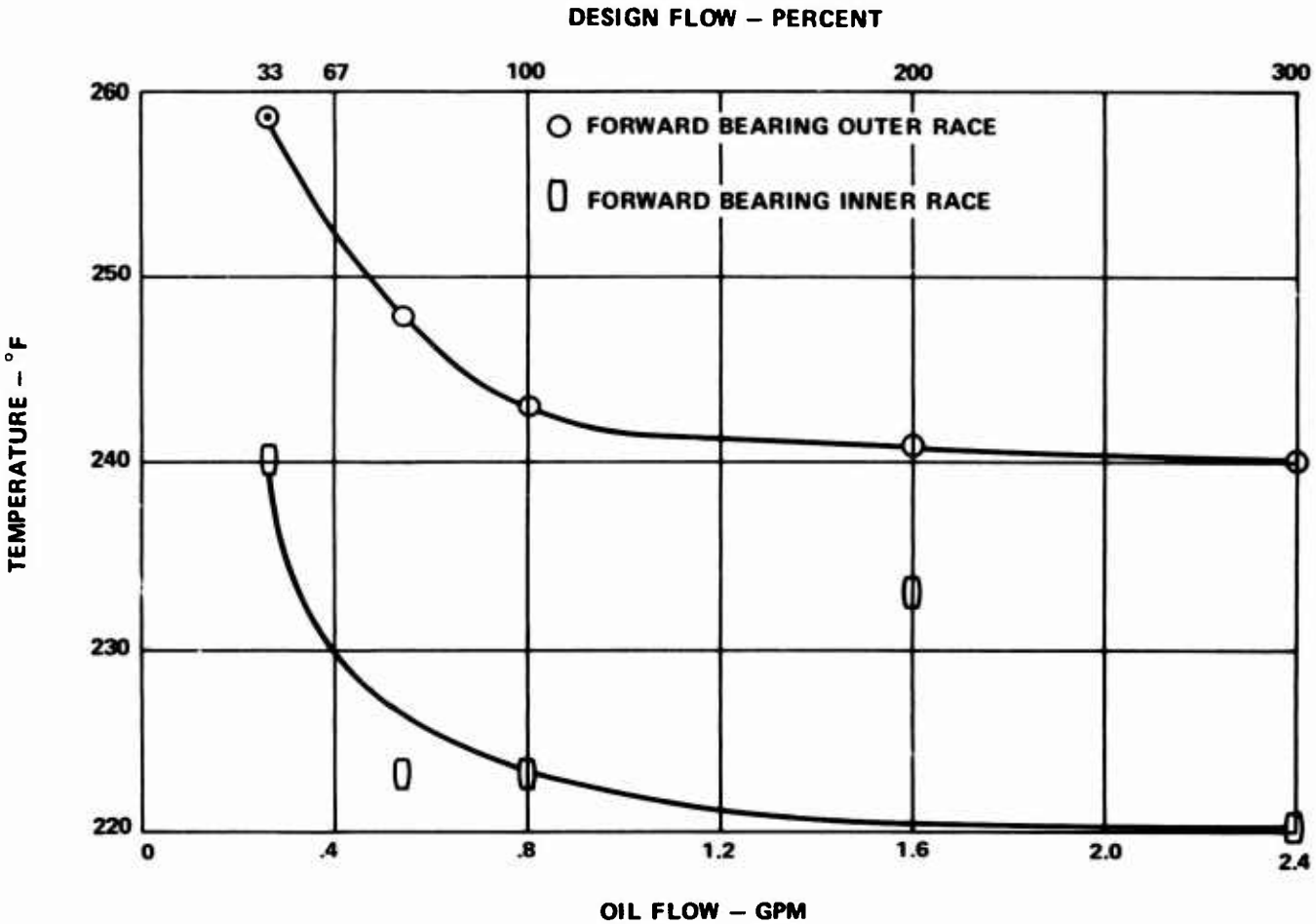

Figure 45. Bearing Race Temperatures Versus Flow, Design B.

TABLE VII. DIFFERENTIAL SPEED TEST RESULTS

Output Shaft (rpm)	Input Shaft (rpm)	Shaft Torque (in.-lb)	Energizing Coil Temperature (°F)	Time (hr)
DESIGN A				
26,500	13,250	7.0	200	6
26,500	17,755	6.6	197	1
26,500	19,875	7.3	197	1
DESIGN B				
26,500	13,250	6.6	229	1
26,500	17,755	6.9	219	6
26,500	19,875	6.9	223	1

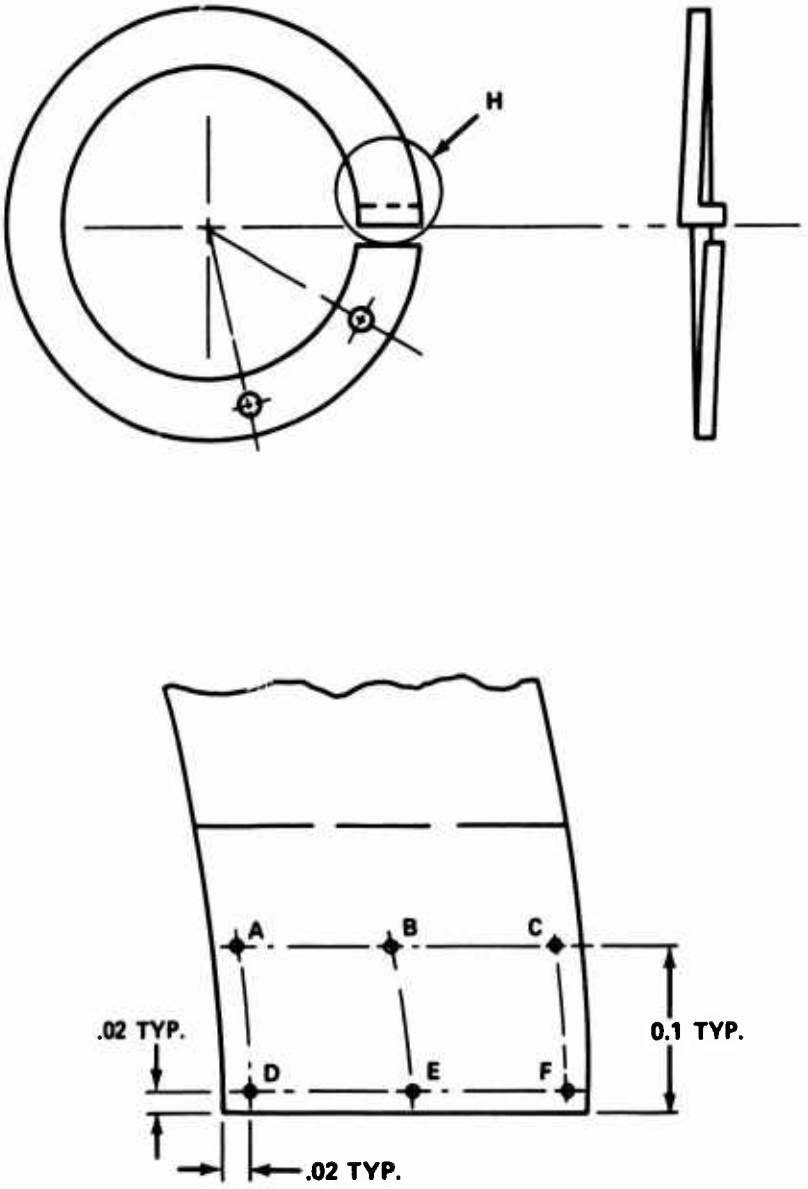

VIEW AT CIRCLE H

LOCATION OF WEAR	A	B	C	D	E	F
DEPTH OF WEAR (IN.)	.0070	.0070	.0097	.0093	.0095	.0103

Figure 46. Energizing Coil Wear Following Differential Speed Test, Design A.

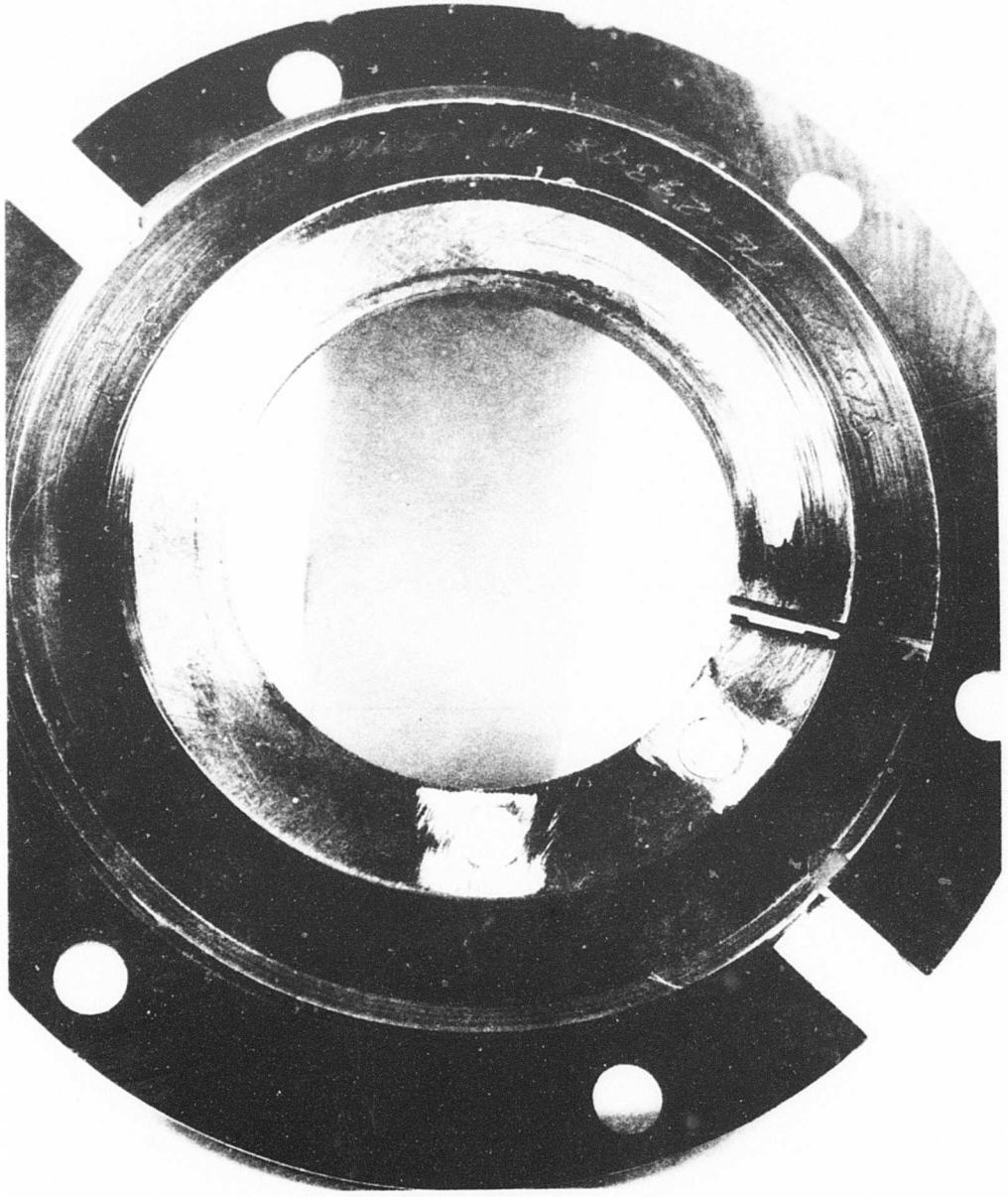

Figure 47. Energizing Coil Condition Following Differential Speed Test, Design A.

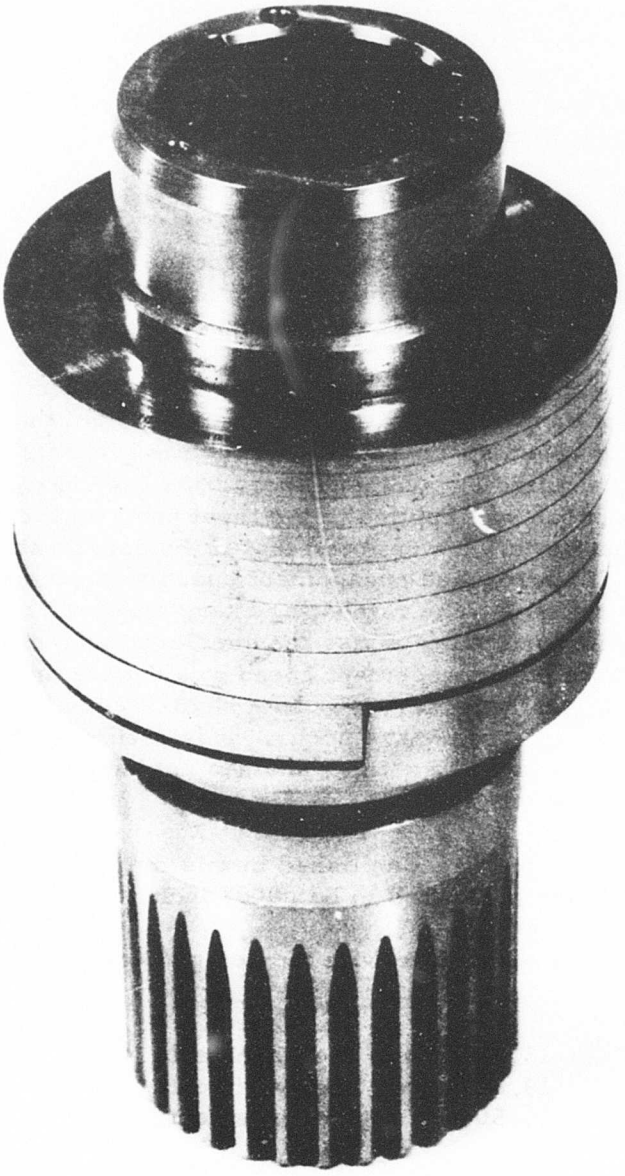

Figure 48. Spring Condition Following Differential Speed Test, Design A.

Figures 49 to 52 illustrate the clutch design B component condition after the differential speed test. In Figures 49 and 50, fretting of the spring arbor may be seen where it fits into the input shaft. In Figure 52, a light groove, .00015 inch deep, is noted where the spring contacted the output shaft. The surface roughness of the output shaft ID where the energizing coils contact increased from 5 to 15 AA as a result of differential speed operation.

DYNAMIC ENGAGEMENT TEST

The design A and B clutches that underwent the overriding and differential speed tests were used in the dynamic engagement tests. Oil flow was set at the 67 percent design flow point (.54 gpm) for both designs.

Difficulty was experienced in engaging the design A clutch. In order to effect an engagement, the test procedure was to hold the output speed at the engagement speed specified and to accelerate the input speed to approach the specified engagement speed. As the engagement sequence commenced, torque was applied to the input shaft as the output prime mover was shut down. It was found that if the acceleration rate of the input shaft as it approached engagement speed was excessive, engagement would not occur. The ratcheting energizing coil could not engage the end of the torque spring unless the acceleration rate of the input shaft as it approached engagement speed was decreasing to zero. In other words, it was necessary that both shaft speeds be approximately synchronized for engagement to occur. It is estimated that the maximum acceleration rate of the input shaft to achieve engagement was 100 revolutions per second squared.

Nine engagements were accomplished in this manner. Axial wear of the energizing coil was measured to be .0007 inch after the test.

No difficulty was experienced with the design B clutch at any of the engaging speeds:

13,250 rpm - 2 engagements
19,875 rpm - 2 engagements
26,500 rpm - 5 engagements

Figure 53 illustrates a typical engagement using an XY plotter hooked up to the input and output shaft speed signals. Note that in Figure 53 the input and output speed scales are dimensionally equal to each other. With both input and output engaged, any accelerations or decelerations

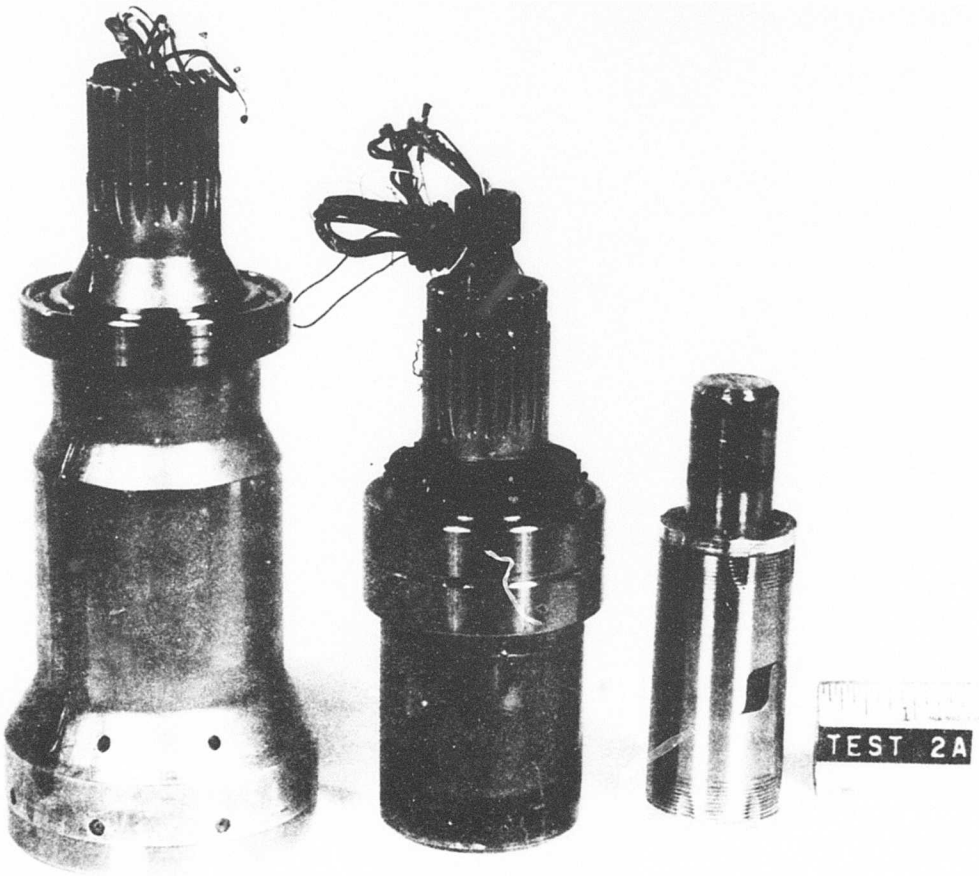

Figure 49. Design B Components Following Differential Speed Test.

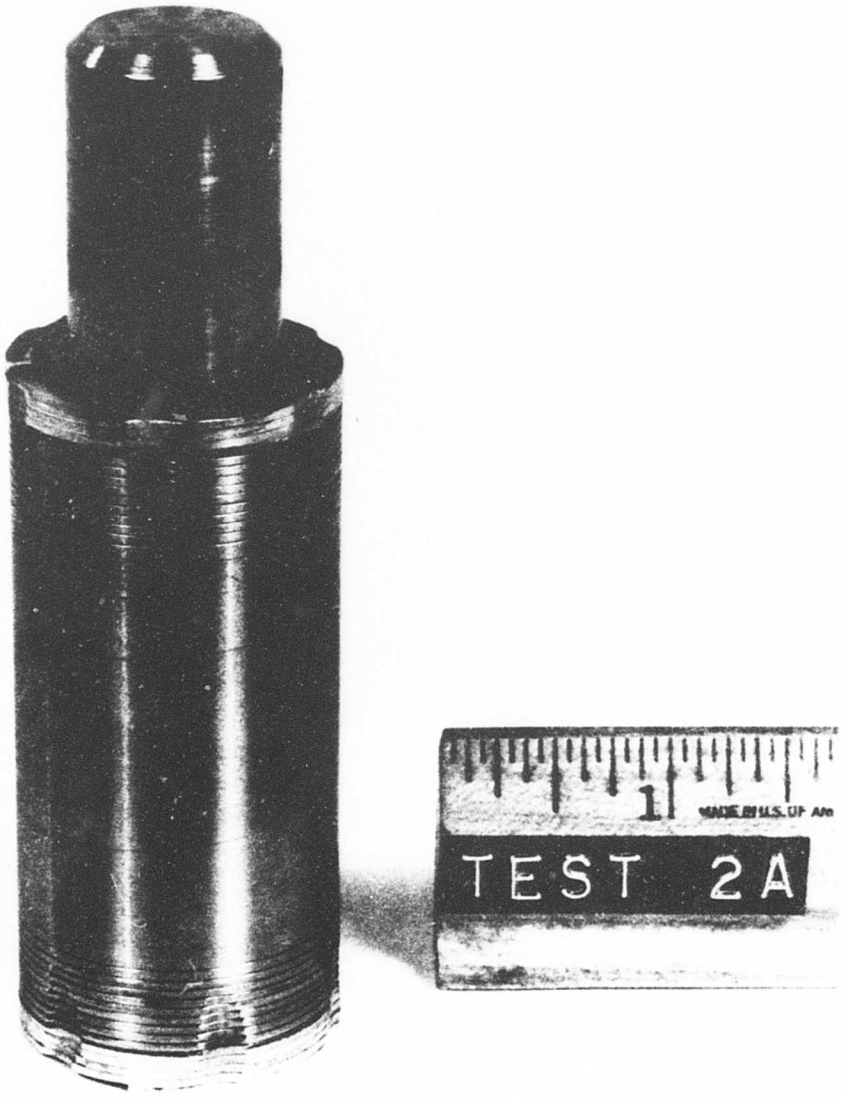

Figure 50. Design B Spring Following Differential Speed Test.

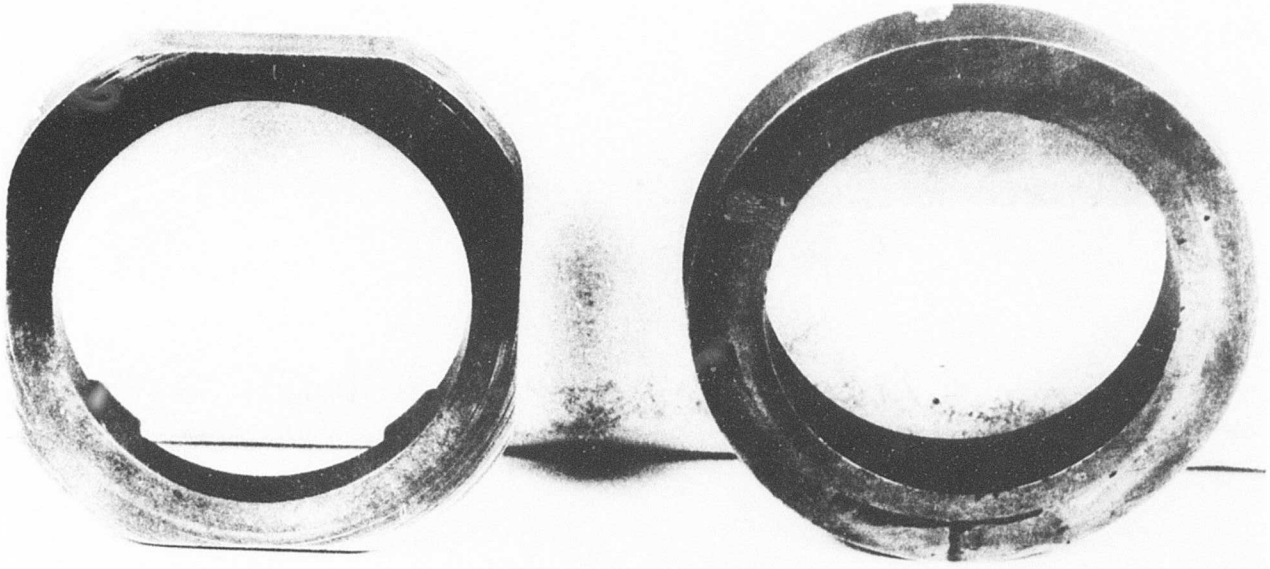

Figure 51. Design B Spacers Following Differential Speed Test.

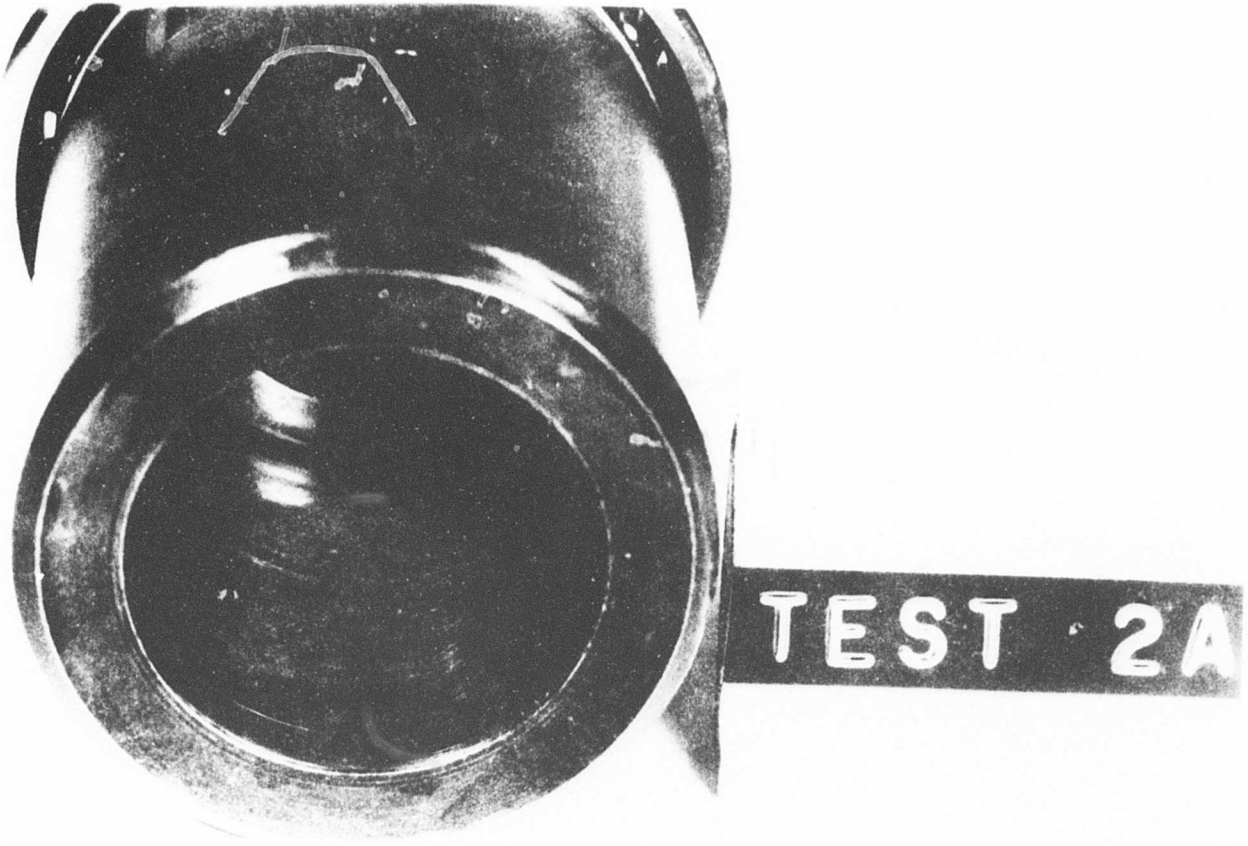

Figure 52. Design B Output Shaft Following Differential Speed Test.

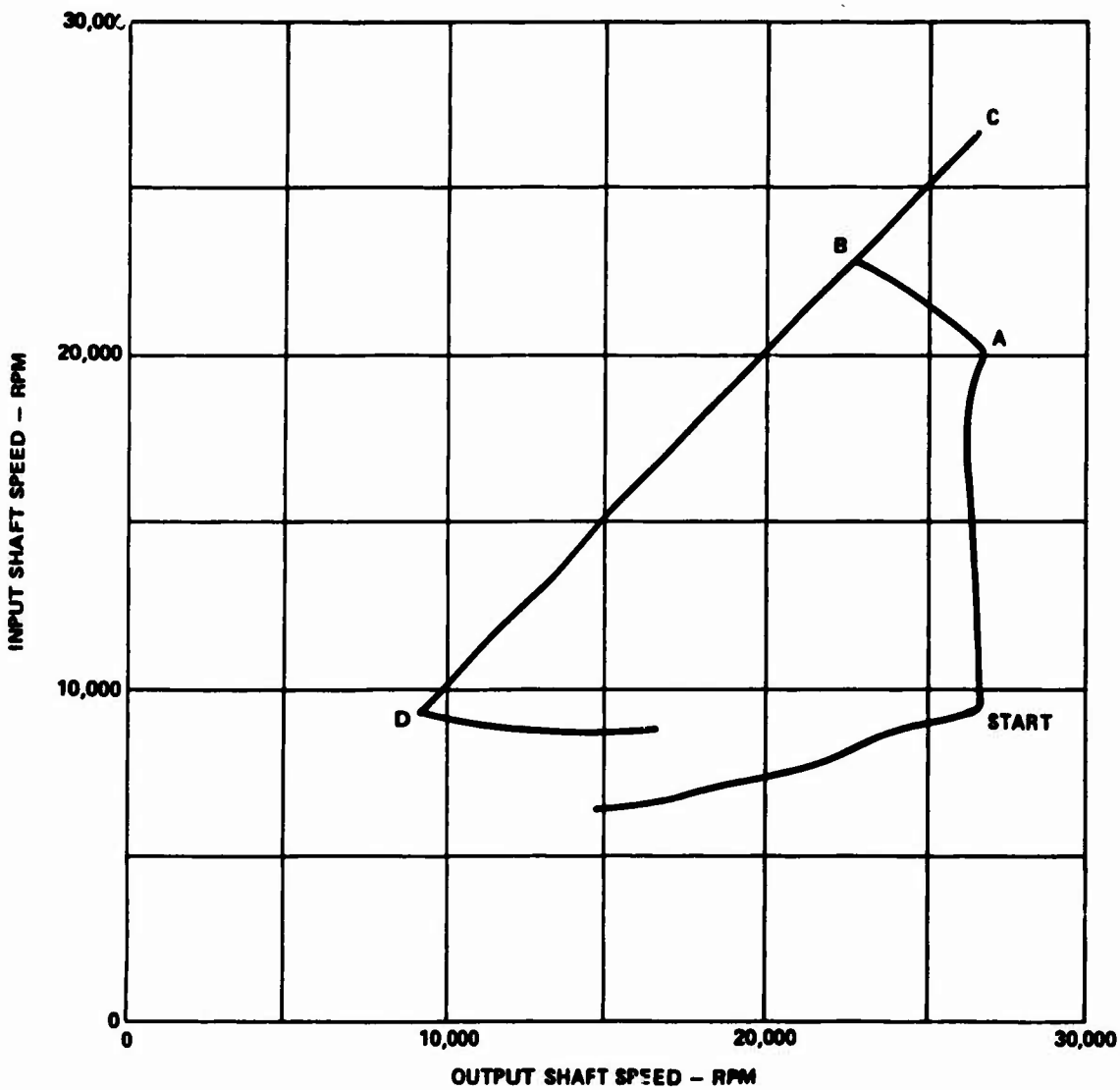

Figure 53. Plot of Dynamic Engagement, Design B.

would result in a 45-degree slope as, for example, line BD in Figure 53. The method employed to reach the start position was to accelerate the output shaft to the engaging speed specified and allow frictional torque to slowly accelerate the input shaft. At the start position, the output speed is held constant at the specified engagement speed, and the input shaft is accelerated. Engagement commences at point A with the input shaft accelerating and the output shaft decelerating. Complete engagement is at point B with both shafts at 22,700 rpm. Engagement time was approximately five seconds. The engaged clutch was then accelerated along the 45° slope to point C, 26,500 rpm. In order to effect a disengagement, the input shaft prime mover was shut down and then put into reverse as torque was applied to the output shaft. In Figure 53, disengagement occurs at point D, 9,300 rpm. Diametral wear of the energizing coils was found to be .0001 inch upon completion of the engagement tests.

STATIC CYCLIC TORQUE FATIGUE TEST

Three separate fatigue tests were conducted on the design A clutch; all of them resulted in failures.

The first test was conducted with a design clearance of .020 inch between the spring OD and the drum ID. The test was conducted for 10^7 load cycles with no indication of trouble. Upon disassembly, it was found that the output shaft had cracked at the lug area (Figure 54). The appearance of the fracture pattern was fatigue in nature (clamshell patterns), emanating from two origins located at the fillets between the lug end stop for the spring and adjoining shaft material. A detailed analysis of the complex stress situation in the vicinity of the lug is presented in Appendix IV.

After the first failure, the output shaft was redesigned with an increased cross section through the failed area and an increased fillet radius. Figure 55 illustrates the changes. The first fatigue test of the redesigned clutch was conducted with a clearance of .087 inch between the spring OD and the drum ID. This was the clearance found to be required to preclude interference up to 26,000 rpm. As torque was applied at the beginning of the fatigue test, the spring failed at an applied static torque of 490 inch-pounds (Figure 56). The tensile stresses at the energizing end coil due to the energizing moment had exceeded the yield point of the material.

Mag. 2X

Figure 54. Design A Fatigue Test Failure 1.

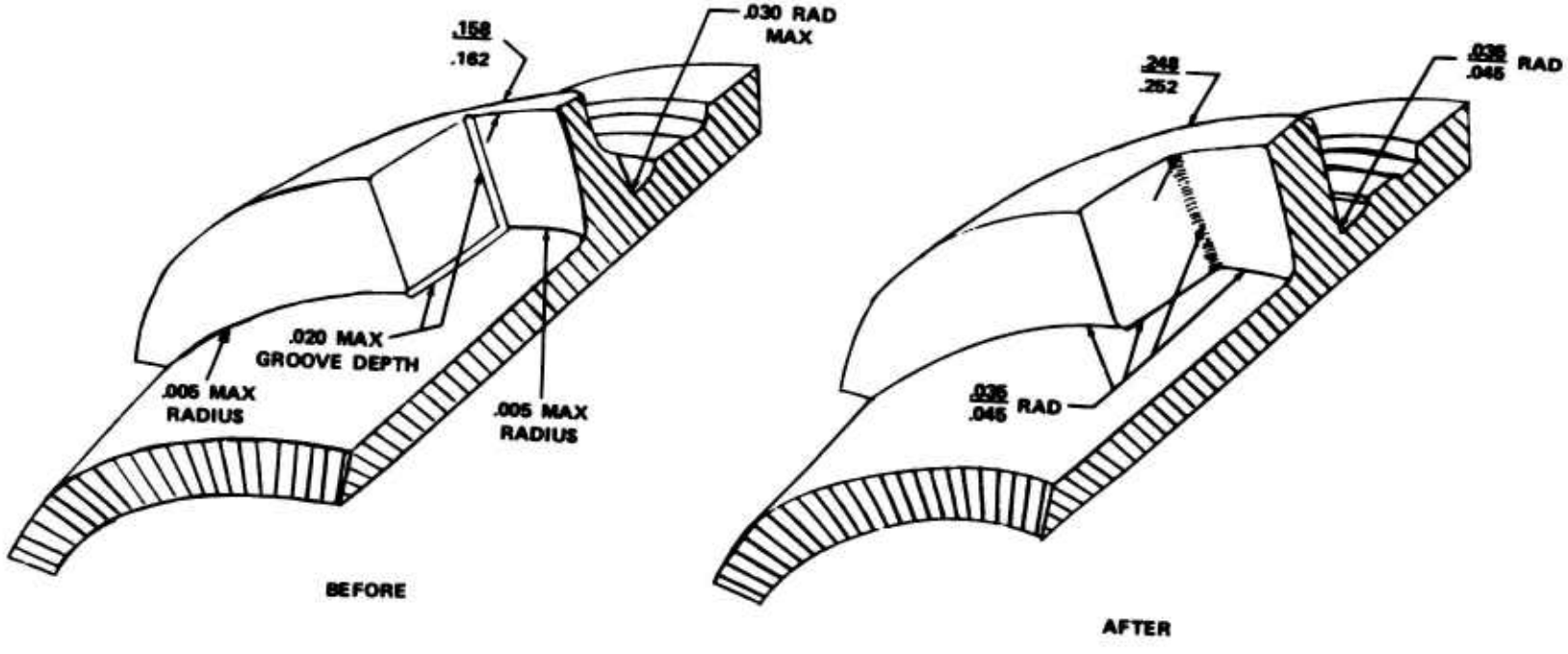

Figure 55. Redesign of Design A.

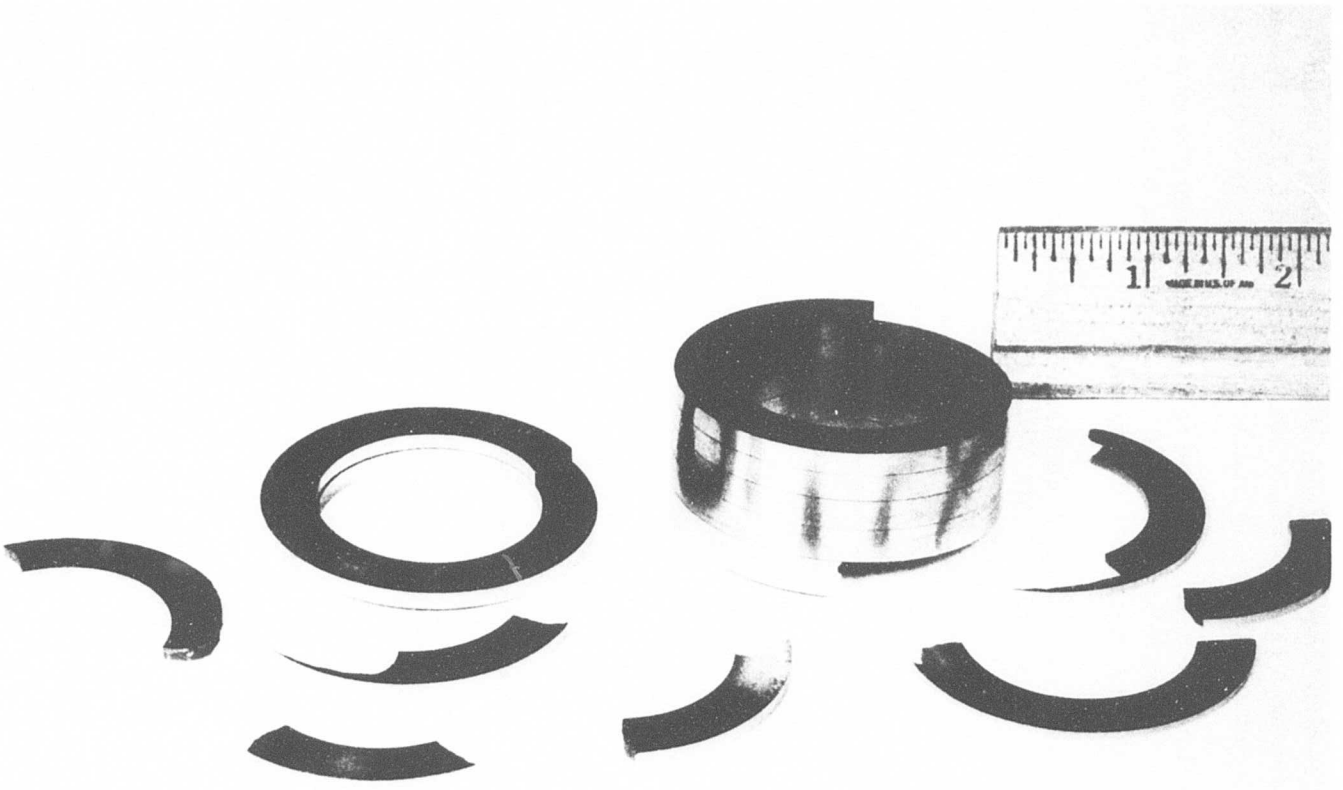

Figure 56. Design A Fatigue Test Failure 2.

A third test was set up with the redesign incorporating a static clearance of .020 inch. A clutch operating with this static clearance would be limited to 23,000 rpm (Figure 13). This test achieved 6.7×10^6 load cycles, when another failure was discovered at the lug area (Figure 57).

Two design B clutches were subjected to the cyclic fatigue test, and both survived 7140 ± 900 inch-pounds for 10^7 cycles with no failures. Magnaflux inspection showed no crack indications.

Angular displacement and outer race diametral growth for both design A and B clutches are listed in Table VIII.

TABLE VIII. CONDITIONS AT MAXIMUM CYCLIC FATIGUE TORQUE, 8040 INCH-POUNDS

Design	Angular Displacement (Deg)	Diametral Growth (In.)
A	26.0	.0012
A	52.8	.0010
B	58.1	.0023
B	65.9	.0020

After the cyclic torque fatigue tests, fretting of the bearing races was noted.

Fretting which could be felt with a .020-inch probe was evident on the inner race of the design A ball bearing (Figure 58). A similar condition was noted on the roller bearing races which was not considered detrimental.

One of the two design B ball bearings showed slight indications of fretting on the inner race (Figure 59).

The fretting experienced may not be representative of an actual application since lubrication conditions would be better in a rotating installation.

Figure 57. Design A Fatigue Test Failure 3.

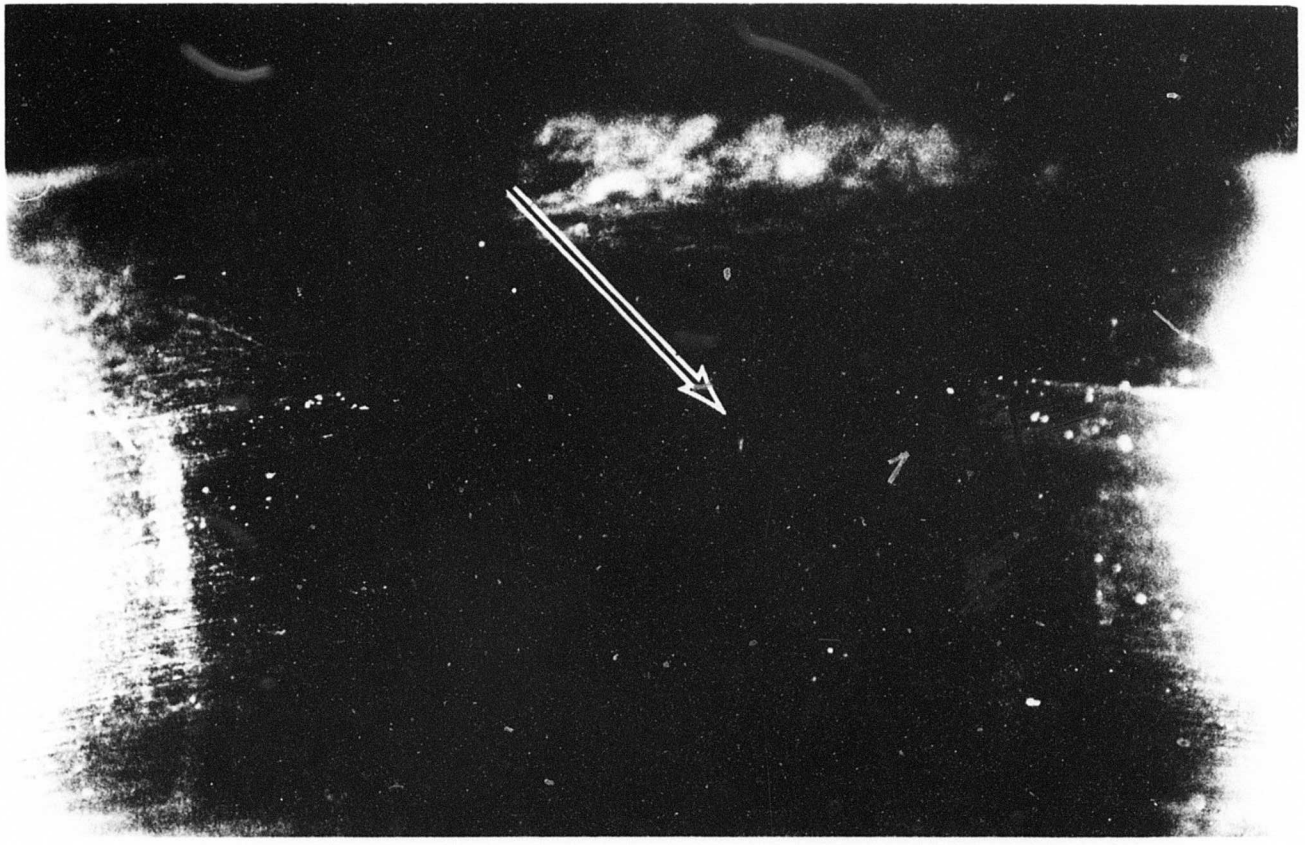

Figure 58. Bearing Fretting, Design A.

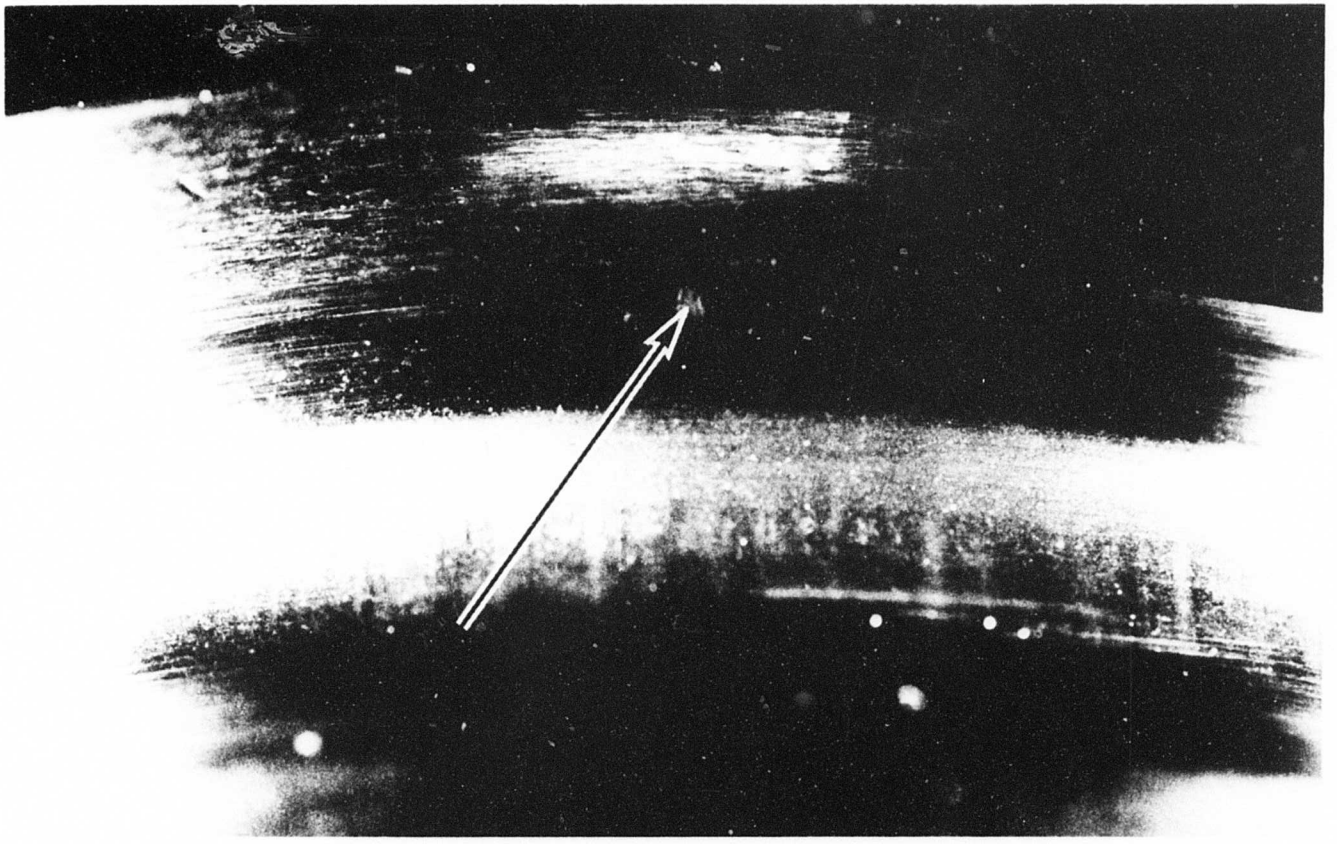

Figure 59. Bearing Fretting, Design B.

Bearing fretting in an application could be forestalled by investigating four areas of improvement:

1. Coating of the bearing races with a dry lubricant

2. Use of dissimilar materials in the bearing balls and races

3. Surface hardening of the balls or races, using such processes as nitriding or chromizing

4. Use of journal or roller bearings.

STATIC OVERLOAD TEST

Only the design B clutch was subjected to the overload test. Design A hardware was not available because of the cyclic fatigue failures.

Two design B clutches were tested to 18,000 inch-pounds without any difficulty. Magnaflux inspection revealed no cracks.

The diametral growth of the output shaft measured during the overload test is shown in Figure 60. The angular displacement of the input shaft versus the output shaft during the overload test is shown in Figure 61. It must be noted that the angular displacement plotted includes windup of the inner and outer race shafts.

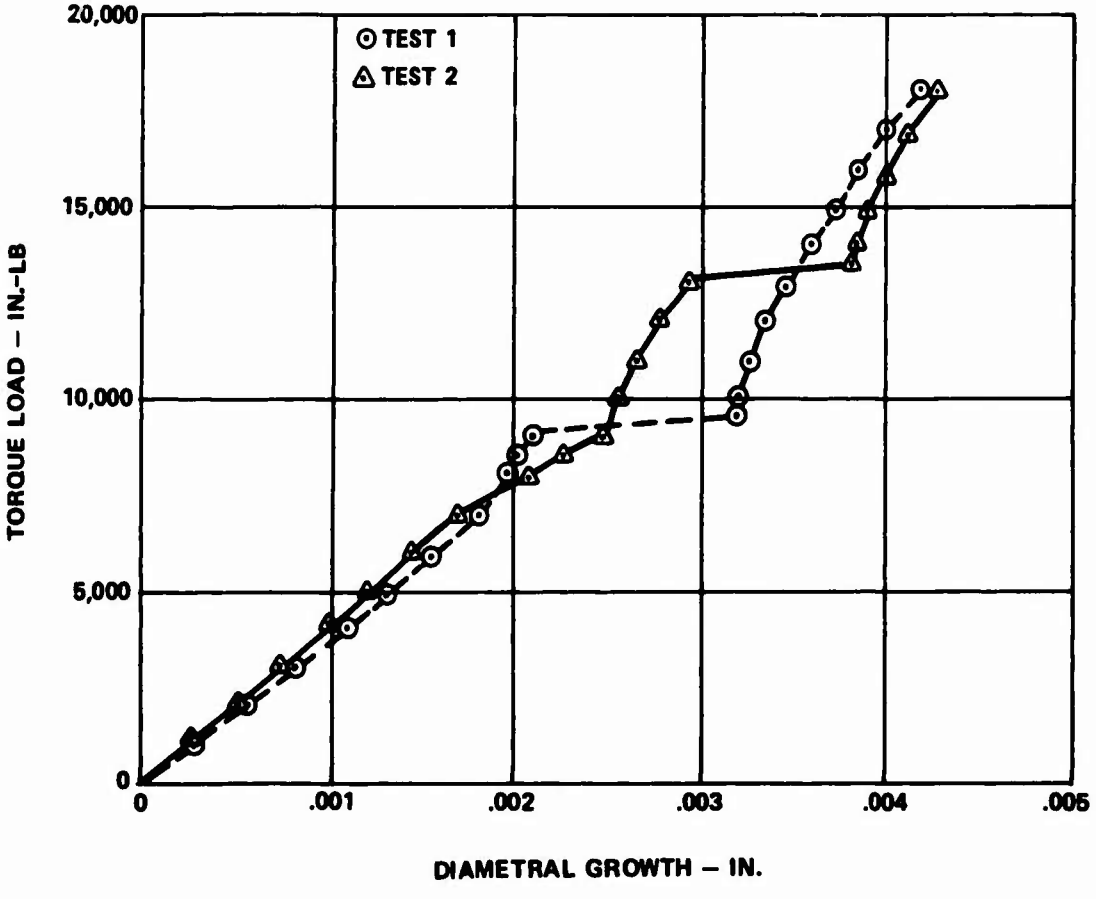

Figure 60. Diametral Growth of Output Shaft, Design B.

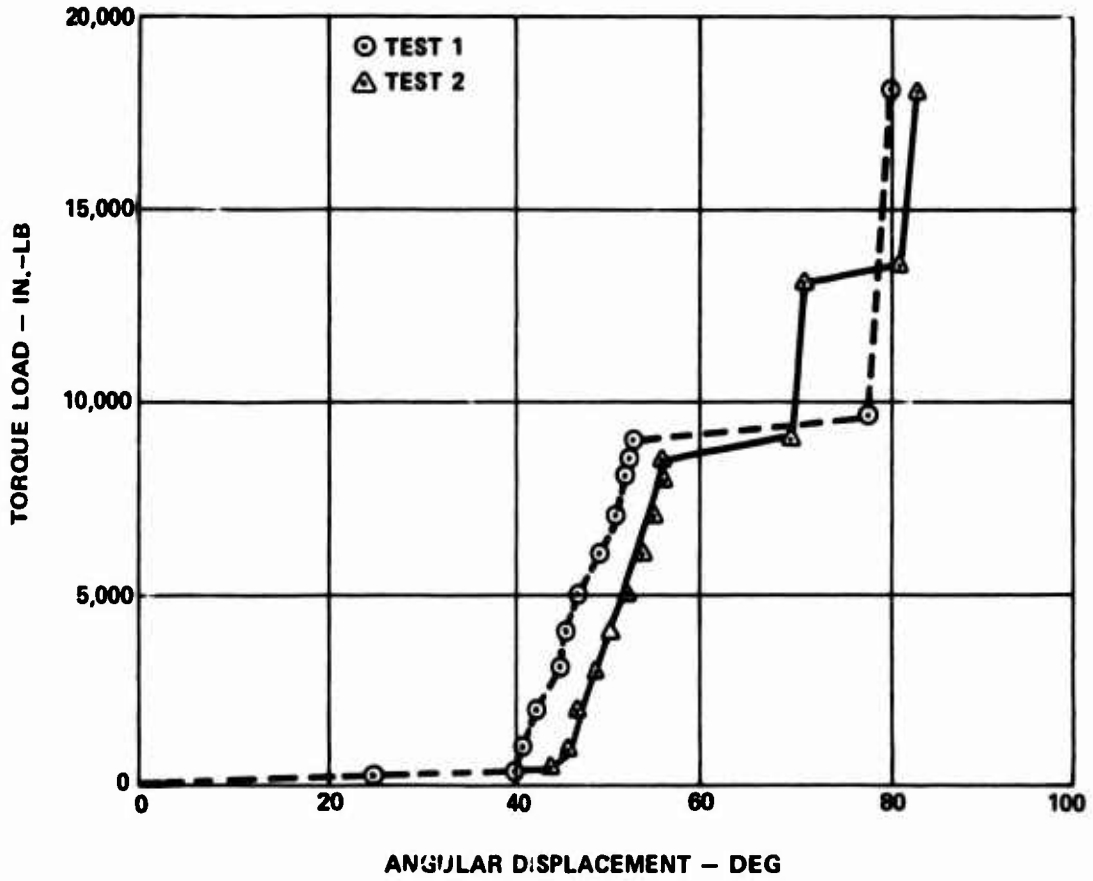

Figure 61. Angular Displacement of Output Shaft, Design B.

METALLURGICAL STUDY

DESIGN A

The clutch spring, energizing coil, and input and output shafts were sectioned and analyzed to determine metallurgical characteristics. Laboratory measurements for the case-carburized input and output shafts are listed in Table IX.

TABLE IX. METALLURGICAL RESULTS, CASE-CARBURIZED RACES, DESIGN A

	Case Depth (in.)	Case Hardness (Rc)	Core Hardness (Rc)	Remarks
Input Shaft	.064	65	33.8	Retained Austenite in case, approx. 10% Required case hardness is 60-63 Rc
Output Shaft	.039	63.5	40	Required case depth is .050-.065 in.

Shaft case hardness versus depth is shown in Figure 62. The spring and energizing coil were made of through-hardened Vascomax 350. The hardness of each was Rc 57. The chemical composition of the springs is listed in Table X.

DESIGN B

The clutch spring and the input and output shafts were made of through-hardened H-11 steel. Hardness of all components was found to be Rc 56-57. No destructive tests were performed in order to preserve clutch hardware.

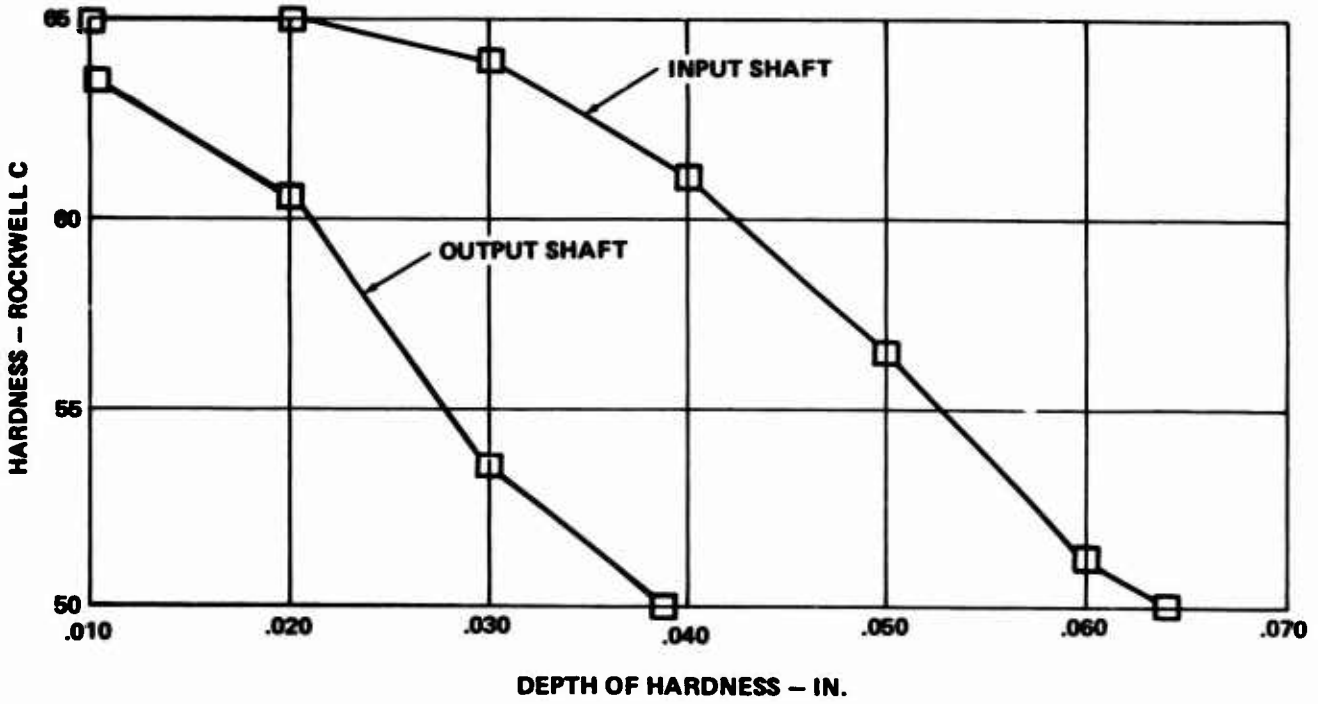

Figure 62. Case Hardness Versus Depth, Input and Output Shafts, Design A.

TABLE X. CHEMICAL COMPOSITION VASCOMAX 350 (PERCENTAGE BY WEIGHT)

Element	Nominal Value	Actual Value	
		Spring Clutch	Energizing Coil
Carbon	0.03 max	0.04	0.01
Nickel	18.00	19.50	19.20
Cobalt	11.80	12.70	12.80
Molybdenum	4.60	5.00	4.90
Titanium	1.35	1.50	1.40

CONCLUSIONS AND RECOMMENDATIONS

CLUTCH DESIGN A

Testing of clutch design A revealed serious failings as follows:

1. The lug on the clutch output shaft presents a critical stress problem. The potential for crack propagation in the fillet areas is great, and much care must be taken in the design of this region. Possibly shot peening would be beneficial.

2. The mathematical model predicting spring growth due to centrifugal force is not accurate. Additional analytical and experimental work is required to properly define clutch geometry. The critical dimension is the gap between the spring outside diameter and the drum inside diameter. It must be small enough to enable the spring to wind into the drum without failure, yet large enough so that the spring outside diameter will not touch the drum inside diameter during full-speed overriding.

3. The inability of the clutch to consistently engage indicates that a redesign is required at the energizing coil end. Increasing the axial spring force will improve the engaging characteristics of the clutch but will lead to more wear during overriding and differential speed operation.

CLUTCH DESIGN B

Clutch design B successfully completed all tests. Oil flow requirements were found to be low: 0.54 gpm. Maximum drag torques were in the order of 8 inch-pounds.

It is recommended that this configuration be endurance tested in the override and differential speed modes of operation to determine the extent of wear that will occur on the silver-plated energizing end coils. Excessive wear will ultimately affect the clutch's ability to engage.

GENERAL

Test results suggest that spring clutches can operate successfully at the design conditions of 1500 hp and 26, 500 rpm.

Design B was satisfactory in every respect, and the design principles are adaptable to other operating conditions.

With extensive development, the weak points uncovered in design A could be corrected and successful operation at the design point achieved. However, more analytical and experimental work is required to apply the design A principles to other applications with confidence.

APPENDIX I
COMPUTER PROGRAM

This computer program was written specifically for a one-way, variable-lead, spring-type overriding clutch affixed to the output shaft. The program calculates the pertinent spring torque and stress data for each coil from energizing lug end to output torque lug end. In addition to this information, the program also prints out the energizing moments, shaft shear stress, and drum hoop stress.

The spring, being fixed to the output shaft, will grow radially outward due to centrifugal force during override and differential speed modes of operation. In order to minimize this growth, the spring is designed to be assembled with a press fit onto the output shaft. Also, an initial clearance between the spring outside diameter and drum inside diameter is assumed so that the spring will not rub into the drum during override.

The subject program is written in FORTRAN IV language and was developed on an IBM 370 system, model 155 computer. Computer running time is five seconds for compile and link edit, and one second per executable case.

INPUT DATA

Card One - Format (IX, 79H)

Identification

Card Two - Format (8F10.8)

Word 1: Speed (rpm)
Word 2: Torque (in.-lb)
Word 3: Number of coils
Word 4: Spring radial height (in.)
Word 5: Spring width, energizing coil (in.)
Word 6: Spring width, last coil (in.)
Word 7: Mean spring diameter in the free state (in.)
Word 8: As-assembled diametral clearance between spring OD and drum ID (in.)

Card Three - Format (8F10.8)

Word 1: Inner shaft diameter (in.)
Word 2: Outer drum diameter (in.)
Word 3: Coefficient of friction between spring and drum for torque transmission

OUTPUT DATA

The computer program output data is shown in Figure 63. The significance of each term is explained as follows:

SPEED, COEFFICIENT OF FRICTION, SPRING HEIGHT, TORQUE -

All of these values are input data: Card 2 Word 1, Card 3 Word 3, Card 2 Word 4, and Card 2 Word 2, respectively.

MODULUS OF ELASTICITY - This value is set as a constant in the early part of the program using the FORTRAN symbol "ELSMOD."

SPRING WIDTH - MEAN - The arithmetical average of the energizing and last coil widths given as input. This value is used to calculate the energizing moment to reduce the drum clearance to zero (M_{CL})*.

INITIAL DRUM CLEARANCE - SPRING OD TO DRUM ID (Δ_{CL}) - Input value Card 2, Word 8.

MEAN SPRING DIA. - FREE (D_{MF}) - Input value Card 2, Word 7.

SPRING DIA. INCREASE - SPEED (Δ D) - Growth of the free torque spring due to centrifugal force. This value is equal to the assembled press fit between the spring and output shaft so that the spring will not grow radially outward away from the shaft at the design point overide speed.

MEAN SPRING DIA. - EXPANDED (D_{ME}) - The mean diameter of the spring as assembled onto the output shaft. This value is the sum of the free-state mean diameter of the spring, plus the amount of design press fit.

SPRING UNWIND ANGLE - INTERFERENCE (θ_D) - The amount the spring must unwind to reduce the press fit to zero.

*Symbols in parentheses are defined in the "Clutch Analysis" section of this report.

SPEED %RPM<	26500.0000000	TORQUE %IN LBS<	3570.0000000
COEFFICIENT OF FRICTION	0.1000000	MODULUS OF ELASTICITY %PSI<	29 MILLION
SPRING HEIGHT %IN<	0.3600000	SPRING WIDTH-MEAN %IN<	0.1500000
INITIAL CLEARANCE-SPRING O.D. TO DRUM I.D. %IN<	0.0170000	MEAN SPRING DIA.-FREE %IN<	1.8030000
SPRING DIA. INCREASE-SPEED %IN<	0.0206491	MEAN SPRING DIA.-EXPANDED %IN<	1.8236491
SPRING UNWIND ANGLE-INTERFERENCE %DEG<	32.6100915	ENERGIZING MOMENT-INTERFERENCE %IN LBS<	193.1147420
SPRING UNWIND ANGLE-CLEARANCE %DEG<	26.5993124	ENERGIZING MOMENT-CLEARANCE %IN LBS<	155.7357343
TOTAL SPRING UNWIND ANGLE %DEG<	59.2094039	TOTAL ENERGIZING MOMENT %IN LBS<	348.8504763

COIL NUMBER	GAIN PER COIL	PER-CENT GAIN IN TORQUE CARRYING CAPACITY %OUTER SURFACE<	TORQUE THROUGH OUTER SURFACE %IN-LBS<	TORQUE THROUGH COIL %IN-LBS<	AXIAL WIDTH PER COIL %IN<	TOTAL STRESS PER COIL %PSI< OUTER	INNER	DRUM HOOP STRESS PER COIL PSI
END-LUG	1.000	-----	0.0	23.424	0.050	-109083.9	106255.9	0.0
1	1.874	0.57	20.484	43.908	0.075	-109436.9	105902.9	18502.1
2	3.514	1.08	38.395	82.303	0.100	-110154.0	105185.8	18936.3
3	6.586	2.02	71.971	154.274	0.125	-111395.0	103944.8	19687.8
4	12.345	3.78	134.906	289.179	0.150	-113488.7	101851.1	20955.5
5	23.141	7.08	252.875	542.054	0.175	-117018.8	98321.0	23093.0
6	43.376	13.28	474.002	1016.056	0.200	-123003.5	92336.3	26716.7
7	81.307	24.89	888.496	1904.553	0.225	-133218.5	82121.3	32901.9
8	152.406	46.65	1665.447	3570.000	0.250	-150770.6	64569.2	43529.7

SHAFT I.D./O.D. %IN<	1.000/ 1.464	SHAFT SHEAR STRESS %PSI<	7414.2
SPRING I.D./O.D. %IN<	1.443/ 2.163	SPRING COMPRESSIVE STRESS-ENERGIZE (PSI).	-21058.4
DRUM I.D./O.D. %IN<	2.201/ 3.120	SPRING BENDING STRESS COMPONENT %PSI<	107669.9
		DRUM HOOP STRESS-MAX (PSI)	43529.7

Figure 63. Computer Program Output Data, Clutch Design A.

ENERGIZING MOMENT - INTERFERENCE (M_D) - The moment required to reduce the press fit to zero. This value is based on the mean spring width of the variable-lead coil and as such is somewhat conservative.

SPRING UNWIND ANGLE - CLEARANCE (θ_{CL}) - The amount the spring must unwind to reduce the initial clearance between the assembled spring OD and drum ID to zero.

ENERGIZING MOMENT - CLEARANCE (M_{CL}) - The moment required to reduce the initial clearance between the assembled spring OD and drum ID to zero.

TOTAL SPRING UNWIND ANGLE - The sum of (θ_D) and (θ_{CL}).

TOTAL ENERGIZING MOMENT - The sum of (M_D) and (M_{CL}). Note: If the system is started from rest, the total energizing moment will be required to unwrap the spring off of the shaft and into the drum. In a twin-engine installation with one engine already in operation, only the energizing moment to reduce the initial clearance to zero, (M_{CL}), will be required for energization, since the output shaft is already overriding at speed when the second engine is being started up. Hence, the speed of the output shaft provides the centrifugal force necessary to reduce the press fit to zero, and the energizing moment (M_D) need no longer be supplied by the second engine.

The next section of data, presented in tabular form, deals with the transmittal load capabilities and stresses in each coil.

COIL NUMBER - The coils are numbered for each full revolution starting with the END-LUG or energizing end.

GAIN PER COIL - The amplification factor for each successive spring coil as defined in the "Clutch Analysis" section.

PERCENT GAIN IN TORQUE CARRYING CAPACITY (Outer Surface) -

$$\frac{G_i - G_{i-1}}{G_n} \times 100$$

where G_i = gain of the coil in question
G_{i-1} = gain of the preceding coil
G_n = total gain of the spring

TORQUE THROUGH OUTER SURFACE (See Figure 64) - The amount of torque that each coil carries through its outside diameter and is equal to the PERCENT GAIN for that coil multiplied by the total transmitted torque.

TORQUE THROUGH COIL (See Figure 64) - The amount of torque being transmitted through the cross section of each coil. The value for the END LUG is found by dividing the total transmitted torque by the total gain of the spring.

$$\text{Example: } \frac{3,570}{152.406} = 23.424 \text{ in.-lb}$$

The torque through each succeeding coil is found by adding the torque through the preceding coil to the torque through the outer surface of the coil in question; i.e., for coil number 3: 82.303 + 71.971 = 154.274 in.-lb.

AXIAL WIDTH PER COIL - The width of each succeeding coil is based on an arithmetical progression with the coils becoming wider towards the output lug end. This was done to make the stresses in each coil more nearly equal and thus conserve axial space.

TOTAL STRESS PER COIL - The stress in the inner and outer surfaces of the coil at any section is comprised of a bending component and a compressive component as derived in Figure 11 of the "Clutch Analysis" section. The bending component (107,669 psi) has been previously calculated for the energizing coil end based on an energizing moment of 348.85 in.-lb. This energizing moment is the amount of torque it takes to unwrap the spring into the drum. The bending stress component, therefore, is constant regardless of the torque being transmitted through the coils, provided that the spring stays wrapped into the drum. The bending component produces tension in the inner surface and compression in the outer surface of the spring.

The compressive component varies for each coil because the torque through the coils varies from 23.42 in.-lb at the energizing end lug to 3570.00 in.-lb at the output end lug; and at the same time, the coil width increases. The compressive component produces compression in both the inner and outer surfaces of the spring.

As an example, the compressive component will be calculated for coil number 3:

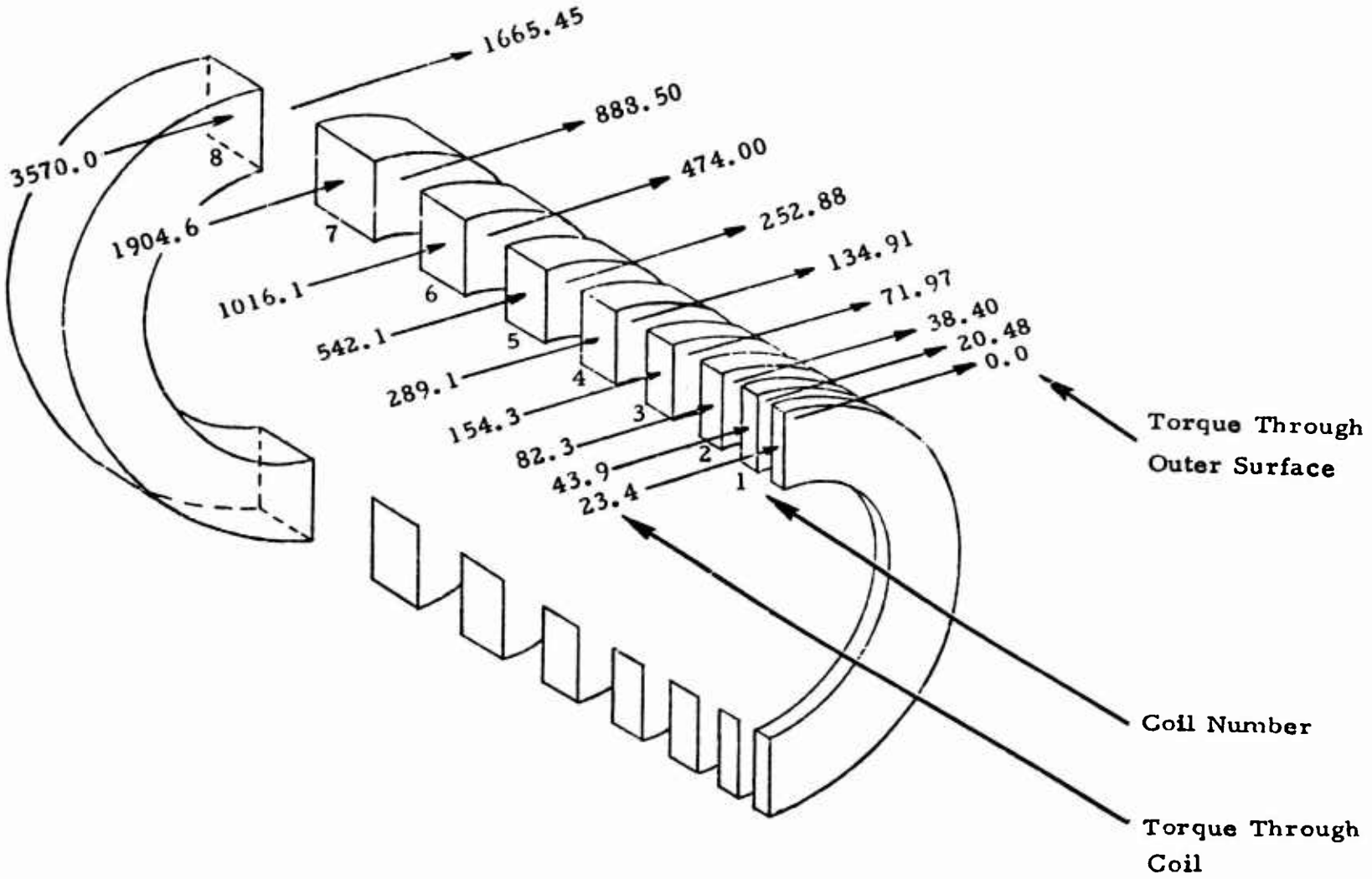

Figure 64. Torque Distribution Through Spring, Clutch Design A.

$$S_c = \frac{2\ T3}{D_{MO}\ b3\ h} = \frac{2\ (154.274)}{(2.201-.36)(.125)(.36)} = 3724 \text{ psi}$$

The stress on the outer surface of the coil equals

$$S_{to} = -107,669 - 3724 = -111,393 \text{ psi}$$

The stress on the inner surface of the coil equals

$$S_{ti} = 107,669 - 3,724 = 103,945 \text{ psi}$$

DRUM HOOP STRESS PER COIL - The hoop stress in the drum is calculated for each coil using the equation defined in the "Clutch Analysis" section. The drum hoop stress variation for each coil is dependent upon the width and torque through the outer surface of the coil in question. A sample calculation of the drum hoop stress for the last coil is shown in the "Clutch Analysis" section.

The last section of output data is presented in two columns; the first column lists component diameters. The significance of each term is explained as follows:

SHAFT ID/OD - The SHAFT ID is an input value, Card 3, Word 1. The SHAFT OD equals (D_{ME}) - (h).

Example: 1.824 - .36 = 1.464

SPRING ID/OD - The free-state SPRING ID equals (D_{MF}) - (h).

Example: 1.803 - .36 = 1.443

The free state SPRING OD equals (D_{MF}) + (h).

Example: 1.803 + .36 = 2.163

DRUM ID/OD - The DRUM ID equals (D_{ME}) + (h) + (Δ_{CL}).

Example: 1.824 + .360 + .017 = 2.201

The DRUM OD is an input value, Card 3, Word 2.

The second column of data represents certain stress values which have all been previously defined and calculated in the "Clutch Analysis" section.

A FORTRAN listing of the computer program follows.

FORTRAN LISTING OF COMPUTER PROGRAM

```
C       SPRING CLUTCH DESIGN - BY AL MEYER
        IMPLICIT REAL*8 (A-H,O-Z)
        KRD=5
        KPR=6
        PI=3.14159265
        DIMENSION G(30), N(30),XL(30),TORQ(30),SCOMP(30),B(30),SHOOP(30)
        ELSMOD=29.0*(10.**6.0)
        POISSN=0.25
        WTDENS=0.282
        GRAVTY=386.4
        WRITE(KPR,1000)
      1 READ(KRD,1001)
        READ(KRD,1002)RPM,TORQUE,COILS,HEIGHT,WIDTH1,WIDTHN,DNAF,DELCL
        READ(KRD,1002)DSHFT1,DDRUMO,FRCOEF
        WRITE(KPR,1001)
        WRITE(KPR,999)
        WRITE(KPR,1010)RPM,TORQUE
        WRITE(KPR,1011)FRCOEF
        WIDTHM=(WIDTHN-WIDTH1)*0.5+WIDTH1
        WRITE(KPR,1012)HEIGHT,WIDTHM
        WRITE(KPR,1013)
        WRITE(KPR,1014)DELCL,DNAF
        DELD=((RPM*RPM)/(0.5*(10.0**13.0)))*((DNAF**5.0)/(HEIGHT*HEIGHT))
        DNAE=DELD+DNAF
        DSHFTO=DNAE-HEIGHT
        THAINT=(360.0*COILS*DELD)/(DELD+DNAF)
        XMINT=(ELSMOD*WIDTHM*(HEIGHT**3.0)*THAINT)/(2376.0*DNAF*COILS)
        THACL=(360.0*COILS*DELCL)/(DELCL+DNAE)
        XMCL=(ELSMOD*WIDTHM*(HEIGHT**3.0)*THACL)/(2376.0*DNAE*COILS)
        THAE=THAINT+THACL
        XME=XMINT+XMCL
        WRITE(KPR,1015)DELD,DNAE
        WRITE(KPR,1016)THAINT,XMINT
        WRITE(KPR,1017)THACL,XMCL
        WRITE(KPR,1018)THAE,XME
C       SPRING GAIN CHARACTERISTICS
        ECONST=2.0*PI*FRCOEF
        GG=DEXP(ECONST)
        NCOILS=COILS+.500
        DO 15 I=1,NCOILS
        XI=I
```

```
   15 G(I)=GG**XI
      XL(1)=(G(1)-1.000)*100.0/G(I)
      DELWTH=(WIDTHN-WIDTH1)/NCOILS
      B(1)=WIDTH1+DELWTH
      DO 16 J=2,NCOILS
      XL(J)=((G(J)-G(J-1))*100.0)/G(I)
   16 B(J)=B(J-1)+DELWTH
      SBEND=6.0*XME/(WIDTHM*HEIGHT*HEIGHT)
      DDRUMI=DNAE+HEIGHT+DELCL
      XSC1=2.0/((DDRUMI-HEIGHT)*HEIGHT)
      DDRUM1=DDRUMI*DDRUMI
      DDRUM2=DDRUMO*DDRUMO
      SHC1=((3.0+POISSN)/32.0)*(WTDENS/GRAVTY)
      SHC2=(PI*RPM/30.0)*(PI*RPM/30.0)
      SHC3=2.0*DDRUM2+DDRUM1-((1.0+3.0*POISSN)/(3.0+POISSN))*DDRUM1
      SHSPED=SHC1*SHC2*SHC3
      SHC4=(DDRUM2+DDRUM1)/(DDRUM2-DDRUM1)
      WRITE(KPR,1019)
      WRITE(KPR,1020)
      WRITE(KPR,1021)
      WRITE(KPR,1022)
      TORQZ=TORQUE/G(I)
      WIDTHZ=WIDTH1
      SCOMZO=-(TORQZ*XSC1/WIDTHZ)-SBEND
      SCOMZI=-(TORQZ*XSC1/WIDTHZ)+SBEND
      WRITE(KPR,1023)TORQZ,WIDTHZ,SCOMZO,SCOMZI
      TORQTC=TORQZ
      DO 17 K=1,NCOILS
      TORQ(K)=XL(K)*TORQUE/100.0
      TORQTC=TORQTC+TORQ(K)
      SCOMP(K)=-((TORQTC*XSC1)/B(K))-SBEND
      SCOMPI=SCOMP(K)+2.0*SBEND
      FNK=(2.0*TORQ(K))/(FRCOEF*DDRUMI)
      FCGK=(PI*B(K)*HEIGHT*WTDENS/GRAVTY)*(DDRUMI-HEIGHT)*SHC2
      AREA=PI*DDRUMI*B(K)
      PRESSI=(FNK+FCGK)/AREA
      SHOOP(K)=PRESSI*SHC4+SHSPED
      N(K)=K
   17 WRITE(KPR,1024)N(K),G(K),XL(K),TORQ(K),TORQTC,B(K),SCOMP(K),SCOMPI
     1,SHOOP(K)
C     SHAFT AND DRUM STRESSES,SPRING ENERGIZING STRESS
      SFTSHR=(16.0*TORQUE*DSHFTO)/(PI*(DSHFTO**4.0-DSHFTI**4.0))
      DSPRGI=DNAF-HEIGHT
      DSPRGO=DNAF+HEIGHT
      SCOMPE=-(XME*XSC1/WIDTHZ)
      WRITE(KPR,1026)DSHFTI,DSHFTO,SFTSHR
      WRITE(KPR,1027)DSPRGI,DSPRGO,SCOMPE
      WRITE(KPR,1028)DDRUMI,DDRUMO,SBEND
      WRITE(KPR,1029)SHOOP(K)
 1000 FORMAT(1H1)
 1001 FORMAT(1X,79H
```

```
     1                                )
 1002 FORMAT(8F10.8)
  999 FORMAT(117X,13HG118-1.0-4/71)
 1010 FORMAT(/' SPEED %RPM<.....a,F16.7,7X,'TORQU
     1E %IN LBS<.....a,F16.7)
 1011 FORMAT(' COEFFICIENT OF FRICTION.....a,F16.7,7X,'MODULU
     1S OF ELASTICITY %PSI<.....      29 MILLIONa)
 1012 FORMAT(' SPRING HEIGHT %IN<.....a,F16.7,7X,'SPRING
     1 WIDTH-MEAN %IN<.....a,F16.7/)
 1013 FORMAT(' INITIAL CLEARANCE-SPRING O.D.a)
 1014 FORMAT('  TO DRUM I.D. %IN<.....a,F16.7,7X,'MEAN S
     1PRING DIA.-FREE %IN<.....a,F16.7)
 1015 FORMAT(/' SPRING DIA. INCREASE-SPEED %IN<.....a,F16.7,7X,'MEAN
     1SPRING DIA.-EXPANDED %IN<.....a,F16.7)
 1016 FORMAT(/' SPRING UNWIND ANGLE-INTERFERENCE %DEG<.a,F16.7,7X,'ENERG
     1IZING MOMENT-INTERFERENCE %IN LBS<..a,F16.7)
 1017 FORMAT(' SPRING UNWIND ANGLE-CLEARANCE %DEG<....a,F16.7,7X,'ENERGI
     1ZING MOMENT-CLEARANCE %IN LBS<.....a,F16.7)
 1018 FORMAT(' TOTAL SPRING UNWIND ANGLE %DEG<.....a,F16.7,7X,'TOTAL
     1ENERGIZING MOMENT %IN LBS<.....a,F16.7)
 1019 FORMAT(//26X,' PER-CENTa,11X,'TORQUEa,9X,'TORQUEa,8X,'AXIALa,12X,'
     1TOTALa,12X,'DRUM HOOPa)
 1020 FORMAT(23X,' GAIN IN TORQUEa,4X,'THROUGH OUTERa,5X,'THROUGHa,8X,'W
     1IDTHa,10X,'STRESS PERa,11X,'STRESSa)
 1021 FORMAT(1X,' COILa,7X,'GAINa,5X,'CARRYING CAPACITYa,6X,'SURFACEa,9X
     1,'COILa,9X,'PER COILa,8X,'COIL %PSI<a,10X,'PER COILa)
 1022 FORMAT( ' NUMBERa,4X,'PER COILa,4X,'%OUTER SURFACE<a,7X,'%IN-LBS<a
     1,6X,'%IN-LBS<a,9X,'%IN<a,6X,'OUTERa,8X,'INNERa,8X,'PSIa)
 1023 FORMAT(/ ' END-LUGa,5X,'1.000a,9X,'-----a,16X,'0.0a,7X,F10.3,6X,F6
     1.3,4X,F9.1,4X,F9.1,9X,'0.0a)
 1024 FORMAT(/I4,6X,F8.3,9X,F5.2,11X,F10.3,5X,F10.3,6X,F6.3,4X,F9.1,4X,F
     19.1,3X,F9.1)
 1026 FORMAT(//' SHAFT I.D./O.D. %IN<.....a,F7.3,'/a,F7.3,10
     1X,'SHAFT SHEAR STRESS %PSI<.....a,2X,F9.1)
 1027 FORMAT(' SPRING I.D./O.D. %IN<.....a,F7.3,'/a,F7.3,10X,
     1'SPRING COMPRESSIVE STRESS-ENERGIZE (PSI).  ',F9.1)
 1028 FORMAT(' DRUM   I.D./O.D. %IN<.....a,F7.3,'/a,F7.3,10X,
     1'SPRING BENDING STRESS COMPONENT %PSI<....  a,F9.1)
 1029 FORMAT(62X,' DRUM HOOP STRESS-MAX (PSI).....',F9.1)
      WRITE(KPR,1000)
      GO TO 1
      END
```

APPENDIX II
SPRING DIAMETRAL GROWTH DUE TO SPEED

The pressure between spring and shaft due to centrifugal force can be determined from the following equation:

$$p_c = \frac{F_C}{A_C} \tag{1}$$

where $F_C = m_S \left(\frac{D_{ME}}{2}\right) w^2 = \left(\frac{b_i\, h\, l}{g}\delta\right)\left(\frac{D_{ME}}{2}\right)\left(\frac{2\pi\eta}{60}\right)^2$

$A_C = b_i l$

Therefore,

$$p_c = \frac{h_\delta}{g}\left(\frac{D_{ME}}{2}\right)\left(\frac{2\pi\eta}{60}\right)^2 \tag{2}$$

An element of a free spring when expanded onto the shaft, assuming no friction, may be represented by the picture below.

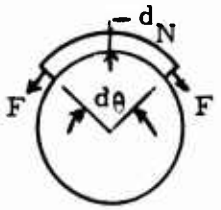

The pressure on the internal surface is

$$p_d = \frac{d_N}{d_A} \tag{3}$$

where $d_N = 2F\left(\sin\frac{d\theta}{2}\right)$

$d_A = b_i\left(\frac{d_{s_o}}{2}\right)d\theta$

For small angles,

$$\sin d\theta = d\theta \tag{4}$$

Therefore,

$$p_d = \frac{2F\, d\theta}{b_i d_{s_o} d\theta} = \frac{2F}{b_i d_{s_o}} \tag{5}$$

But

$$F = \frac{2T_S}{D_{ME}} \tag{6}$$

where T_S = moment required to unwrap the free spring to the diameter of the shaft

Hence,

$$p_d = \frac{4T_S}{b_i d_{s_o} D_{ME}} \tag{7}$$

The relationship between the moment and resulting angular deflection as defined in spring handbooks is expressed as follows:

$$T_S = \frac{E b_i h^3}{6 D_{MF}} \quad \frac{\phi}{N} \tag{8}$$

The relationship between angular deflection and diametral growth is derived as follows: The arc length of the free spring equals the arc length of the expanded spring

$$D_{MF}\, \theta_F = D_{ME}\, \theta_E \tag{9}$$

By definition

$$\Delta D = D_{ME} - D_{MF}, \quad 2\pi \phi = \theta_F - \theta_E \tag{10}$$

Therefore,

$$2\pi \phi = \theta_F - \theta_F \left(\frac{D_{MF}}{D_{ME}}\right) = \theta_F \left(1 - \frac{D_{MF}}{D_{ME}}\right) = \theta_F \left(\frac{D_{ME} - D_{MF}}{D_{ME}}\right)$$

$$= \theta_F \left(\frac{\Delta D}{D_{ME}}\right) \tag{11}$$

But

$$\theta_F = 2\pi N \tag{12}$$

Therefore,

$$\frac{\phi}{N} = \frac{\Delta D}{D_{ME}} \tag{13}$$

Substitution of Equation (13) into (8) yields

$$T_S = \left(\frac{E b_i h^3}{6 D_{MF}}\right)\left(\frac{\Delta D}{D_{ME}}\right) \tag{14}$$

Substitution of Equation (14) into (7) yields

$$P_d = \left(\frac{4}{b_i d_{s_o} D_{ME}}\right)\left(\frac{E b_i h^3}{6 D_{MF}} \frac{\Delta D}{D_{ME}}\right)$$

$$= \frac{2 E \eta^3 \Delta D}{3 d_{s_o} D_{MF} D_{ME}^2} \tag{15}$$

Equating the pressure relationships of equations (15) and (2) and solving for ΔD yields

$$\Delta D = \left(\frac{3 d_{s_o} D_{MF} D_{ME}^2}{2 E h^3}\right)\left(\frac{h\delta}{g}\right)\left(\frac{D_{ME}}{2}\right)\left(\frac{2\pi\eta}{60}\right)^2$$

$$= \left(\frac{3\delta\pi^2}{Eg(60)^2}\right)\left(\frac{d_{s_o} D_{MF} D_{ME}^3 \eta^2}{h^2}\right)$$

$$= \left(\frac{3(.282)\pi^2}{(29\times10^6)(386.4)(3600)}\right)\left(\frac{d_{s_o} D_{MF} D_{ME}^3 \eta^2}{h^2}\right)$$

$$= (2.07)(10^{-13})\left(\frac{d_{s_o} D_{MF} D_{ME}^3 \eta^2}{h^2}\right) \qquad (16)$$

Rounding off and approximating all diameters by D_{MF} results in

$$\boxed{\Delta D = \frac{(2)(10^{-13})\,(D_{MF}^5 \eta^2)}{h^2}} \qquad (17)$$

APPENDIX III
RAW DATA, OVERRIDE TEST

CLUTCH DESIGN A

Oil Flow (gpm)	Output Shaft Speed (rpm)	Shaft Torque (in.-lb)	Reaction Torque (in.-lb)	Oil-In Temp. (°F)	Oil-Out Temp. (°F)	Torque Calculated Using Oil ΔT (in.-lb)
2.4	26,000	1.3	4.9	201	213	5.9
	25,000	1.5	4.6	200	216	8.2
	20,000	1.7	3.1	200	206	3.8
	15,000	1.5	2.1	199	204	4.3
	10,000	1.0	1.1	200	203	3.8
	5,000	0.6	.6	199	202	7.7
1.6	26,000	0.7	4.9	200	207	2.3
	25,000	0.5	4.5	200	206	2.0
	20,000	0.9	2.8	201	202	.4
	15,000	0.6	1.7	202	200	-
	10,000	0.6	1.0	200	200	-
	5,000	0.5	.7	200	196	-
.8	26,000	-	4.2	202	207	.8
	25,000	-	4.0	204	214	1.7
	20,000	-	2.6	202	198	-
	15,000	-	1.6	200	198	-
	10,000	-	1.0	200	195	-
	5,000	-	.6	204	200	-
.54	26,000	1.1	4.0	198	193	-
	25,000	1.2	3.7	196	196	-
	20,000	1.3	2.4	194	186	-
	15,000	1.3	1.7	196	180	-
	10,000	1.1	1.0	197	178	-
	5,000	0.8	.4	196	177	-
.26	26,000	6.4	3.1	199	216	.9
	25,000	6.1	2.9	199	222	1.3
	20,000	3.8	2.2	200	196	-
	15,000	2.3	1.5	200	185	-
	10,000	1.1	.9	201	183	-
	5,000	0.6	.6	200	194	-

CLUTCH DESIGN B

Oil Flow (gpm)	Output Shaft Speed (rpm)	Shaft Torque (in.-lb)	Reaction Torque (in.-lb)	Oil-In Temp. (°F)	Oil-Out Temp. (°F)	Torque Calculated Using Oil ΔT (in.-lb)
2.4	26,500	8.4	8.2	200	232	15.4
	25,000	7.7	7.8	200	230	15.3
	20,000	5.9	6.0	200	226	16.5
	15,000	4.1	4.2	200	219	16.1
	10,000	3.3	3.6	200	213	16.6
	5,000	2.1	2.4	200	207	17.8
1.6	26,500	8.3	7.8	201	229	9.0
	25,000	7.8	7.2	200	224	8.1
	20,000	5.6	6.0	200	218	7.6
	15,000	4.1	4.2	200	212	6.8
	10,000	3.0	3.0	200	210	8.5
	5,000	1.7	2.1	200	203	5.0
.8	26,500	7.9	7.2	200	230	4.8
	25,000	7.4	7.2	200	228	4.8
	20,000	5.9	6.0	200	218	3.8
	15,000	4.5	4.2	200	210	2.8
	10,000	2.9	3.0	200	208	3.4
	5,000	2.0	2.1	200	204	3.4
.54	26,500	6.6	6.0	200	239	4.2
	25,000	6.3	5.4	200	234	3.8
	20,000	4.8	4.8	200	224	3.4
	15,000	4.2	4.2	200	218	3.4
	10,000	2.8	3.0	200	210	2.8
	5,000	1.6	2.1	200	203	1.6
.26	26,500	6.2	4.8	200	263	3.4
	25,000	5.6	4.5	200	260	3.4
	20,000	4.5	3.9	200	240	2.8
	15,000	4.1	3.3	200	236	3.4
	10,000	2.7	2.7	200	214	2.0
	5,000	1.7	1.8	200	206	1.8

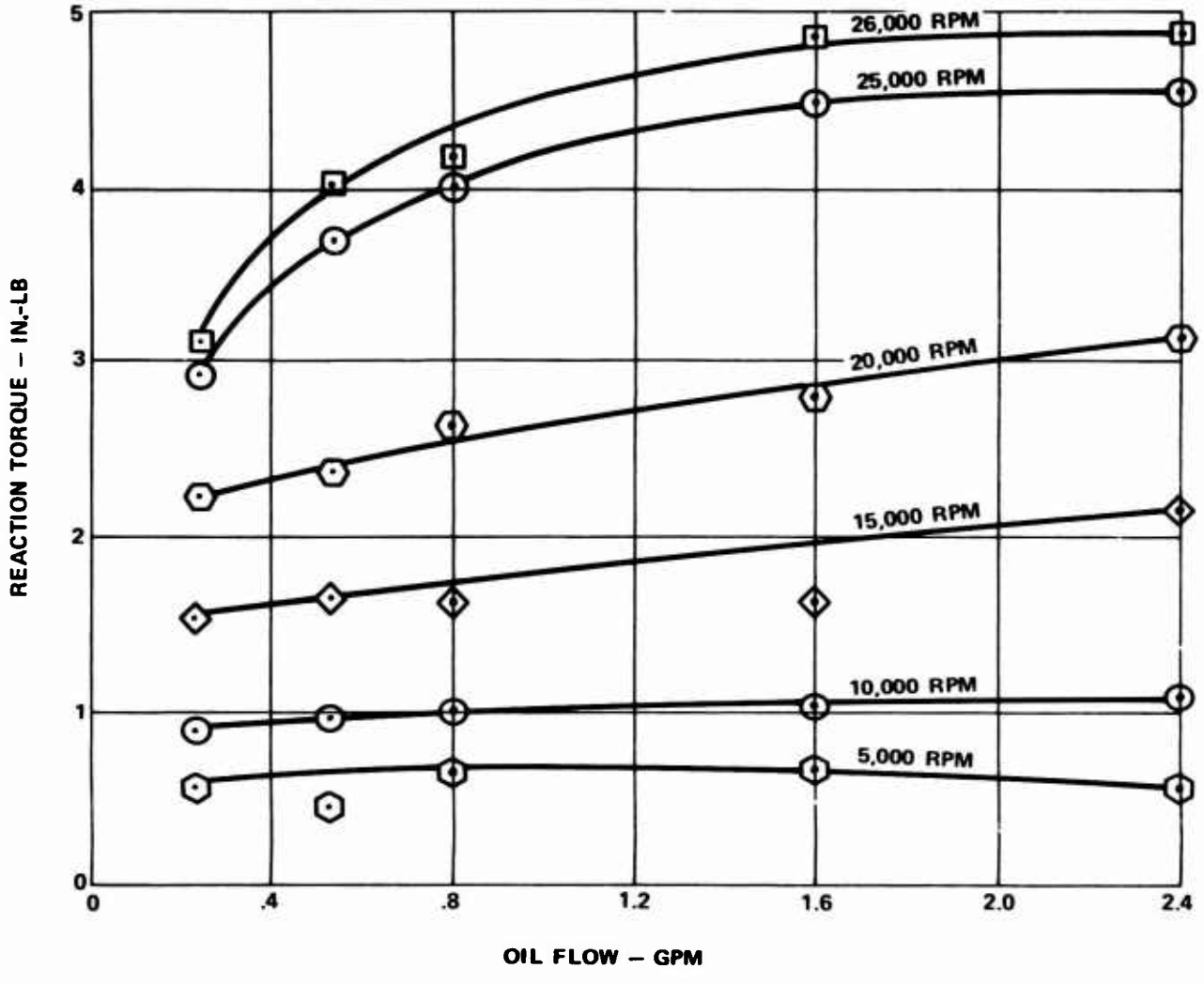

Figure 65. Reaction Torque Versus Oil Flow at Various Speeds, Design A Full-Speed Override (Input Stationary).

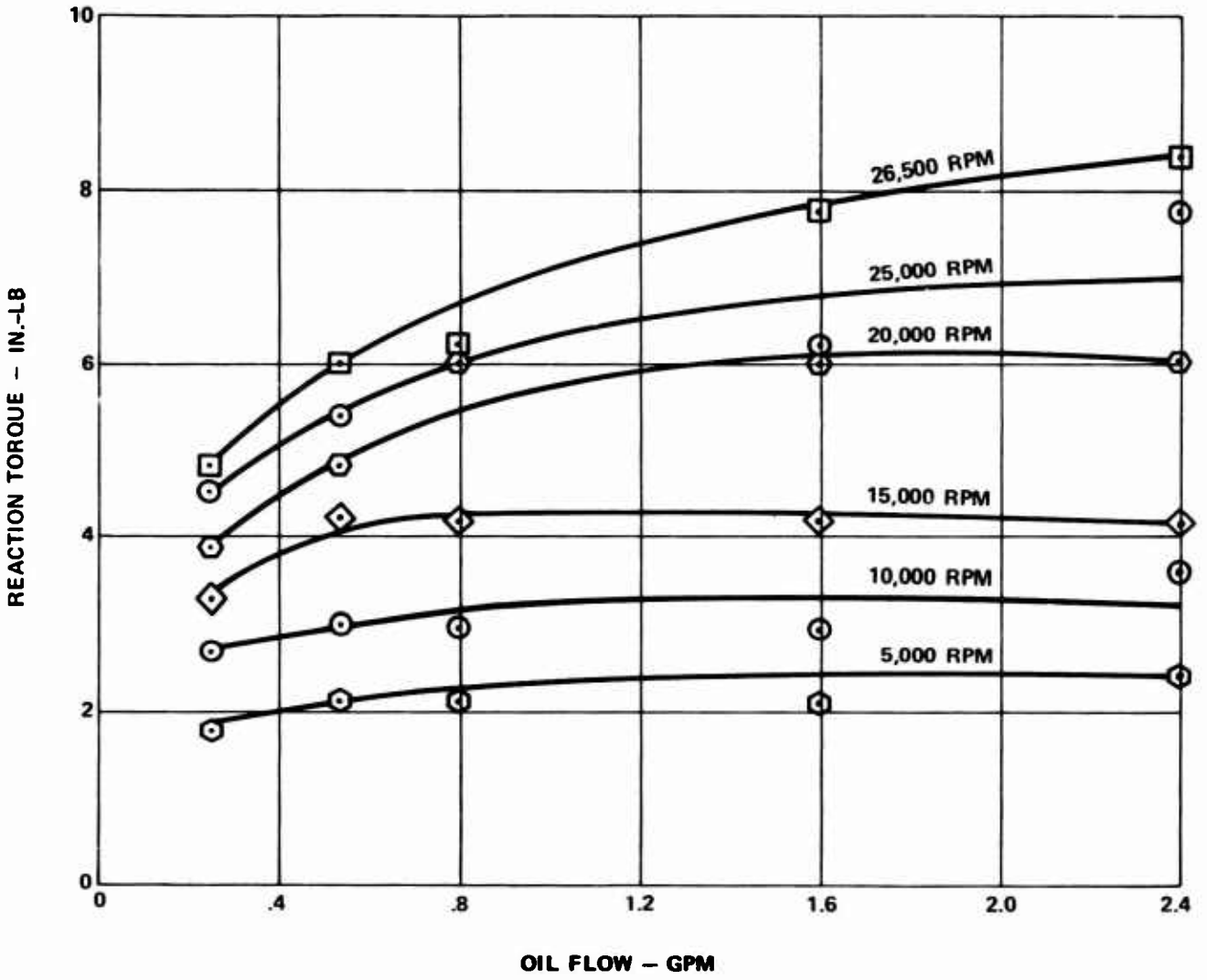

Figure 66. Reaction Torque Versus Oil Flow at Various Speeds, Design B Full-Speed Override (Input Stationary).

APPENDIX IV
DESIGN A STRESS ANALYSIS

The critical section of the spring clutch assembly is located at the lug of the inner race. In this region, the combined axial bending and torsional shear stress field of the shaft portion of the race is altered by the reaction at the lug to the applied torque.

A sketch of a sector of the inner race is shown in Figure 67. Relatively high stress concentrations can be expected at the junction between the shaft and the lug and also at the junction between the shoulder and the lug (i.e., along path A-B-C of Figure 67). Because of the complex geometry and the proximity of the load P to the fillet region, no exact theoretical solutions for the stress/strain distributions in this region are obtainable. Therefore, an expirical expression developed by R. B. Heywood * was used in conjunction with a photoelastic investigation of the stresses produced in loaded projections in order to estimate the peak stresses and strains in the lug. To simplify the analysis, the stiffening effect of the shoulder was neglected; hence, in this respect the analysis is somewhat conservative.

The geometry and nomenclature associated with the Heywood analysis of a loaded projection are shown in Figure 68. The same terminology is used in Figure 69, which constitutes a tabular presentation of various geometric quantities pertinent to the analysis of the lug as functions of the size of the fillet radius, R (see column 7 of Figure 69). The elastic stress concentration factor is shown in column 12 of Figure 69. Columns 13 and 14 give the nominal bending and proximity stress terms, respectively, per unit value of P/t, whereas the nominal tensile stress at the fillet (again per unit value of P/t) is listed in column 15. Since the width of the section, t (see column 11), decreases with an increase of fillet radius, the quantity P/t increases correspondingly; however, the same conditions produce a decrease in the stress concentration factor, K, thereby producing effects upon the peak tensile stress at the fillet which tend to offset one another.

*Heywood, R. B., TENSILE FILLET STRESSES IN LOADED PROJECTIONS, Proc. IME, Vol. 159, WEI 45, 1948.

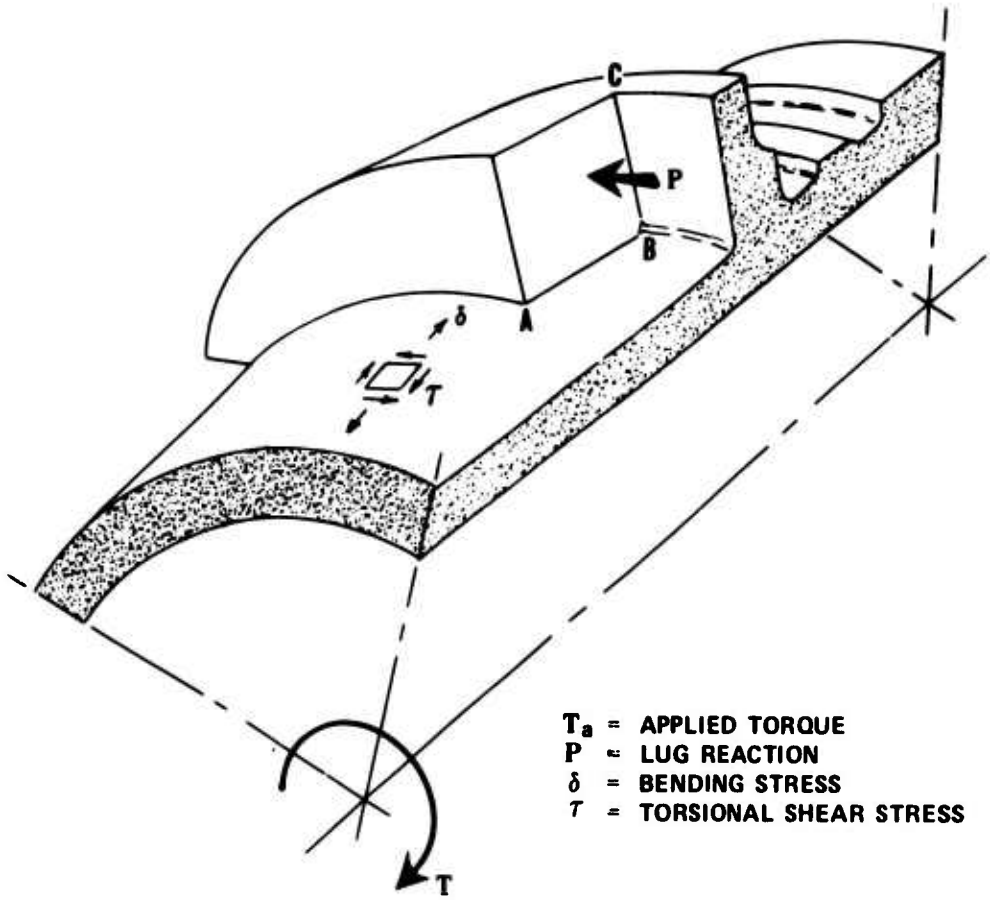

Figure 67. Inner Race, Spring Clutch Assembly.

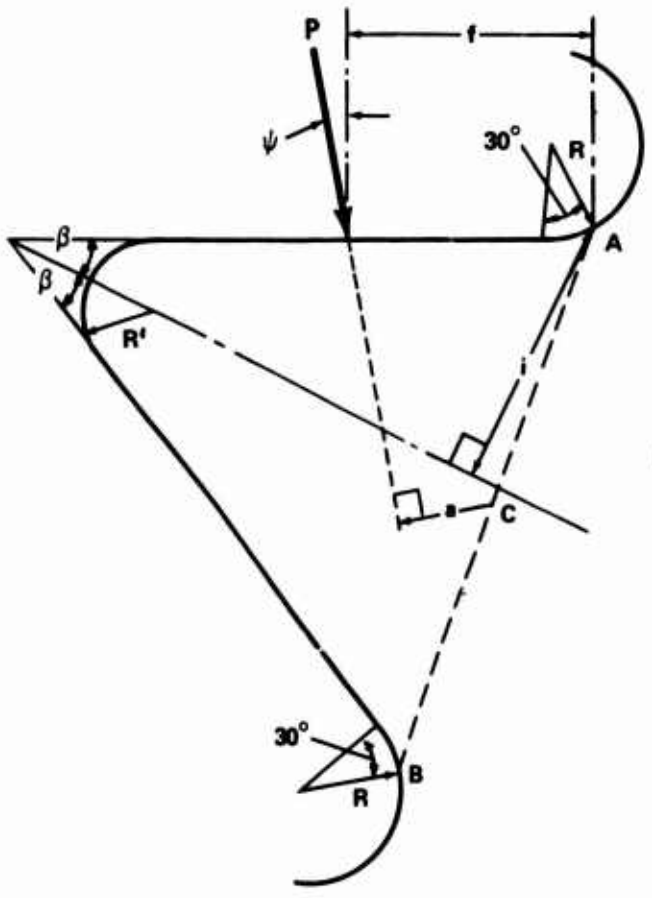

σ_{max} = K (M + L)

where

σ_{max}	=	maximum tensile fillet; stress
K	=	stress concentration factor = $1 + 0.26\ (i/R)^{0.7}$
M	=	nominal bending stress = $[1.5a/i^2]\ P/t$
L	=	proximity stress = $[\sqrt{0.36/(fi)}\ (1 + \frac{1}{4} \sin \psi)]\ P/t$
a	=	moment arm
f	=	distance from point of load application to point at which maximum tensile fillet stress occurs
i	=	dimension defining weakest semisection
t	=	width of section
P	=	applied load
ψ	=	angle of inclination of load from surface normal
β	=	semiangle of projection

Figure 68. Geometry Required for Heywood Analysis of Loaded Projection.

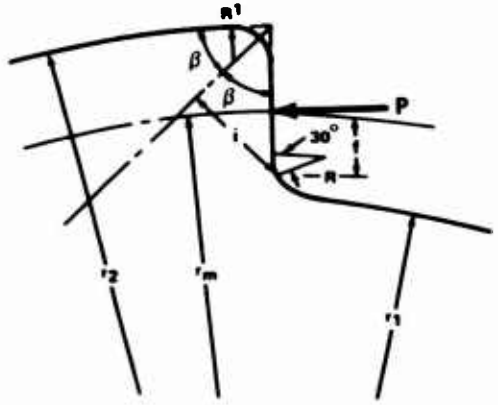

Case No.	1 r_1 (in.)	2 r_2 (in.)	3 r_m (in.)	4 β (°)	5 ψ (°)	6 R^1 (in.)	7 R (in.)	8 a (in.)	9 f (in.)	10 i (in.)	11 t (in.)	12 k	13 $\frac{1.5a}{i^2}$	14 $\sqrt{\frac{0.36}{fi}}$	15 $\frac{1.5a}{i^2} + \sqrt{\frac{0.36}{fi}}$
1	0.7325	1.0925	0.9125	45	0	0.010	0.010	0.175	0.175	0.252	0.229	3.49	4.13	2.86	6.99
2	↓	↓	↓	↓	↓	↓	0.020	0.170	0.170	0.249	0.219	2.52	4.10	2.91	7.01
3	↓	↓	↓	↓	↓	↓	0.030	0.165	0.165	0.247	0.209	2.14	4.06	2.97	7.04
4	↓	↓	↓	↓	↓	↓	0.040	0.160	0.160	0.244	0.198	1.92	4.02	3.04	7.06
5	0.7325	1.0925	0.9125	45	0	0.010	0.050	0.155	0.155	0.242	0.188	1.78	3.98	3.10	7.08

Figure 69. Summary of Lug Geometry, Inner Race.

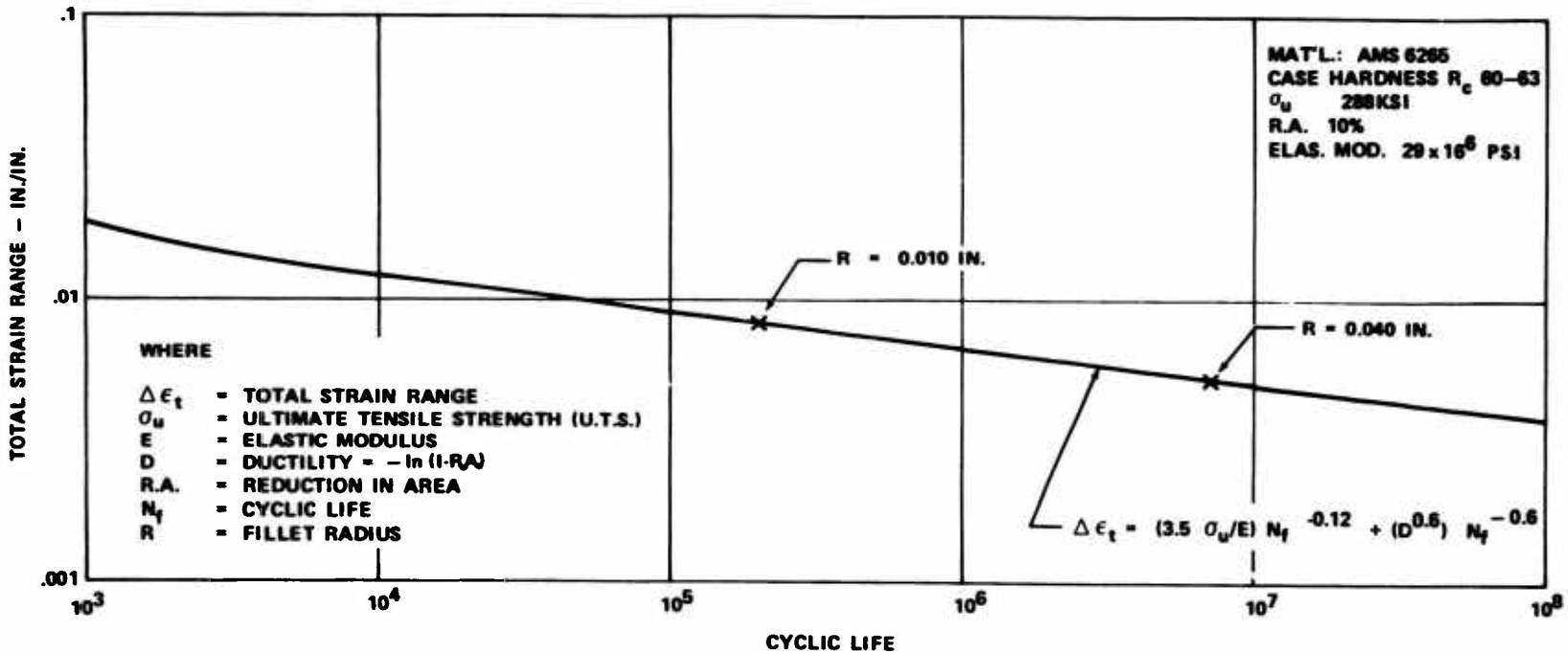

Figure 70. Fatigue Curve, Strain Controlled Cycling.

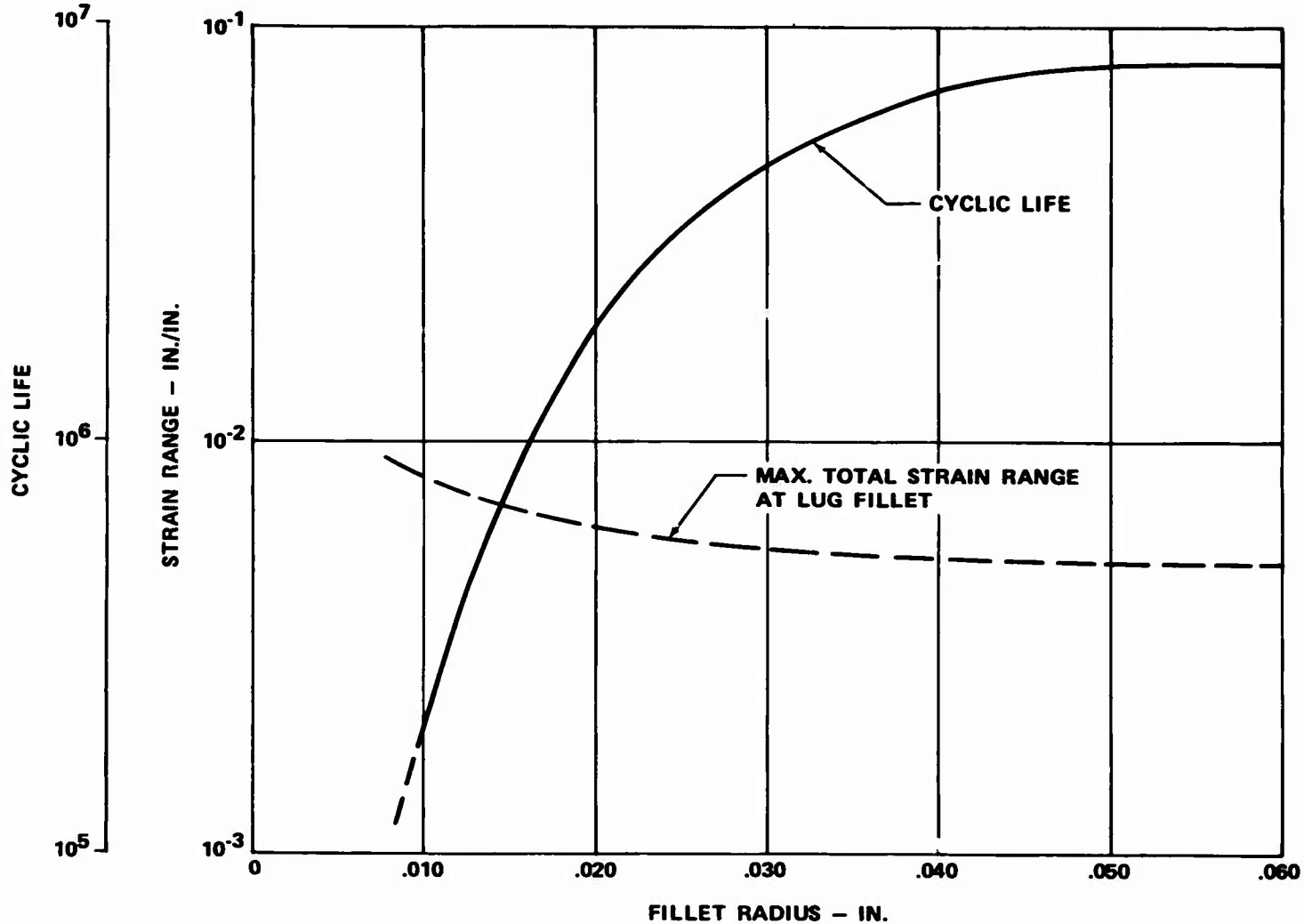

Figure 71. Effect of Fillet Size on Predicted Strain Range and Cyclic Life of the Inner Race (Lug Analysis).

The fatigue curve used in the analysis is shown in Figure 70. This curve, which is based upon fully-reversed strain-controlled cycling, was constructed from S. S. Manson's "universal slopes" equation*.

Figure 71 is a plot of the calculated fatigue life of the inner race versus the size of the lug fillet radius, R. This plot was obtained by use of the geometric parameters shown in Figure 69, the fatigue curve of Figure 70, and an estimated total strain range taken to be twice the elastic strain computed by using the elastic modulus for the inner-race material and the maximum tensile stress at the fillet for a vibratory torque of 1000 in.-lb. (When Figure 70 is used, the tacit assumption is made that the strain at the fillet is fully reversed; consequently, the steady torque of 7100 in.-lb was not considered in the analysis.) Because of the approximate nature of the analysis, the results of Figure 71 can only be interpreted as indicating the relative merits of one fillet size with respect to another. Thus, the average life expectancy of an inner race with a 0.040-inch fillet radius should be on the order of 35 times that of one with a 0.010-inch fillet radius.** However, no such increase in life was evident from the two tests which were conducted. This lack of conformity with the analytical results can be attributed to either or both of the following factors:

1. The limitations of the analysis itself.

2. The significance of the small number of tests in view of the scatter inherent in all fatigue tests.

*Manson, S. S., FATIGUE: A COMPLEX SUBJECT - SOME SIMPLE APPROXIMATIONS, The William M. Murray Lecture, 1964, Experimental Mechanics, Vol. 5, No. 7, July 1965, pp. 193-226.

**From Figure 71, the indicated cyclic life of a race with a 0.040-inch fillet radius is 7.0×10^6, whereas that of a race with a 0.010-inch fillet radius is 2.0×10^5. Thus, the relative life expectancy of the former is $7.0 \times 10^6 / (2.0 \times 10^5) = 35$ times that of the latter.

As regards the limitations of the analysis, certain simplifying assumptions were necessary to make the problem solvable. For this reason the results presented in Figure 71 were interpreted only in terms of the relative life of one inner-race design with respect to another, rather than in terms of the individual values of cyclic life. The prediction of an actual fatigue life on the basis of Figure 71 requires that the fatigue life of a reference design be known in advance, thereby establishing a scale factor between observed and calculated lives. This has not been attempted in the present report, since the average cyclic lives of both inner-race designs for the given loading conditions are unknown.

The scatter of results which is associated with all forms of fatigue testing implies that a large variation in cyclic life will be observed in the neighborhood of the endurance limit (or at high values of average cyclic life in those instances when no endurance limit is observed); therefore, it is quite possible that the life scatter bands for the two inner-race designs under consideration do in fact overlap. Thus, the analysis described in the present report is not invalidated by the results of the two fatigue tests.